CANADIAN THESES

THÈSES CANADIENNES

NOTICE

The quality of this microfiche is heavily dependent upon the quality of the original thesis submitted for microfilming. Every effort has been made to ensure the highest quality of reproduction possible.

If pages are missing, contact the university which granted the degree.

Some pages may have indistinct print especially if the original pages were typed with a poor typewriter ribbon or if the university sent us an inferior photocopy.

Previously copyrighted materials (journal articles, published tests, etc.) are not filmed.

Reproduction in full or in part of this film is governed by the Canadian Copyright Act, R.S.C. 1970, c. C-30.

AVIS

La qualité de cette microfiche dépend grandement de la qualité de la thèse soumise au microfilmage. Nous avons tout fait pour assurer une qualité supérieure de reproduction.

S'il manque des pages, veuillez communiquer avec l'université qui a conféré le grade.

La qualité d'impression de certaines pages peut laisser à désirer, surtout si les pages originales ont été dactylographiées à l'aide d'un ruban usé ou si l'université nous a fait parvenir une photocopie de qualité inférieure.

Les documents qui font déjà l'objet d'un droit d'auteur (articles de revue, examens publiés, etc.) ne sont pas microfilmés.

La reproduction, même partielle, de ce microfilm est soumise à la Loi canadienne sur le droit d'auteur, SRC 1970, c. C-30.

THIS DISSERTATION HAS BEEN MICROFILMED EXACTLY AS RECEIVED

LA THÈSE A ÉTÉ MICROFILMÉE TELLE QUE NOUS L'AVONS REÇUE

PERFORMANCE OF FH/QPSK, FH/QPR, FH/MSK UNDER FREQUENCY SELECTIVE FADING AND PARTIAL BAND TONE JAMMING

Fazal Noor

A Thesis

in

The Department

of

Electrical Engineering

Presented in Partial Fulfillment of the Requirements
for the Degree of Master of Engineering at
Concordia University
Montréal, Québec, Canada

July, 1986

ISBN 0-315-32261-6

ABSTRACT

Performance of FH/QPSK, FH/QPR, and FH/MSK Under Frequency Selective Fading and Partial Band Tone Jamming

Fazal Noor

The performance of each of the following coherent modulation techniques namely, quadriphase-shift-keying (QPSK), minimum-shift-keying (MSK), and quadrature-partial-response (QPR), each employing frequency hopping (FH), is presented. The systems are assumed to be operating in the presence of partial-band tone jammer. The channel over which the signals are transmitted is frequency-selective Rician fading modeled as wide-sense-stationary-uncorrelated-scattering (WSSUS). The probability of bit error for each system is derived both with and without the use of error-correction coding and a comparison for the two cases is made on the basis of equal information rates and equal spread bandwidths. The use of error correction-coding is employed to improve the performance of the systems.

ACKNOWLEDGEMENTS

I wish to acknowledge my heartfelt gratitude to Professor A.K. Elhakeem for suggesting the problem, for his guidance and assistance during the entire preparation of this thesis.

I gratefully acknowledge the encouragement and full support provided by my parents, sisters and brothers.

Table of Contents

LIST OF SYMBOLS

A	amplitude of the transmitted signal.
a_m, b_m	transmitted symbols in QPR system.
$\hat{a}_m$, $\hat{b}_m$	estimate of the transmitted symbols.
c_n d_n	precoded symbols in the QPR system.
$d_I(t)$, $d_Q(t)$	are the in-phase and quadrature symbols taking on values ± 1.
$E[\cdot]$	expected value.
E_b	energy per bit.
E_b/N_J	energy per bit to jammer spectral density.
E_b/N_o	energy per bit to additive noise spectral density.
FH/QPSK	frequency hopping quadrature phase shift keying.
FH/MSK	frequency hopping minimum shift keying.
FH/QPR	frequency hopping quadrature partial response.
$H_T(\omega)$	QPR pulse shaping transmitter filter.
$H_R(\omega)$	receiver filter in frequency domain.
$h_T(t)$	transmitter filter in time domain.
$h_R(t)$	receiver filter in time domain.
I_{s_i}	intersymbol interference of the signal.
I_{J_i}	intersymbol interference of the jammer.
J	jammer power per slot.
J_T	total jammer power.
$\bar{J}(t)$	jammer signal waveform.

$\bar{J}_F(t)$	faded component of the jammer signal.
M	number of jammed channels.
MSK	minimum shift keying.
N	number of frequencies available.
n(t)	additive white Gaussian noise of two sided spectral density $\eta_o/2$.
$N_c(t)$, $N_s(t)$	statistically independent low-pass white Gaussian noise processes with single-sided noise spectral density N_o W/Hz.
P(t)	rectangular pulse.
P_b	probability of bit error.
PLL	phase-locked loop.
P_I, P_Q	probability of error in the in-phase and quadrature channels.
Q(x)	Gaussian probability integral.
r(t)	is the received signal.
$r_d(t)$	is the dehopped signal.
Re { }	real part of the argument.
S	average transmitted power.
s(t)	is the transmitted signal.
$s_F(t)$	is the faded component of the transmitted signal.
Si ( )	sine integral function defined as $\mathrm{Si}(x) = \int_0^x \frac{\sin y}{y}\, dy$.
T	bit duration.
u(t)	unit step function.
ω_o	oscillator frequency.

ω_k	is the kth hopping frequency.
W_{ss}	spreading bandwidth.
$Z_Q(t)$, $Z_I(t)$	quadrature and in-phase demodulated signals.
Z_{Qm}, Z_{Im}	sampled values of $Z_Q(t)$, $Z_I(t)$.
γ_s	transmission coefficient of the signal channel.
γ_J	transmission coefficient of the jammer channel.
λ	takes on value of ± 1 depending upon whether or not the channel is jammed.
$\beta_s(\tau)$, $\beta_J(\tau)$	independent zero mean complex Gaussian random processes representing the low-pass equivalent impulse response of the channel.
θ_k	is the random phase generated by the frequency synthesizer in the kth interval.
ϕ_k	is the random phase of the jammer.
$\delta(\cdot)$	Dirac delta function.
$\rho(\tau)$	multipath delay spread of the channel.
$\eta_o/2$	two-sided spectral density of additive white Gaussian noise.
σ_N^2	variance of the noise.
σ_Q^2	variance of the signal in quadrature channel.
ρ	fraction of the total channels jammed.

LIST OF FIGURES

LIST OF TABLES

CHAPTER ONE

Introduction

1.1 Thesis outline:

In the present chapter a brief explanation of frequency hopping, jammer model and channel model is given. In chapter two, chapter three and chapter four the analysis and numerical results are presented of FH/QPSK, FH/MSK, and FH/QPR, respectively. In chapter five comparison of FH/QPSK, FH/MSK, and FH/QPR is made. Finally chapter six ends with the conclusion.

1.2 Frequency Hopping:

In conventional communication systems, the two primary communication resources are the transmitted power and channel bandwidth. A general system design objective would be to use these two resources as efficiently as possible. For example, space communication links are typically power limited. In power-limited channels, coding schemes are generally used to save power at the expense of bandwidth, whereas in band-limited channels "spectrally efficient modulation" techniques would be used to save bandwidth. The primary objective of spectrally efficient modulation is to maximize the bandwidth efficiency, defined as the ratio of data rate to channel bandwidth (in units of bits/s/Hz).

On the other hand, in spread spectrum communications the channel bandwidth employed is much larger than that used in conventional communication systems. The two main modulation techniques employed in spread spectrum are direct-sequence and frequency-hopping. Some of the advantages of spread

spectrum communication are

1) selective addressing capability

2) low-density output signals

3) message privacy/security

4) interference rejection

and the disadvantages are that they

1) employ more bandwidth than conventional systems

2) employ more hardware than used by conventional systems.

There has been a growing interest in investigating various digital modulation techniques in conjunction with FH [1]. Baseband signals with faster spectral roll-off characteristics and amenability to saturated amplification at the transmitter have also been the subject of intense investigation for over a decade [2]. While phase coherence at all hopping frequencies between the transmitter and the receiver is not viable [4] several researchers have assumed this [5],[6]. Recently, Behraman [7] designed a low cost MSK/FH modem and greater emphasis was placed on the nature of the channel. Also, Milstein [8] has analyzed the performance of FH/FSK system under frequency selective fading and partial band tone jamming. Noncoherent MFSK is the most practical and traditional modulation technique in conjunction with FH [1],

Although it is possible to built coherent frequency hopping transmitters and coherent receivers operating side by side but as these systems are separated, then the signal must pass through the atmosphere where it is no longer coherent when it reaches the receiver due to differences in phases from one frequency to another. In the analysis of coherent frequency hopping, the following assumptions are

made

1). Precise phase coherence in transmitter and receiver frequency synthesizer is accomplished.

2). Accurate model of the link between the transmitter and receiver with precise delay compensation is accomplished.

We analyze in here the following coherent modulation techniques namely, quadriphase-shift-keying (QPSK), minimum-shift-keying (MSK), and quadrature-partial-response (QPR), frequency-hopping (FH) systems operating in partial band tone jamming and frequency selective fading, again with the assumption that phase coherence will be maintained at all frequency hops. Figure 1.1 shows a general block diagram of a FH system operating in a frequency selective environment and in the presence of a jammer. The frequency of the FH signal changes pseudorandomly over a wide band as shown in figure 1.2. The specific order in which frequencies are occupied is a function of a code sequence. The bandwidth of a frequency hopping signal is δf times the number of frequency slots available, where δf is the frequency separation between slots (typically equal to basic data bandthwidth). The processing gain of a frequency hopping system is defined as the number of channels employed. Error correction coding is employed to improve the performance of the system.

1.3 Multi-tone Jammer:

We assume an intelligent jammer that has knowledge of the form of data and spread spectrum modulation, including such items as data rate, spreading bandwidth and hop rate, but no knowledge of the code for selecting for determining the spectrum-spreading hop frequencies.

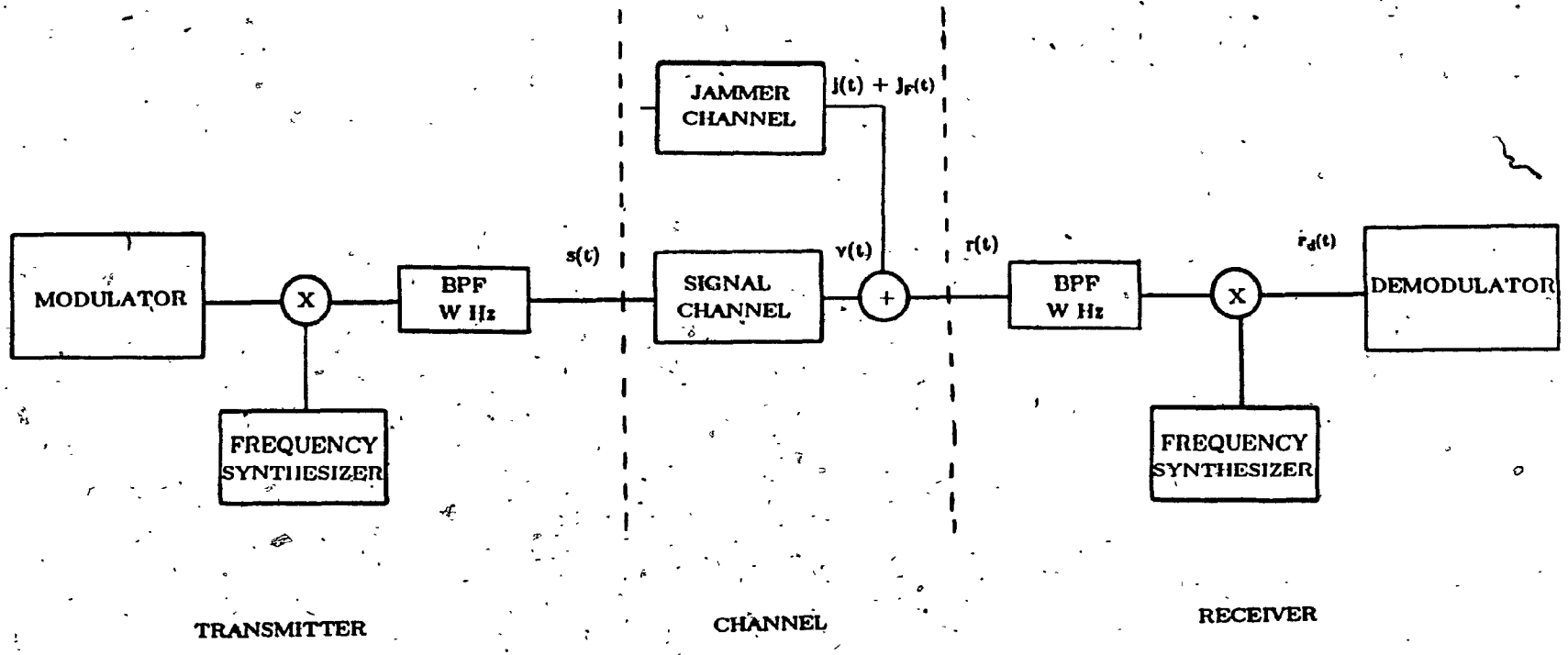

Figure 1.1 Block diagram of FH system operating in a frequency-selective fading channel and in presence of a multi-tone jammer.

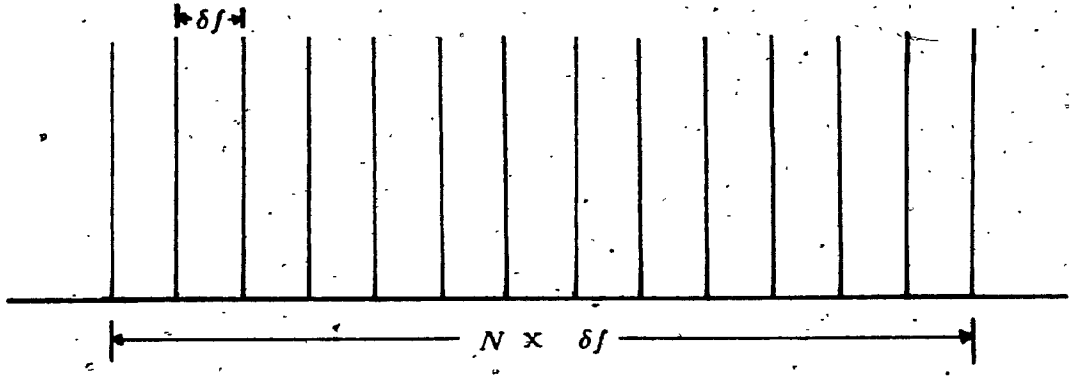

Figure 1.2 Frequency-hopping signal spectrum.

The partial-band jammer $J(t)$ is assumed to have a total power J_T which is evenly divided among M jammer tones. Therefore each tone has a power of

$$J = \frac{J_T}{M} \tag{1.1}$$

Furthermore, since the jammer is assumed to have knowledge of the exact location of the spreading bandwidth W_{ss} and the number N of hops in this bandwidth. We shall assume that the jammer will randomly locate each of his M tones coincident with M of the N hop frequencies. Thus,

$$\rho = \frac{M}{N} \tag{1.2}$$

represents the fraction of the total band which is jammed with tones, each having power J.

1.4 Channel Model

The channel model which assumes wide-sense-stationary-uncorrelated-scattering (WSSUS) is used in the analysis. This is a representative model for practical radio links and troposcatter channels [11],[16]. If $x(t)\cos(\omega_o t + \theta)$ is the input to this channel, then the corresponding output is given by

$$y(t) = \mathrm{Re}\left\{[x(t) + \gamma\int \beta(\tau)\, x(t-\tau)\, d\tau] \exp j(\omega_o t + \theta)\right\} \tag{1.3}$$

where γ is the transmission coefficient for the fading channel. $\beta(\tau)$ is defined as an independent, zero mean, complex Gaussian random process representing the low-pass equivalent impulse response of the frequency selective channel. The correlation function of $\beta(\tau)$ is denoted from [9],[11] as

$$\frac{1}{2}E\{\beta(\tau_1)\beta^*(\tau_2)\} = \rho(\tau_1)\,\delta(\tau_1-\tau_2) \tag{1.4}$$

and assuming [11],[13],[14]

$$E\{\beta(\tau_1)\beta(\tau_2)\} = 0 \tag{1.5}$$

where $\rho(\tau)$ for practical WSSUS channels is a real function of τ and $\delta(\tau)$ is the dirac delta function. As in [9],[11]-[12] $\rho(\tau)$ is the multipath-delay spread of the channel chosen as

$$\rho(\tau) = \begin{cases} \frac{1}{2T}\left(1 - \frac{|\tau|}{2T}\right) & |\tau| \leq 2T \\ 0 & \textit{otherwise} \end{cases} \tag{1.6}$$

and this limits the intersymbol interference that the channel generates to just adjacent symbols. The former assumption in (1.5) implies that the in-phase and quadrature components of $\beta(\tau)$ have the same statistical properties and are uncorrelated with one another.

CHAPTER TWO

FH/QPSK SYSTEM UNDER FREQUENCY SELECTIVE FADING CHANNEL AND PARTIAL BAND TONE JAMMING

2.1 Introduction :

The performance of frequency-hopping quadriphase-shift-keying (FH/QPSK) system is presented operating over a frequency-selective channel and partial band tone jamming.

In the analysis of FH/QPSK system, conventional type QPSK transmitter and receiver structures are employed. The channel model which assumes wide-sense-stationary-uncorrelated-scattering (WSSUS) described in the introduction is used in the analysis.

In section three, the numerical results are obtained by evaluating the expressions for the probability of bit error derived in the analysis.

2.2 Analysis:

The system to be analyzed is shown in figure 2.1. The modulator and demodulator structures shown are those normally employed for coherent detection in AWGN background.

The transmitted signal can be expressed as

$$s(t) = \sqrt{S} \sum_k \left[d_I(t) \cos(\omega_o t) + d_Q(t) \sin(\omega_o t) \right] \cdot \cos(\omega_k t + \theta_k) P(t - 2kT) \qquad (2.1)$$

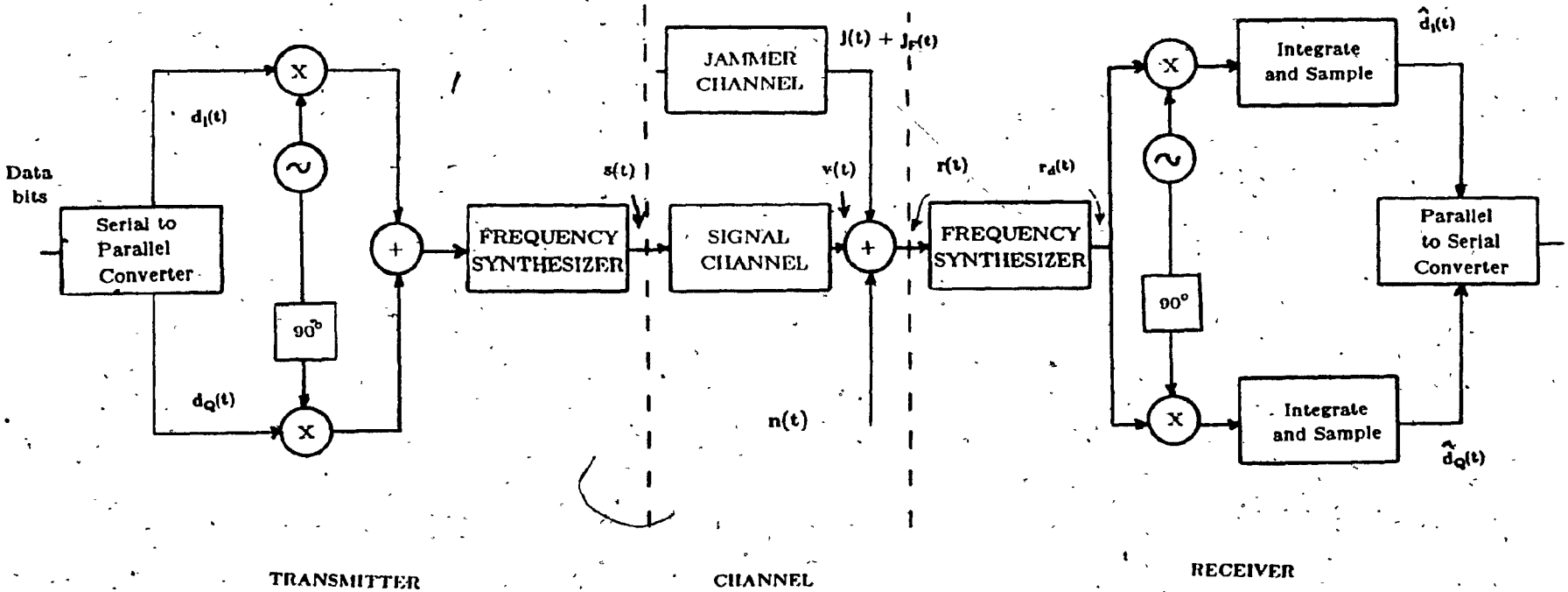

Figure 2.1. Block diagram of FH/QPSK system.

where S is the average transmitted power, $d_I(t)$, $d_Q(t)$ are the in-phase and quadrature symbols taking on values ± 1, ω_k is the *kth* hopping frequency and θ_k is the random phase generated by the frequency synthesizer in the *kth* interval. It is assumed that the hopping rate is equal to information symbol rate, so that the hopping frequency ω_k changes every $2T$ seconds. Thus, in a given-symbol interval, the signal frequency is constant and the jammer, if transmitting a tone at that frequency, affects the entire symbol interval. The pulse shape is defined as

$$P(t) = \begin{cases} 1 & 0 \le t \le 2T \\ 0 & \textit{elsewhere} \end{cases} \tag{2.2}$$

The signal component after propagating through the signal channel is given by

$$v(t) = s(t) + s_F(t) \tag{2.3}$$

where $s(t)$ is the specular component and $s_F(t)$ is the faded component

$$s_F(t) = \sqrt{S}\,\gamma_s\ \mathrm{Re}\Big\{ \sum_k \int_{-\infty}^{\infty} \beta_s(\tau) \Big[d_I(t-\tau) + j d_Q(t-\tau) \Big] \cdot P(t-2kT-\tau)\, d\tau \cdot \exp\, j\,[(\omega_o+\omega_k)t+\theta_k] \Big\} \tag{2.4}$$

and at the output of the jammer channel the specular and faded component of the jammer signal is

$$\bar{J}(t) = \lambda\ \mathrm{Re}\Big\{ \Big[\sqrt{2J} + \gamma_J \sqrt{2J} \int_{-\infty}^{\infty} \beta_J(\tau)\, d\tau \Big] \cdot \exp\, j\,[(\omega_o+\omega_k)t+\phi_k] \Big\} \tag{2.5}$$

where J is the power per tone, $\beta_J(\tau)$ is the low-pass impulse response and has the same statistical properties as $\beta_s(\tau)$ and ϕ_k is random phase uniformly distributed

in $[0, 2\pi]$.

Then the received signal $r(t)$ is given by

$$r(t) = s(t) + s_F(t) + \bar{J}(t) + \bar{J}_F(t) + n(t) \tag{2.6}$$

where $n(t)$ is the additive white Gaussian noise of two sided spectral density $\eta_0/2$.

Assuming that a coherent frequency synthesizer is available at the receiver. That is it is capable of estimating and correcting for the phase errors caused by the transmitter synthesizer, the channel and the receiver synthesizer. Then at the receiver, $r(t)$ is first dehopped by the dehopper to give

$$\begin{aligned} r_d(t) = {} & \sqrt{S}\left[d_I(t)\cos(\omega_o t) + d_Q(t)\sin(\omega_o t)\right] \\ & + \sqrt{S}\,\mathrm{Re}\left\{\sum_k \int_{-\infty}^{\infty} \beta_s(\tau)\left[d_I(t-\tau) + j d_Q(t-\tau)\right]\right. \\ & \left. P(t-2kT-\tau)\,\delta\omega_o\omega_k \; d\tau \cdot \exp\, j\,\omega_o t\right\} \\ & + \mathrm{Re}\left\{\sum_k P(t-2kT)\,\delta\omega_o\omega_k\left[\sqrt{2J} + \gamma_J\sqrt{2J}\int_{-\infty}^{\infty}\beta_J(\tau)d\tau\right]\right. \\ & \left. \cdot \exp\, j\,[(\omega_o+\omega_k)t + \phi_k]\right\} \\ & + N_c(t) \end{aligned} \tag{2.7}$$

In the above equation $\delta\omega_o\omega_k$ represents the action of the dehopper on the signal and the jammer. It equals one if the frequency at the *kth* hop equals what it was on the zeroth hop, otherwise it is equal to zero.

After that the dehopped signal $r_d(t)$ is multiplied by the in-phase and quadrature reference signals followed by integrate and dump filters of duration equal to

the information symbol interval $2T$ to produce the in-phase and quadrature decision variables.

$$Z_I = \sqrt{S}\,T\; d_{I_0} + 2\sqrt{J}\,T\,\cos\phi$$
$$+ \int_0^{2T} \mathrm{Re}\left\{ \left[\sum_k P(t-2kT)\delta\omega_o\omega_k\,\gamma_J\sqrt{2J}\int_{-\infty}^{\infty}\beta_J(\tau)d\tau \right] \exp\, j(\omega_o t+\phi) \right\}$$
$$+ \sqrt{S}\,\mathrm{Re}\left\{ \sum_k \int_{-\infty}^{\infty} \beta_s(\tau)\left[d_I(t-\tau) + j\, d_Q(t-\tau) \right] \right.$$
$$\left. \cdot\, P(t-2kT-\tau)\delta\omega_o\omega_k\, d\tau \cdot \exp\, j\omega_o t \right\}$$
$$+ N_I \qquad (2.8)$$

$$Z_Q = \sqrt{S}\,T\, d_{Q_0} + 2\sqrt{J}\,T\,\sin\phi$$
$$+ \int_0^{2T} \mathrm{Re}\left\{ \left[\sum_k P(t-2kT)\delta\omega_o\omega_k\,\gamma_J\sqrt{2J}\int_{-\infty}^{\infty}\beta_J(\tau)d\tau \right] \exp\, j(\omega_o t+\phi) \right\}$$
$$+ \sqrt{S}\,\mathrm{Re}\left\{ \sum_k \int_{-\infty}^{\infty} \beta_s(\tau)\left[d_I(t-\tau) + j\, d_Q(t-\tau) \right] \right.$$
$$\left. \cdot\, P(t-2kT-\tau)\delta\omega_o\omega_k\, d\tau \cdot \exp\, j\omega_o t \right\}$$
$$+ N_Q \qquad (2.9)$$

where

$$N_I = \int_0^{2T} N_c(t)\, dt \qquad (2.10)$$

$$N_Q = -\int_0^{2T} N_s(t)\, dt \qquad (2.11)$$

are zero mean Gaussian random variables with variance $N_o\, T$.

The receiver estimate of the d_I and d_Q are obtained by passing Z_I and Z_Q through hard limiters giving

$$\hat{a} = sgn\ Z_I; \qquad \hat{b} = sgn\ Z_Q \tag{2.12}$$

Hence the conditional probability of bit error derived in Appendix A is given by (Restricting intersymbol interference to only the adjacent symbols and so the dependence is only on ω_{-1}, ω_1 frequencies of these symbols)

$$P_b(e \mid \phi,\lambda_J,d_{Q_{-1}},d_{Q_0},d_{Q_1},d_{I_{-1}},d_{I_1},\omega_{-1},\omega_1) = Q\left(\frac{1+\sqrt{N_J/\rho E_b}\cos\phi}{\left[\frac{N_o}{2E_b}+\frac{\gamma_s^2}{2}I_{s_1}+\frac{\gamma_J^2}{4}\frac{N_J}{\rho E_b}I_{J_1}\right]^{1/2}}\right) \tag{2.13}$$

Averaging over all possible combinations of data bits

$$P_b(e \mid \phi,\lambda_J,\omega_{-1},\omega_1) = \frac{1}{32}\sum_{i=1}^{32} P_b(e \mid \phi,\lambda_J,d_{Q_{-1}},d_{Q_0},d_{Q_1},d_{I_{-1}},d_{I_1},\omega_{-1},\omega_1) \tag{2.14}$$

where the values of $d_{Q_{-1}}$, d_{Q_0}, d_{Q_1}, $d_{I_{-1}}$, d_{I_1} take all possible 32 combinations i.e. {(1,1,1,1,1), (1,1,1,1,-1), (1,1,1,-1,1) ..., etc }. Averaging over λ_J, ϕ yields

$$P_b(e \mid \omega_{-1},\omega_1) = \frac{M}{N}\frac{1}{2\pi}\int_0^{2\pi} P(e \mid \lambda_J=1,\phi,\omega_{-1},\omega_1)\,d\phi + \left(1-\frac{M}{N}\right)P(e \mid \lambda_J=0,\omega_{-1},\omega_1) \tag{2.15}$$

where $\frac{M}{N}$ is the probability of M frequencies jammed out of N and $1-\frac{M}{N}$ is probability of unjammed channels. Finally, for the four possible cases of intersymbol interference $\delta\omega_o\omega_k$ assumed (i.e. conditions of ω_{-1}, ω_1 compared to ω_o).

$$P_b = \frac{1}{N^2}P(e \mid \omega_{-1}=\omega_o,\omega_1=\omega_o) + \frac{N-1}{N^2}P(e \mid \omega_{-1}=\omega_o,\omega_1\neq\omega_o)$$

$$+\frac{N-1}{N^2}P(e\mid \omega_{-1}\neq\omega_o,\omega_1=\omega_o)+\left(\frac{N-1}{N}\right)^2 P(e\mid \omega_{-1}\neq\omega_o,\omega_1\neq\omega_o) \tag{2.16}$$

where $\frac{1}{N}$ is the probability that the frequency equals that frequency on the ω_o hop and $1-\frac{1}{N}$ is the probability that the frequency does not equal to the frequency on the zeroth hop.

In order to improve the performance of the FH/QPSK system in the presence of a jammer, it useful to employ error-correction coding. The information rate and spread bandwidth is kept constant, therefore making the number of slots available for hopping decrease by the information rate of the code [9] (for fair comparison to prevail). For example, if the uncoded FH/QPR system uses N slots, the (23,12) Golay encoded system will then have $\frac{12}{23}N$ slots to hop with. For Golay Code the probability of bit error in the decoded sequence can be shown to be given approximately by [9],

$$P \approx \frac{1}{n}\sum_{i=e+1}^{n} i\binom{n}{i} P_b{}^i (1-P_b)^{n-i} \tag{2.17}$$

where P_b is given by (2.16) except that E_b/N_o is decreased by the rate of the code. That is the energy-per-symbol of the coded system is 12/23 of the energy-per-symbol of the uncoded system. Also $n=23$ is code length of the Golay code and $e=3$ is the number of correctable errors.

2.3 Numerical Results:

In this section the probability of bit error is evaluated for the uncoded and coded system and the results are plotted.

Figures 2.2-A to 2.2-C show the effect of varying M, the number of jammed slots on the probability of bit error for the uncoded (N=1917) and coded (N=1000) systems. We consider first the case of no fading ($\gamma_s = 0$, $\gamma_J = 0$) and

compare the curves of figures 2.2-A to 2.2-C for $E_b/N_J = 30, 15, 1\ dB$, respectively (keeping $E_b/N_o = 20\ dB$ fixed). One observes that for E_b/N_J equal to 15 dB there exists value of M equal to 70 and 40 and for E_b/N_J equal to 30 dB there exists a value of M equal to 40 and 20 for the uncoded and coded systems, respectively, which maximizes the probability of bit error. Similarly, for E_b/N_J equal to 1 dB (fig. 2.2-C) it is seen that there exists value of $M = 1110$ and $M = 580$ which maximizes the probability of error. Secondly in the case of fading, for the values $\gamma_s = \gamma_J = .2, .5$ the performance is seen to be more sensitive for $E_b/N_J = 15, 30\ dB$ (figures 2.2-A and 2.2-B) compared to the case of $E_b/N_J = 1\ dB$ (fig. 2.2-C). Although the performance of the coded system is superior to the uncoded system, the coded system is more sensitive to the increase in power of the scatter component than the uncoded system.

In figures 2.3-A to 2.3-F, we show the effect of varying E_b/N_o on the performance of P_b. For the set of figures 2.3-A to 2.3-C and 2.3-D to 2.3-F the value of E_b/N_J is fixed at 15 dB and 1 dB, respectively. Figures 2.3-A and 2.3-C show the performance for suboptimal values of $M = 1$, $M = 1000$ (coded) and $M = 1917$ (uncoded) (from the viewpoint of the jammer). It is observed that P_b decreases with increasing E_b/N_o flatting out at large values of E_b/N_o whereas in fig. 2.3-B (for worst case $M = 70$ uncoded and $M = 40$), the performance is worst. Worth noting too is the performance sensitivity to values of γ_s and γ_J for both cases of suboptimal and worst case M. It is seen that performance is less sensitive to γ_s, γ_J for worst case M than in the case of suboptimal values of $M = 1$, 1000 (coded), 1917 (uncoded). Similar conclusions are drawn from figures 2.3-D to 2.3-F, the worst case M being 580 jamming tones for the coded system and 1110 tones for the uncoded system.

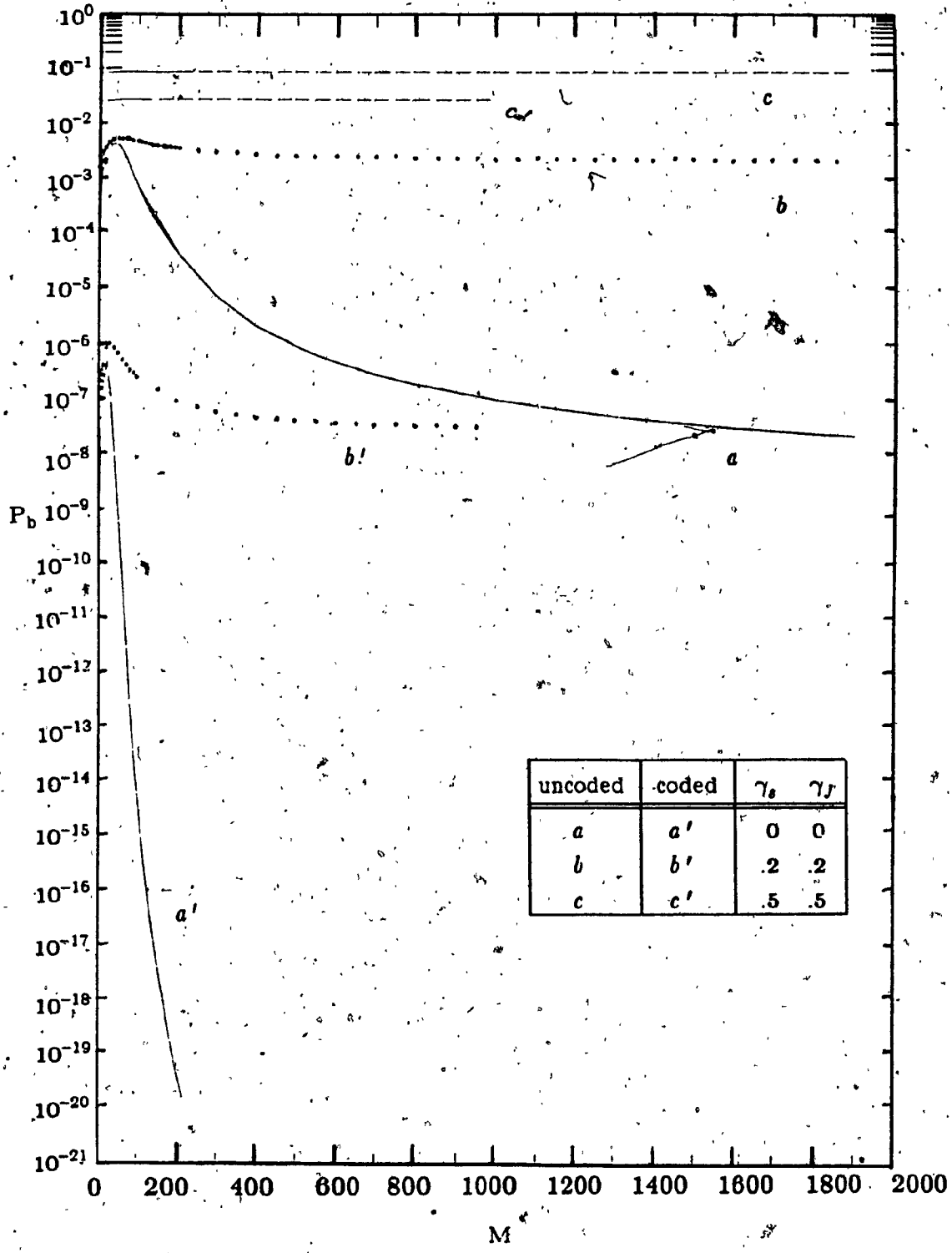

Fig. 2.2-A. P_b versus M for E_b/N_o = 20 dB and E_b/N_J = 30 dB.

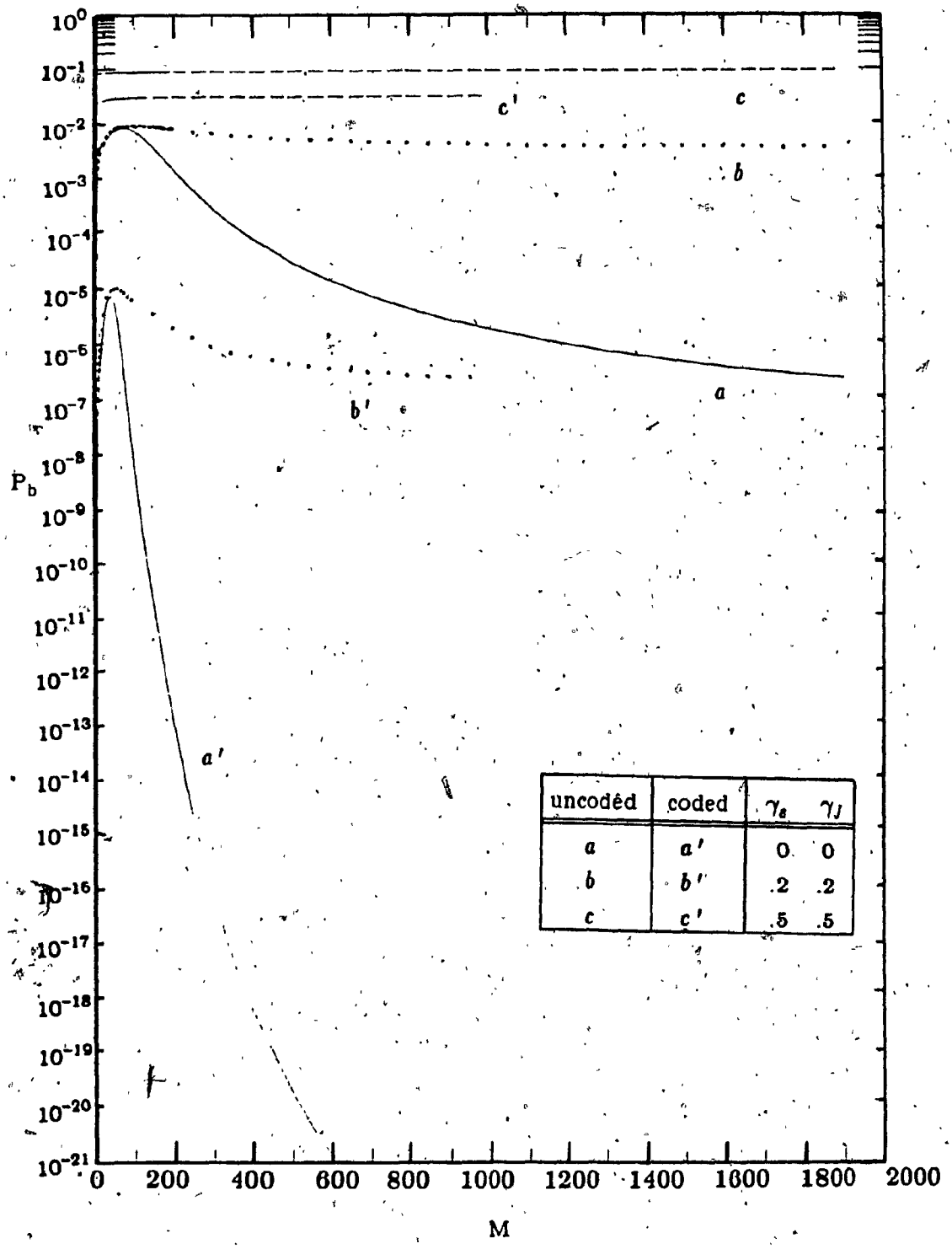

Fig. 2.2-B. P_b versus M for $E_b/N_o = 20$ dB and $E_b/N_J = 15$ dB.

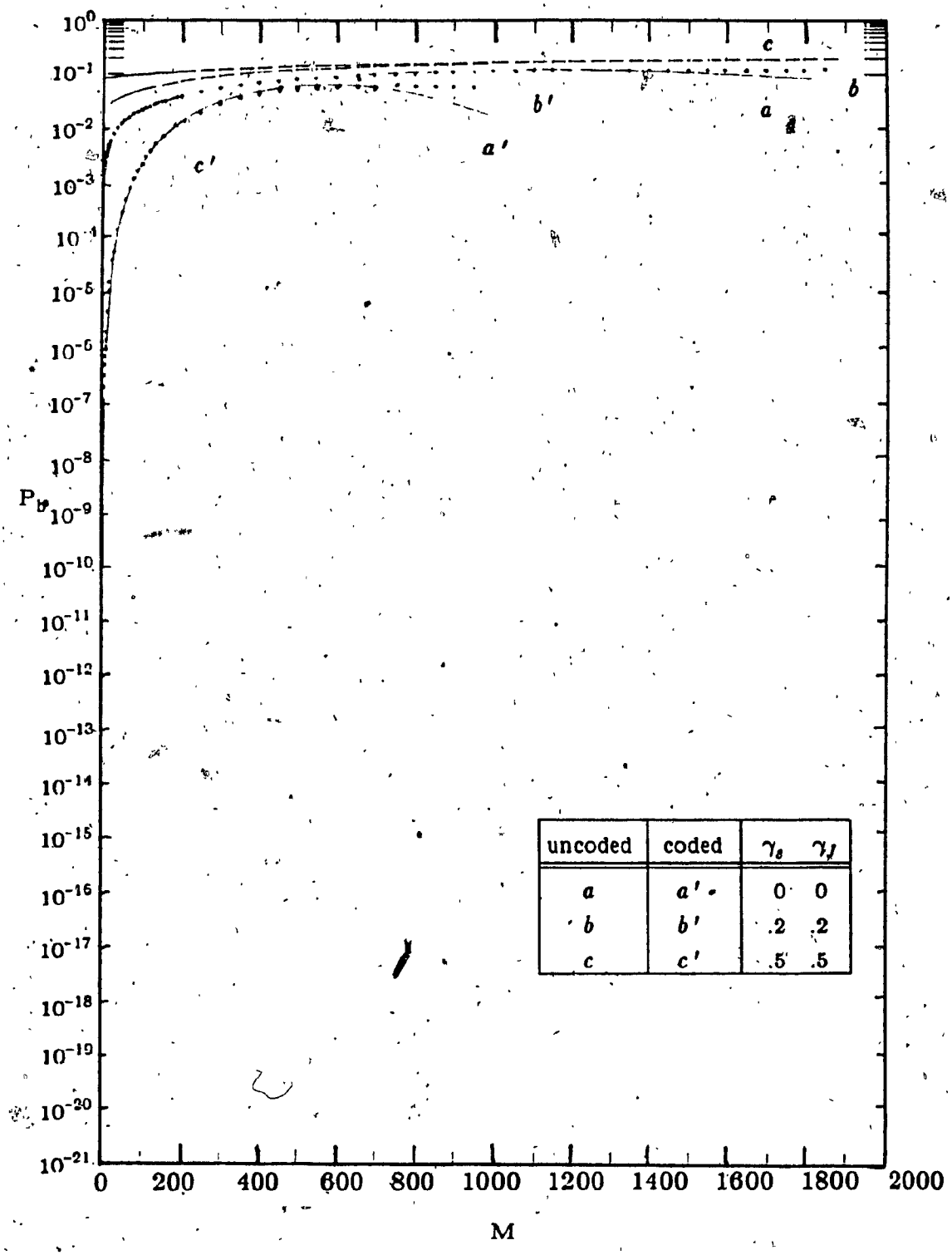

Fig. 2.2-C. P_b versus M for $E_b/N_o = 20$ dB and $E_b/N_J = 1$ dB.

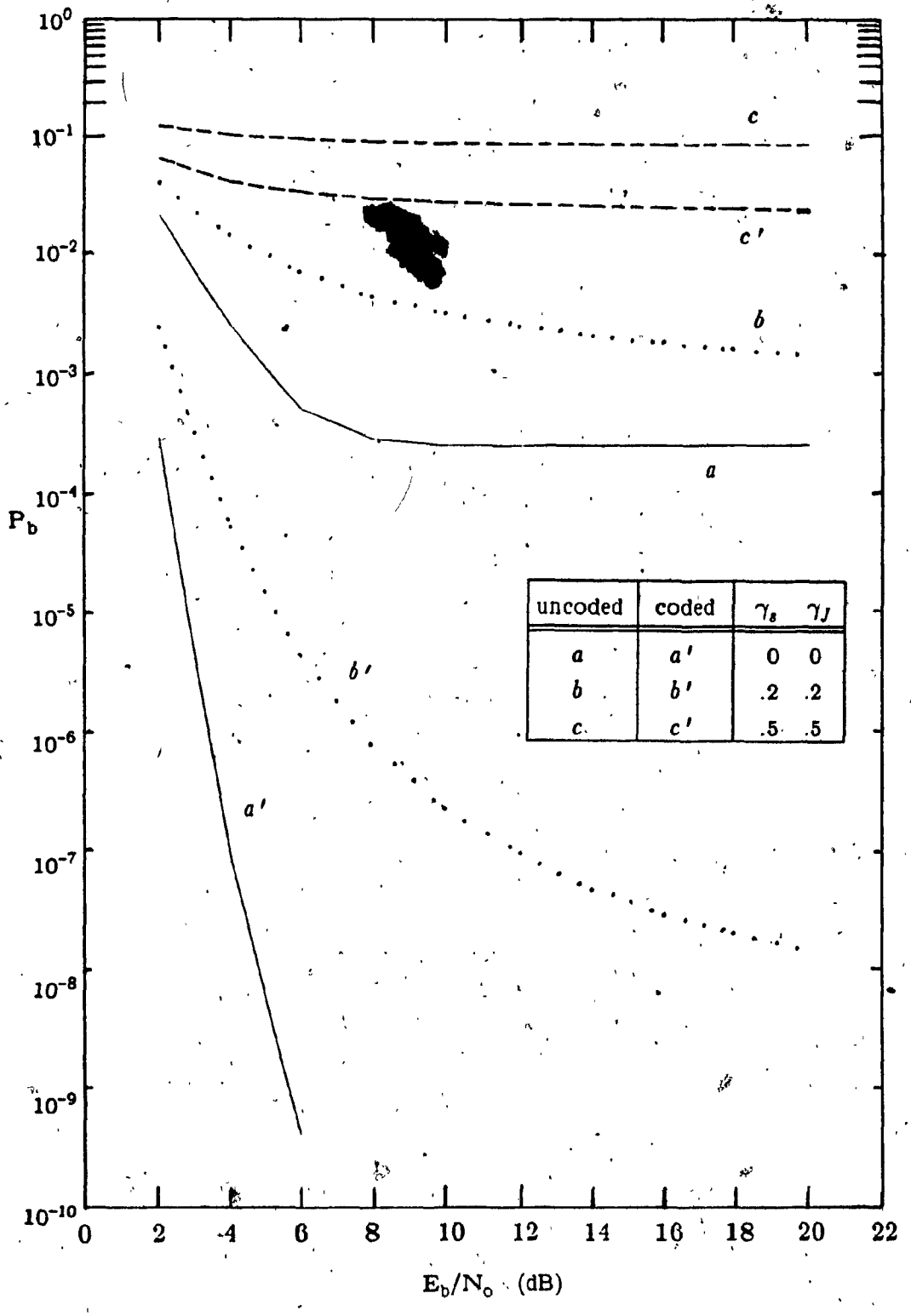

Fig. 2.3-A. P_b versus E_b/N_o for $E_b/N_J = 15$ dB and $M = 1$.

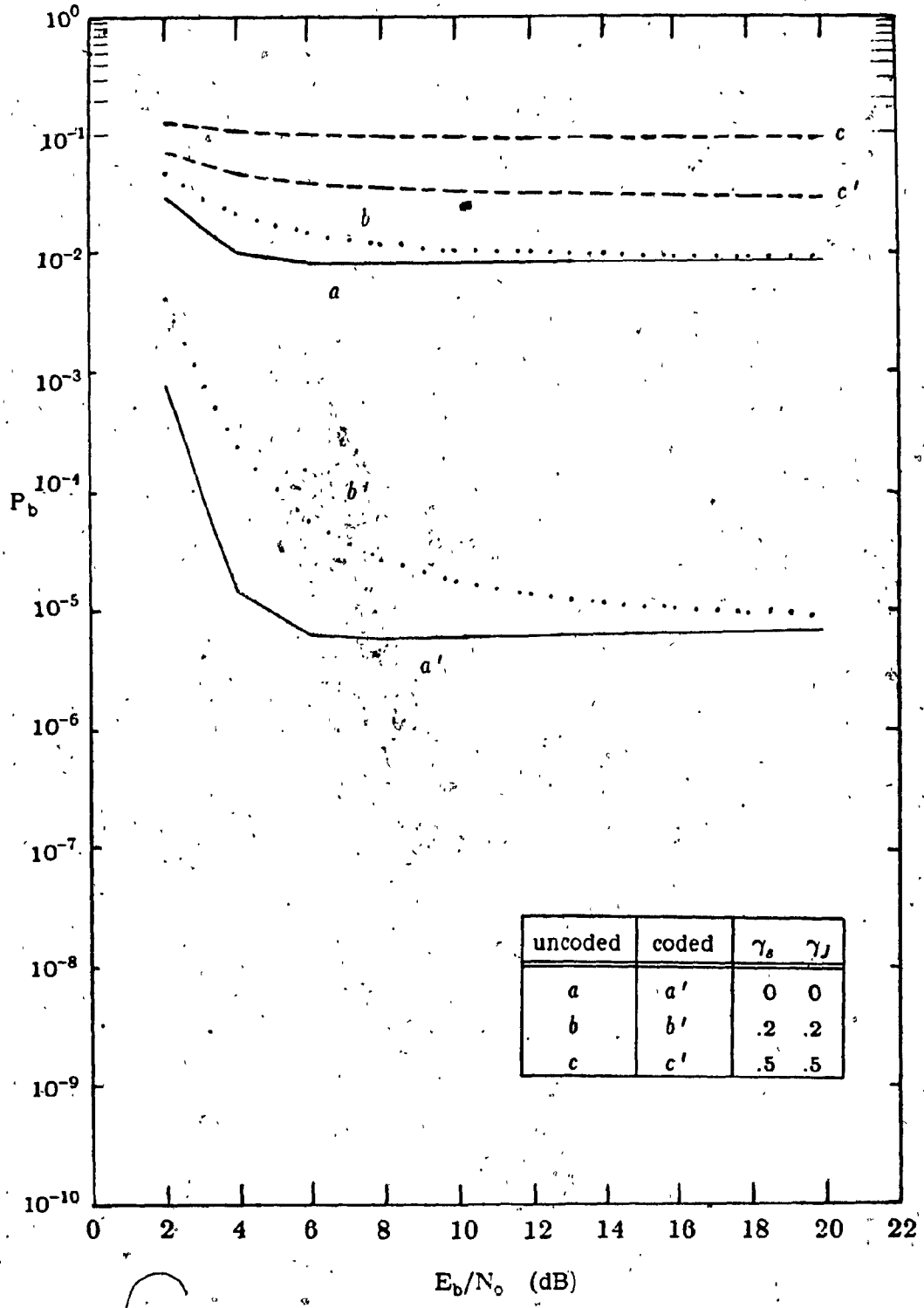

Fig. 2.3-B. P_b versus E_b/N_o for $E_b/N_J = 15$ dB and worst case M.

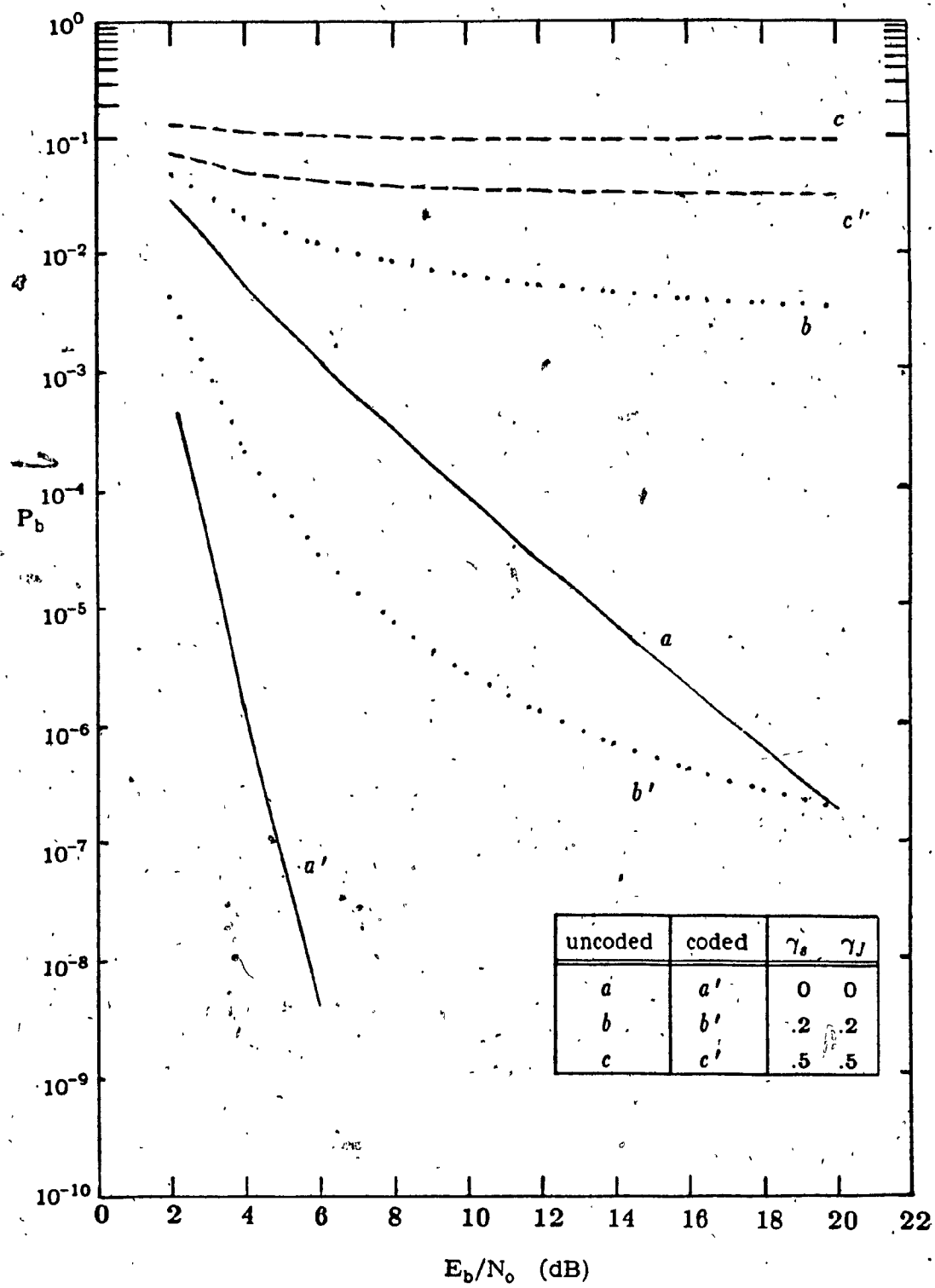

Fig. 2.3-C. P_b versus E_b/N_o for $E_b/N_J = 15$ dB and $M = 1000$ (coded), and $M = 1917$ (coded).

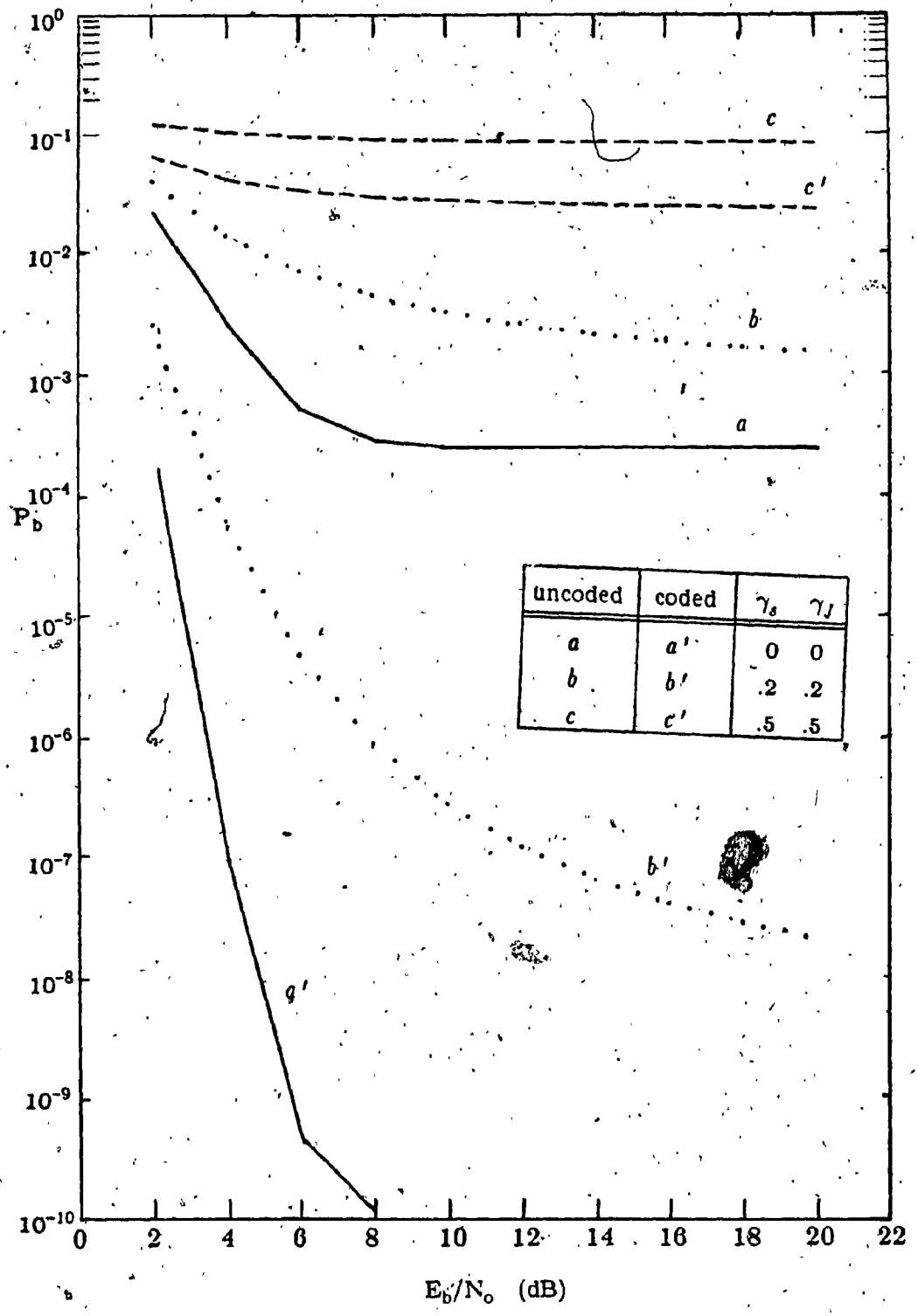

Fig. 2.3-D. P_b versus E_b/N_o for $E_b/N_J = 1$ dB and $M = 1$.

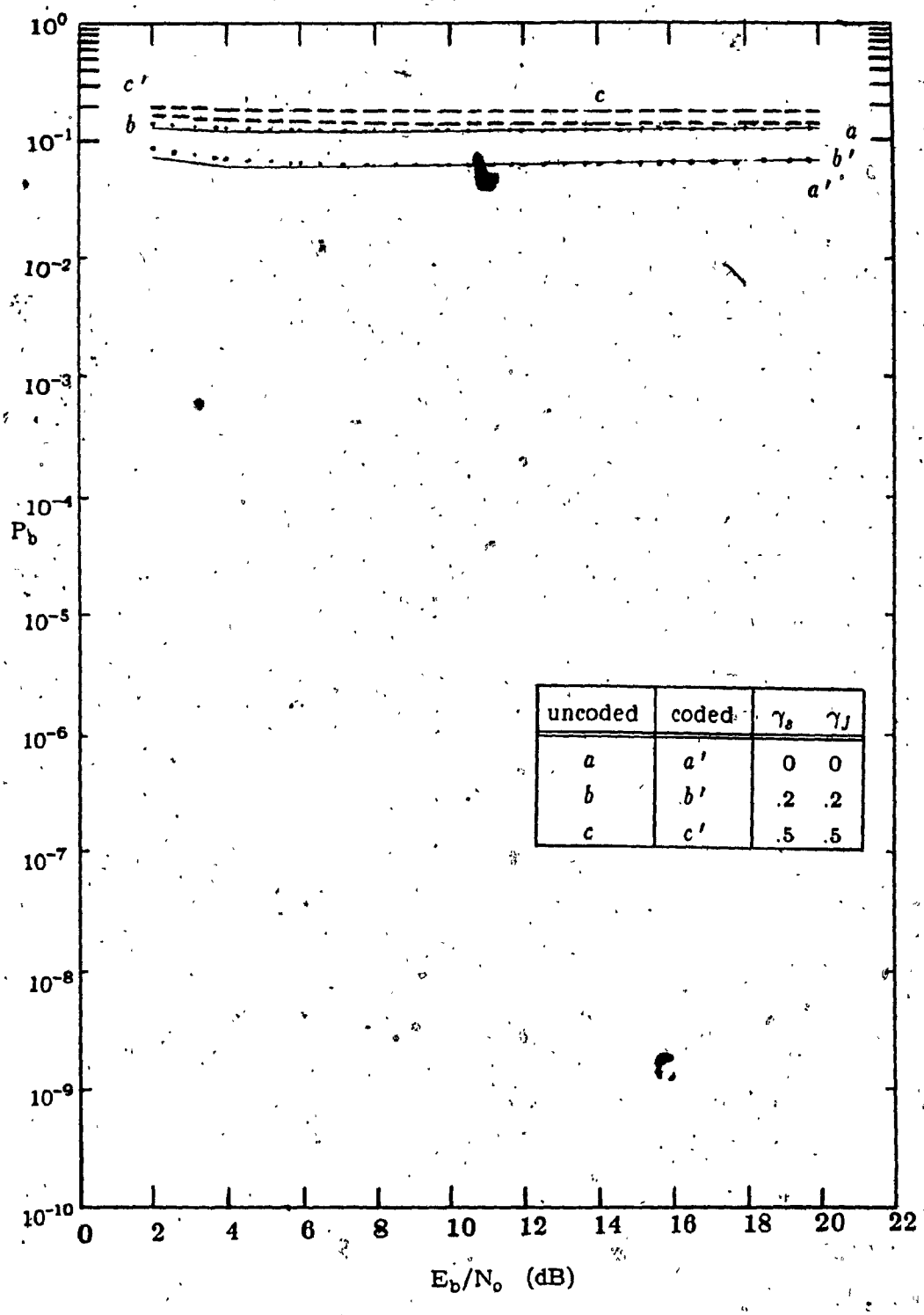

Fig. 2.3-E. P_b versus E_b/N_o for $E_b/N_J = 1$ dB and worst case M.

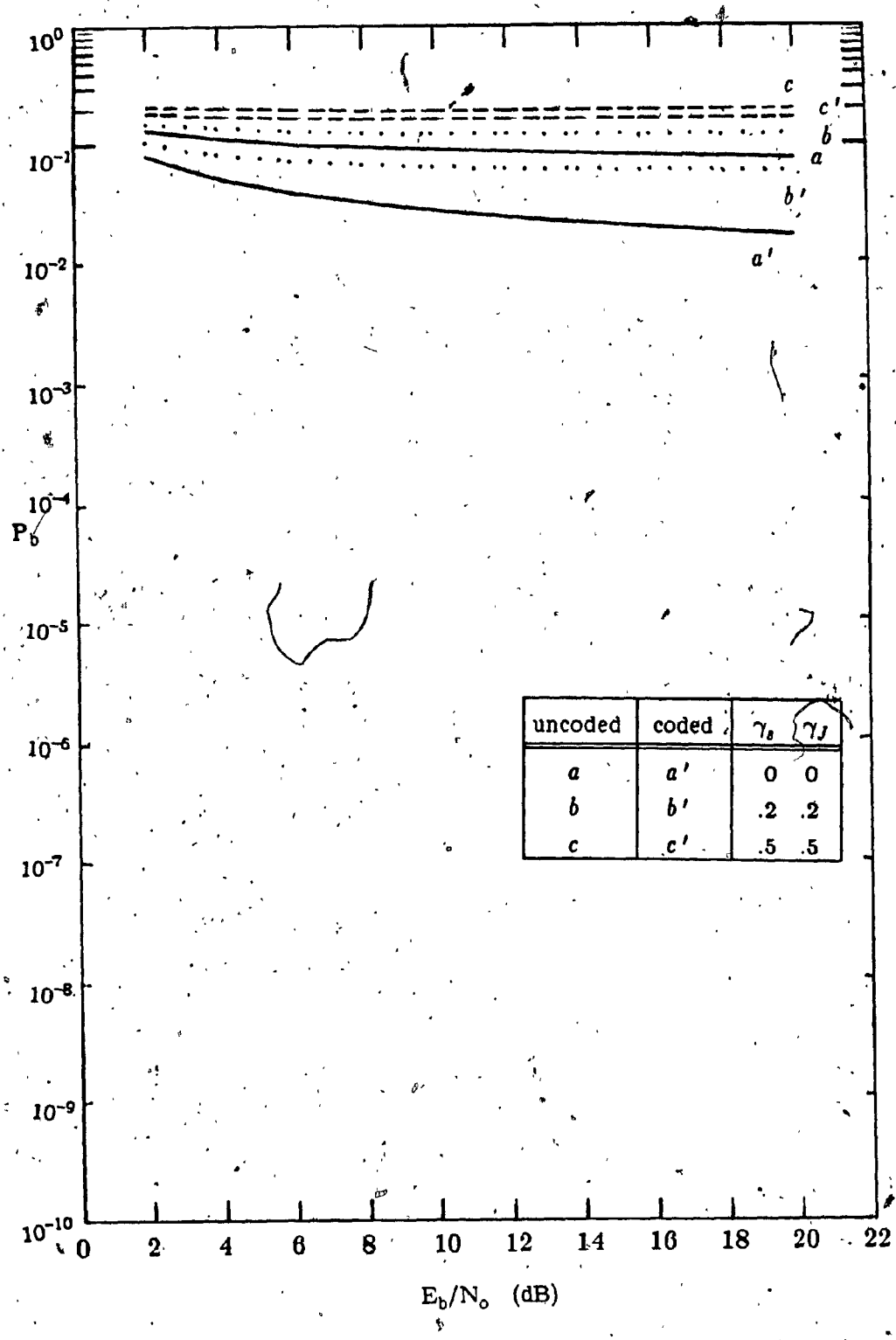

Fig. 2.3-F. P_b versus E_b/N_o for $E_b/N_J = 1$ dB and M = 1000 (coded), and M = 1917 (uncoded).

CHAPTER THREE

FH/MSK SYSTEM UNDER FREQUENCY SELECTIVE FADING CHANNEL AND PARTIAL BAND TONE JAMMING

3.1 Introduction:

In this chapter, the performance of frequency-hopping minimum-shift-keying (FH/MSK) system is presented operating over a frequency-selective channel and partial band tone jamming.

In the analysis of FH/MSK system, conventional type MSK transmitter and receiver structures are employed. Again the channel model which assumes wide-sense-stationary-uncorrelated-scattering (WSSUS) described in the introduction is used in the analysis.

In section three, the numerical results are obtained by evaluating the expressions for the probability of bit error derived in the analysis.

3.2 Analysis:

The system to be analyzed is shown in figure 3.1. The transmitted signal can be expressed as

$$s(t) = \sqrt{2}\,A \sum_{k} \left[d_I(t)\, I_k(t) \cos\frac{\pi t}{2T} \cos\left[(\omega_o + \omega_k)t + \theta_k\right] + d_Q(t)\, P(t-2kT) \sin\frac{\pi t}{2T} \sin\left[(\omega_o + \omega_k)t + \theta_k\right] \right] \qquad (3.1)$$

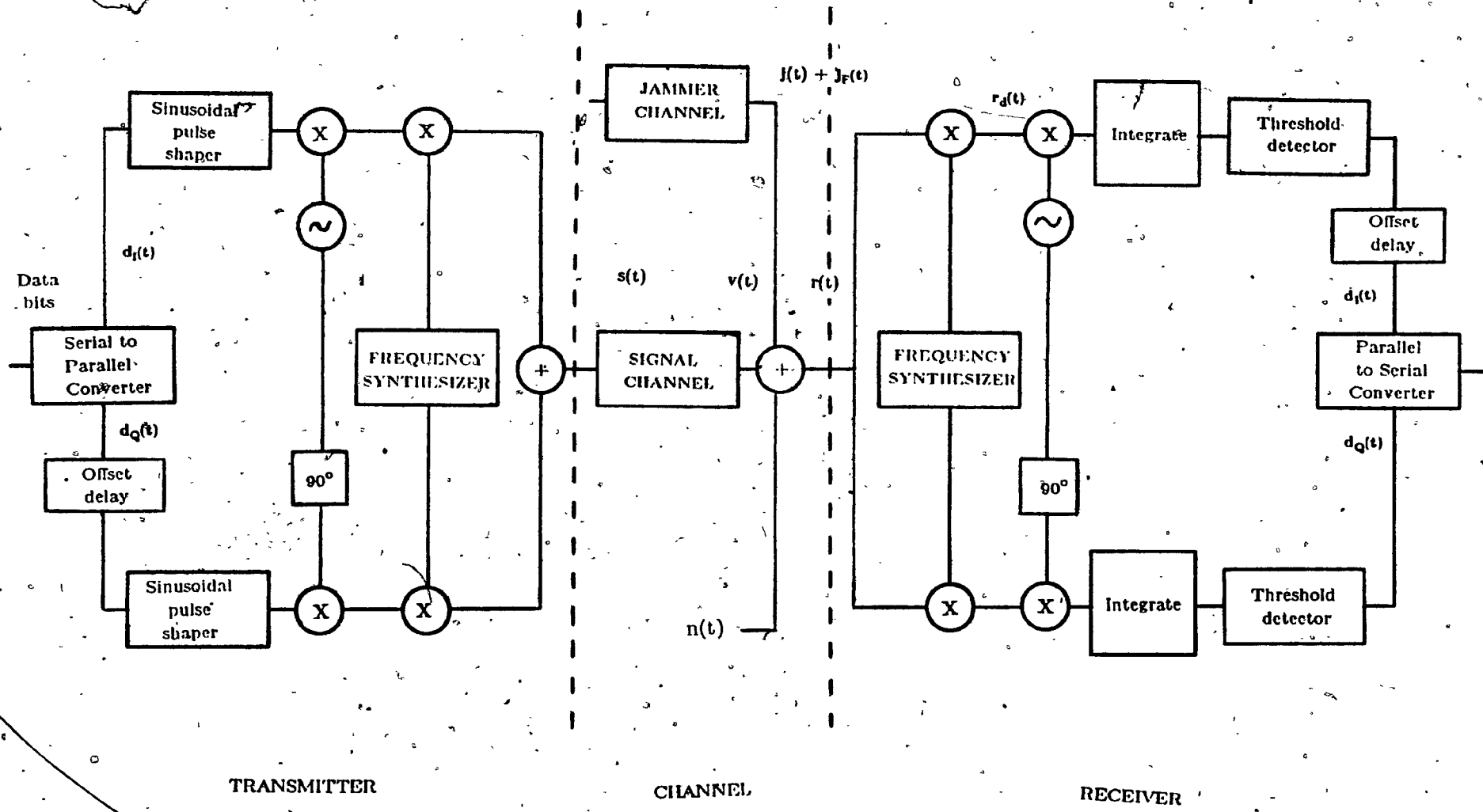

Figure 3.1. Block diagram of FH/MSK system.

where A is the amplitude of the transmitted signal, $d_I(t)$, $d_Q(t)$ are the in-phase and quadrature symbols taking on values ± 1, ω_k is the *kth* hopping frequency and θ_k is the random phase generated by the frequency synthesizer in the *kth* interval. Again it is assumed that the hopping rate is equal to information symbol rate, so that the hopping frequency ω_k changes every $2T$ seconds. Therefore, in a given symbol interval, the signal frequency is constant and the jammer, if transmitting a tone at that frequency, affects the entire symbol interval. The pulse shape is defined for the quadrature and in phase channel as

$$P(t) = \begin{cases} 1 & 0 \le t \le 2T \\ 0 & \textit{elsewhere} \end{cases} \qquad I(t) = \begin{cases} 1 & -T \le t \le T \\ 0 & \textit{elsewhere} \end{cases} \tag{3.2}$$

The signal component after propagating through the signal channel is given by

$$v(t) = s(t) + s_F(t) \tag{3.3}$$

where $s(t)$ is the specular component and $s_F(t)$ is the faded component

$$s_F(t) = \sqrt{2}A\,\gamma_s \operatorname{Re}\Bigg\{ \sum_k \int_{-\infty}^{\infty} \beta_s(\tau) \Bigg[d_I(t-\tau) I_k(t-\tau) \cos\frac{\pi(t-\tau)}{2T}$$

$$- j\, d_Q(t-\tau) P(t-2kT-\tau) \sin\frac{\pi(t-\tau)}{2T} \Bigg] d\tau$$

$$\exp j[(\omega_o+\omega_k)t+\theta_k] \Bigg\} \tag{3.4}$$

and at the output of the jammer channel the specular and faded component of the jammer signal is

$$\bar{J}(t) = \lambda_J \operatorname{Re}\Bigg[\Bigg\{ \sqrt{2J} + \gamma_J \sqrt{2J} \int_{-\infty}^{\infty} \beta_J(\tau) d\tau \Bigg\}$$

$$\cdot \exp j[(\omega_o+\omega_k)t+\phi_k] \Bigg] \tag{3.5}$$

where J is the power per tone, $\beta_J(\tau)$ is the low-pass impulse response and has the same statistical properties as $\beta_s(\tau)$ and ϕ_k is random phase uniformly distributed in $[0, 2\pi]$. Also it is assumed that the jammer distributes his power evenly in the in-phase and in the quadrature channel.

Then the received signal r(t) is given by

$$r(t) = s(t) + s_F(t) + \bar{J}(t) + \bar{J}_F(t) + n(t) \tag{3.6}$$

where $n(t)$ is the additive white Gaussian noise of two sided spectral density $\eta_0/2$.

Again assuming that a coherent frequency synthesizer is available at the receiver. That is it is capable of estimating and correcting for the phase errors caused by the transmitter synthesizer, the channel and the receiver synthesizer. Then at the receiver, $r(t)$ is first dehopped by the dehopper to give

$$\begin{aligned} r_d(t) = {} & \sqrt{2}\,A\; d_I(t) \cos\frac{\pi t}{2T} \cos\omega_0 t \\ & + \sqrt{2}\,A\; I(t)P(t)d_Q(t) \sin\frac{\pi t}{2T} \sin\omega_0 t \\ & + \sqrt{2}\,A\,\gamma_s \mathrm{Re}\left\{ \sum_k \int_{-\infty}^{\infty} \beta_s(\tau) \left[d_I(t-\tau) I_k(t-\tau) \cos\frac{\pi(t-\tau)}{2T} \right.\right. \\ & \left.\left. - j\, d_Q(t-\tau) P(t-2kT-\tau) \sin\frac{\pi(t-\tau)}{2T} \right] \delta\omega_0\,\omega_k\; d\tau \exp j\omega_0 t \right\} \\ & + \mathrm{Re}\left\{ \sum_k P(t-2kT)\,\delta\omega_0\,\omega_k \left[\lambda_J \sqrt{2J} + \lambda_J\,\gamma_J \sqrt{2J} \int_{-\infty}^{\infty} \beta_J(\tau) d\tau \right] \right. \\ & \left. \cdot \exp j(\omega_0 t + \phi) \right\} \\ & + N_c(t) \end{aligned} \tag{3.7}$$

In the above equation $\delta\omega_o\omega_k$ represents the action of the dehopper on the signal and the jammer. It equals one if the frequency at the *kth* hop equals what it was on the zeroth hop, otherwise it is equal to zero.

After that the dehopped signal $r_d(t)$ is multiplied by the in-phase and quadrature reference signals followed by integrate and dump filters of duration equal to the information symbol interval $2T$ to produce the in-phase and quadrature decision variables.

$$
\begin{aligned}
Z_I = {} & AT d_{I_0} + \frac{248\sqrt{JT}}{63\pi}\cos\phi \\
& + 2A\,\gamma_s \int_{-T}^{T} \mathrm{Re}\left\{ \sum_j \int_{-\infty}^{\infty} \beta_s(\tau) \left[d_I(t-\tau) I_j(t-\tau) \cos\frac{\pi}{2T}(t-\tau) \right.\right. \\
& \left.\left. - j\, d_Q(t-\tau) P(t-2jT-\tau) \sin\frac{\pi}{2T}(t-\tau) \right] \delta\omega_o\omega_j\, d\tau_1 \exp j\omega_o t \right\} \\
& \cdot \cos\frac{\pi}{2T} t \cos\omega_o t\, dt \\
& + 2\lambda\gamma_J \int_{I}^{T} \mathrm{Re}\left\{ \sum_j P(t-2jT)\,\delta\omega_o\omega_j \int_{J}^{\infty} \beta_J(\tau) \exp j(\omega_o t + \phi) \right\} \\
& \cdot \cos\frac{\pi t}{2T} \cos\omega_o t\, dt \\
& + N_I
\end{aligned}
\tag{3.8}
$$

The probability of error conditioned on ϕ, λ_J, ω_{-1}, ω_1, $d_{Q_{-1}}$, d_{Q_0}, d_{Q_1}, $d_{I_{-1}}$, d_{I_1} and assuming $d_{I_0} = 1$ is given by (from Appendix B)

$$
P(e \mid \phi, \lambda_J, \omega_{-1}, \omega_1, d_{Q_{-1}}, d_{Q_0}, d_{Q_1}, d_{I_{-1}}, d_{I_1}) = Q\left[\frac{AT + \frac{248\sqrt{JT}}{63\pi}\cos\phi}{\left[4N_o T + 2A^2\gamma_s^2 T^2 I_{s_1} + \frac{\lambda_J \gamma_J^2 J T^2}{\pi^2} I_{J_1} \right]^{1/2}} \right] \tag{3.9}
$$

Averaging over all possible combinations of data bits

$$P_b(e \mid \phi, \lambda_J, \omega_{-1}, \omega_1) = \frac{1}{32} \sum_{i=1}^{32} P_b(e \mid \phi, \lambda_J, d_{Q_{-1}}, d_{Q_0}, d_{Q_1}, d_{I_{-1}}, d_{I_1}, \omega_{-1}, \omega_1) \tag{3.10}$$

where the values of $d_{Q_{-1}}$, d_{Q_0}, d_{Q_1}, $d_{I_{-1}}$, d_{I_1} take all possible 32 combinations i.e. (1,1,1,1,1), (1,1,1,1,-1), (1,1,1,-1,1) ..., etc }. Averaging over λ_J, ϕ^* yields

$$P(e \mid \omega_{-1}, \omega_1) = \frac{M}{N} \frac{1}{2\pi} \int_0^{2\pi} P(e \mid \lambda_J = 1, \phi, \omega_{-1}, \omega_1)\, d\phi + \left(1 - \frac{M}{N}\right) P(e \mid \lambda_J = 0, \phi, \omega_{-1}, \omega_1) \tag{3.11}$$

Finally, for the four possible cases of intersymbol interference $\delta\omega_o\, \omega_k$ assumed (i.e. conditions of ω_{-1}, ω_1 compared to ω_o).

$$P_b = \frac{1}{N^2} P(e \mid w_{-1} = \omega_o, \omega_1 = \omega_o) + \frac{N-1}{N^2} P(e \mid w_{-1} = \omega_o, \omega_1 \neq \omega_o) + \frac{N-1}{N^2} P(e \mid w_{-1} \neq \omega_o, \omega_1 = \omega_o) + \left(\frac{N-1}{N}\right)^2 P(e \mid w_{-1} \neq \omega_o, \omega_1 \neq \omega_o) \tag{3.12}$$

In order to improve the performance of the FH/MSK system in the presence of a jammer, it useful to employ error-correction coding. The information rate and spread bandwidth is kept constant, therefore making the number of slots available for hopping decrease by the information rate of the code [9]. Employing (23,12) Golay code the probability of bit error in the decoded sequence can be shown to be given approximately by [9],

$$P \approx \frac{1}{n} \sum_{i=e+1}^{n} i \binom{n}{i} P_b^{\,i} (1 - P_b)^{n-i} \tag{3.13}$$

where P_b is given by (36) except that E_b/N_o is decreased by the rate of the code. That is the energy-per-symbol of the coded system is 12/23 of the energy-

per-symbol of the uncoded system.

3.3 Numerical Results:

In this section the probability of bit error is evaluated for the uncoded and coded system and the results are plotted.

Figures 3.2-A to 3.2-C show the effect of varying M, the number of jammed slots on the probability of bit error for the uncoded (N=1917) and coded (N=1000) systems. We consider first the case of no fading ($\gamma_s = 0$, $\gamma_J = 0$) and compare the curves of figures 3.2-A to 3.2-C for $E_b/N_j = 30, 15, 1\ dB$, respectively (keeping $E_b/N_o = 20\ dB$ fixed). One observes that for E_b/N_j equal to 15 dB there exists value of M equal to 60 and 30 and for E_b/N_j equal to 30 dB there exists a value of M equal to 30 and 20 for the uncoded and coded systems, respectively, which maximizes the probability of bit error. Similarly, for E_b/N_j equal to 1 dB (fig. 3.2-C) it is seen that there exists value of M equal to 870 and 460 for the uncoded and coded systems, respectively, which maximizes the probability of bit error. Secondly in the case of fading, for the values $\gamma_s = \gamma_J = .2, .5$ the performance is seen to be more sensitive for $E_b/N_j = 15, 30\ dB$ (figures 3.2-A and 3.2-B) compared to the case of $E_b/N_j = 1\ dB$ (fig. 3.2-C). Although the performance of the coded system is superior to the uncoded system, the coded system is more sensitive to the increase in power of the scatter component than the uncoded system.

In figures 3.3-A to 3.3-F, we show the effect of varying E_b/N_o on the performance of P_b. For the set of figures 3.3-A to 3.3-C and 3.3-D to 3.3-F the value of E_b/N_j is fixed at 15 dB and 1 dB, respectively. Figures 3.3-A and 3.3-C show the performance for suboptimal values of $M = 1$, $M = 1000$ (coded) and $M = 1917$ (uncoded) (from the viewpoint of the jammer). It is observed that P_b decreases with increasing E_b/N_o flatting out at large values of E_b/N_o, whereas

In fig. 3.3-B (for worst case $M = 60$), the performance is worst. Worth noting too is the performance sensitivity to values of γ_s and γ_I for both cases of suboptimal and worst case M. It is seen that performance is less sensitive to γ_s, γ_I for worst case M than in the case of suboptimal values of $M = 1$, 1000 (coded), 1917 (uncoded). Similar conclusions are drawn from figures 3.3-D to 3.3-F.

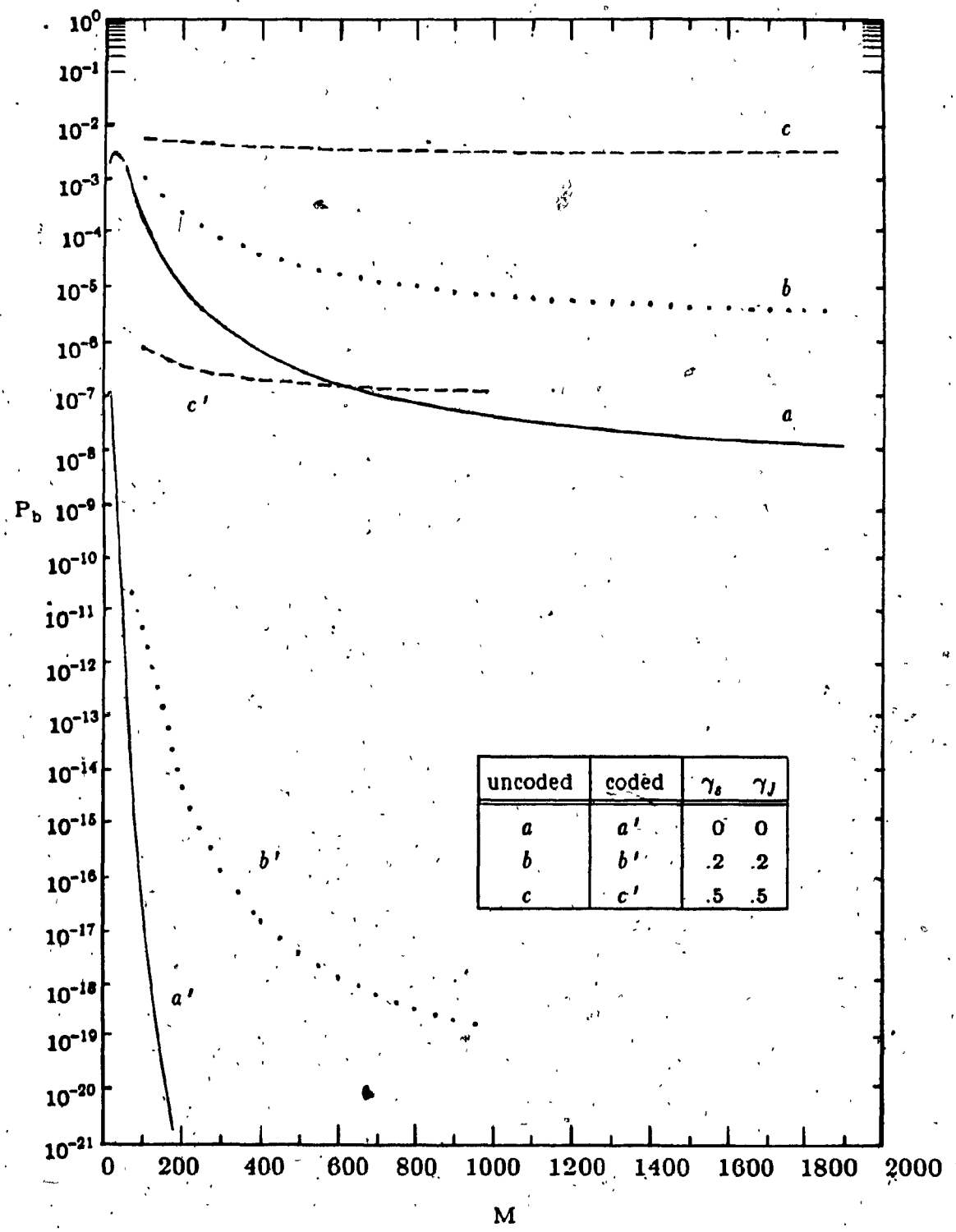

Fig. 3.2-A. P_b versus M for $E_b/N_o = 20$ dB and $E_b/N_J = 30$ dB.

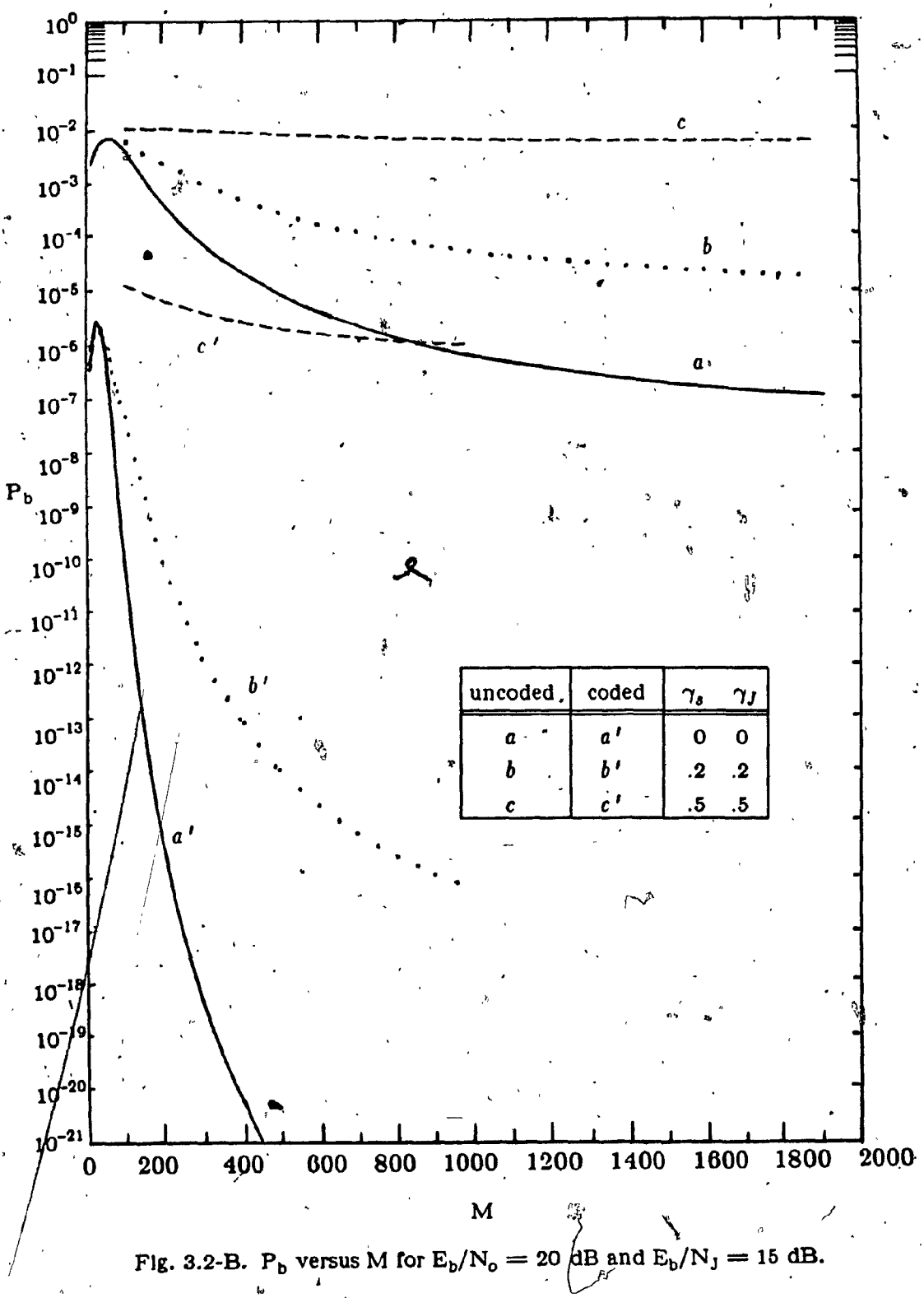

Fig. 3.2-B. P_b versus M for $E_b/N_o = 20$ dB and $E_b/N_J = 15$ dB.

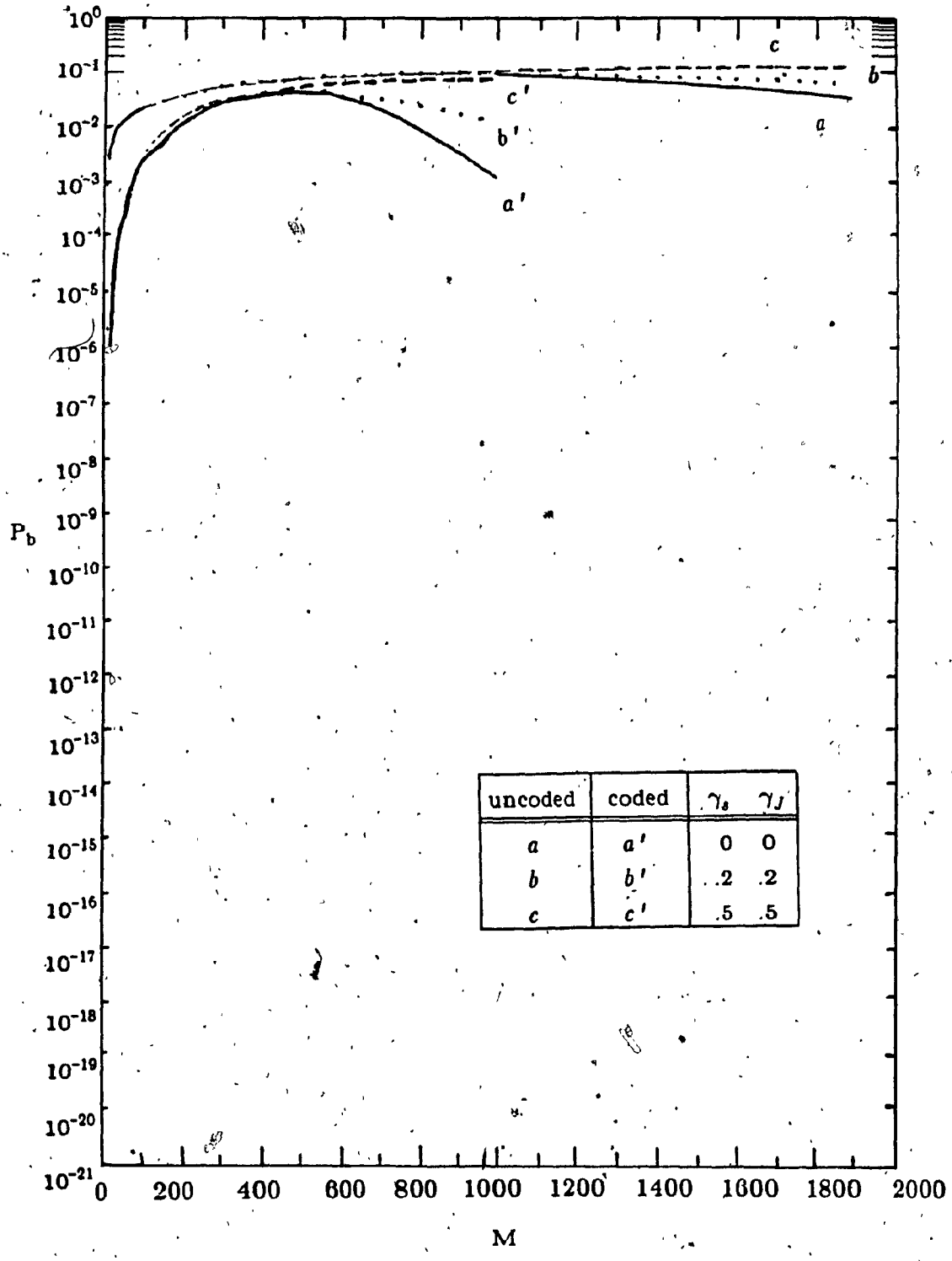

Fig. 3.2-C. P_b versus M for $E_b/N_o = 20$ dB and $E_b/N_J = 1$ dB.

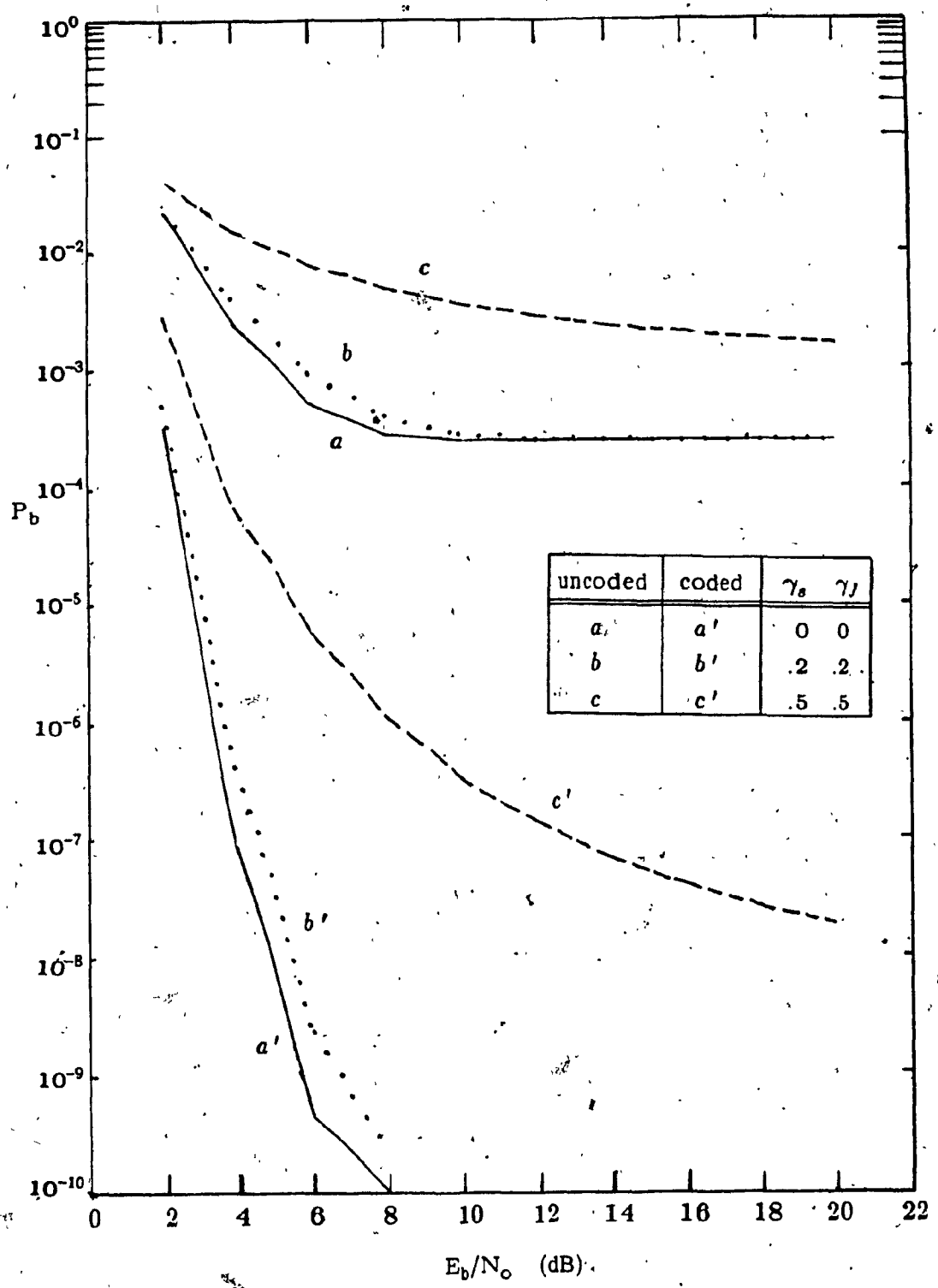

Fig. 3.3-A. P_b versus E_b/N_o for $E_b/N_J = 15$ dB and $M = 1$.

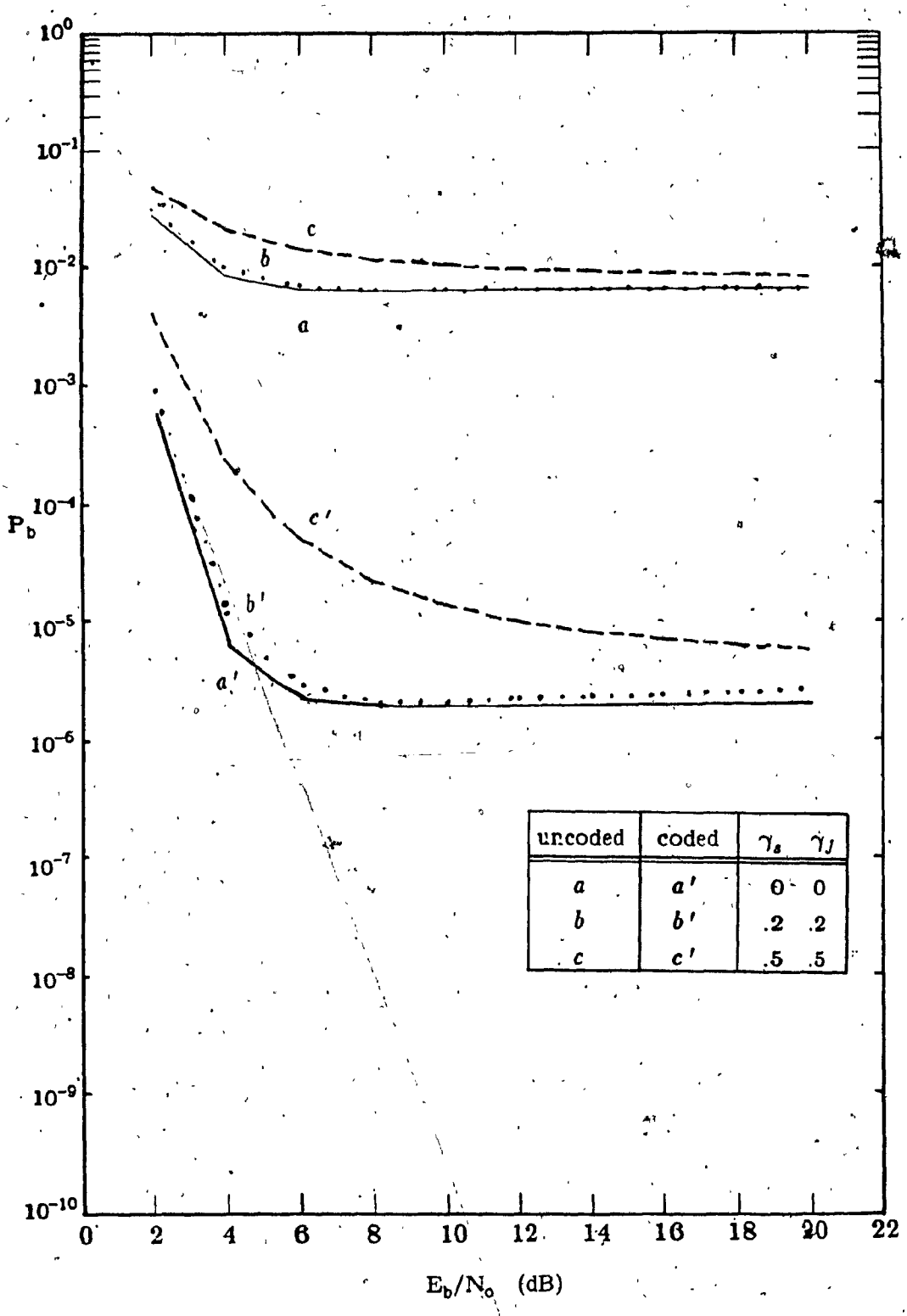

Fig. 3.3-B. P_b versus E_b/N_o for $E_b/N_J = 15$ dB and worst case M.

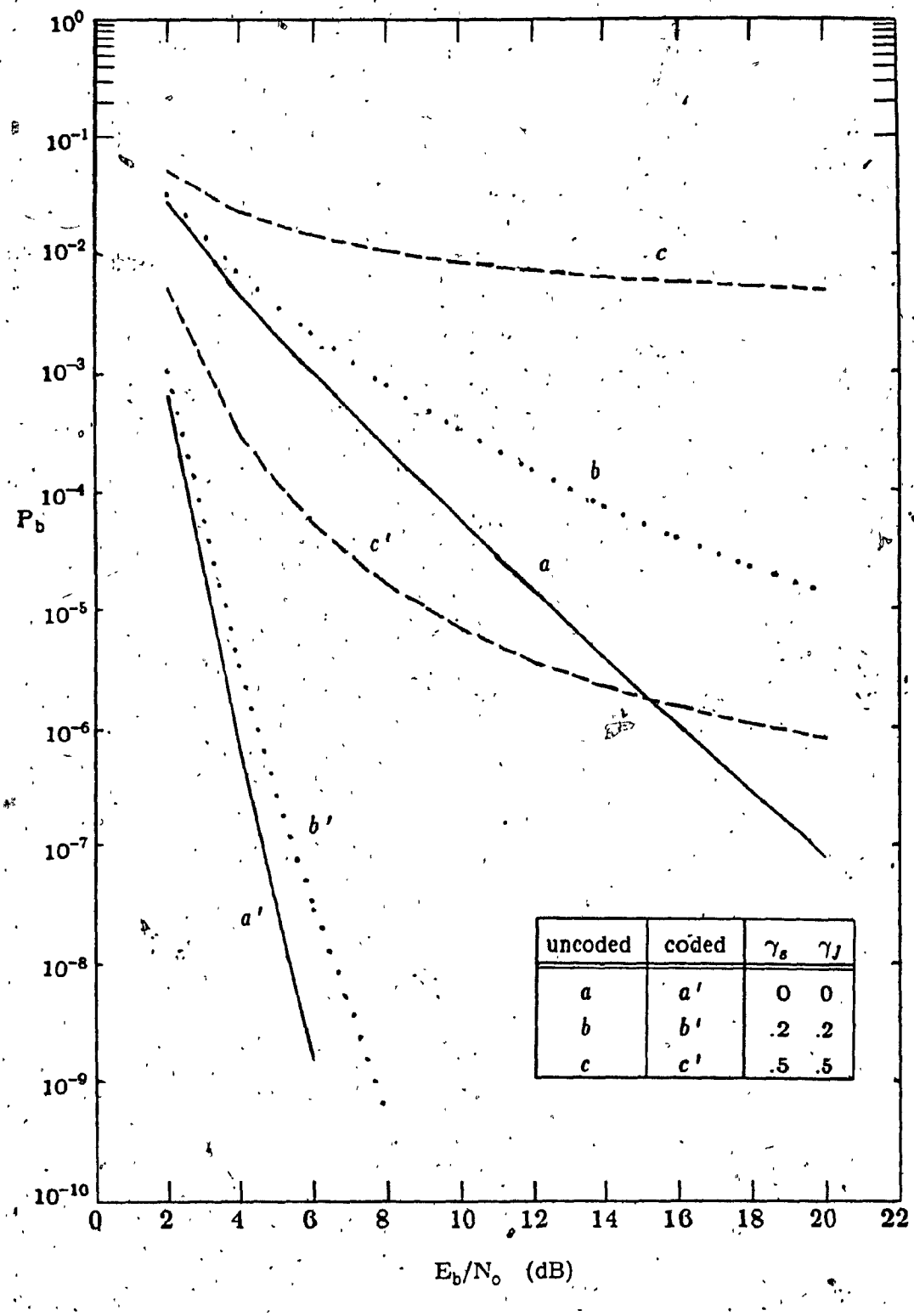

Fig. 3.3-C. P_b versus E_b/N_o for $E_b/N_j = 15$ dB and $M = 1000$ (coded), and $M = 1917$ (uncoded).

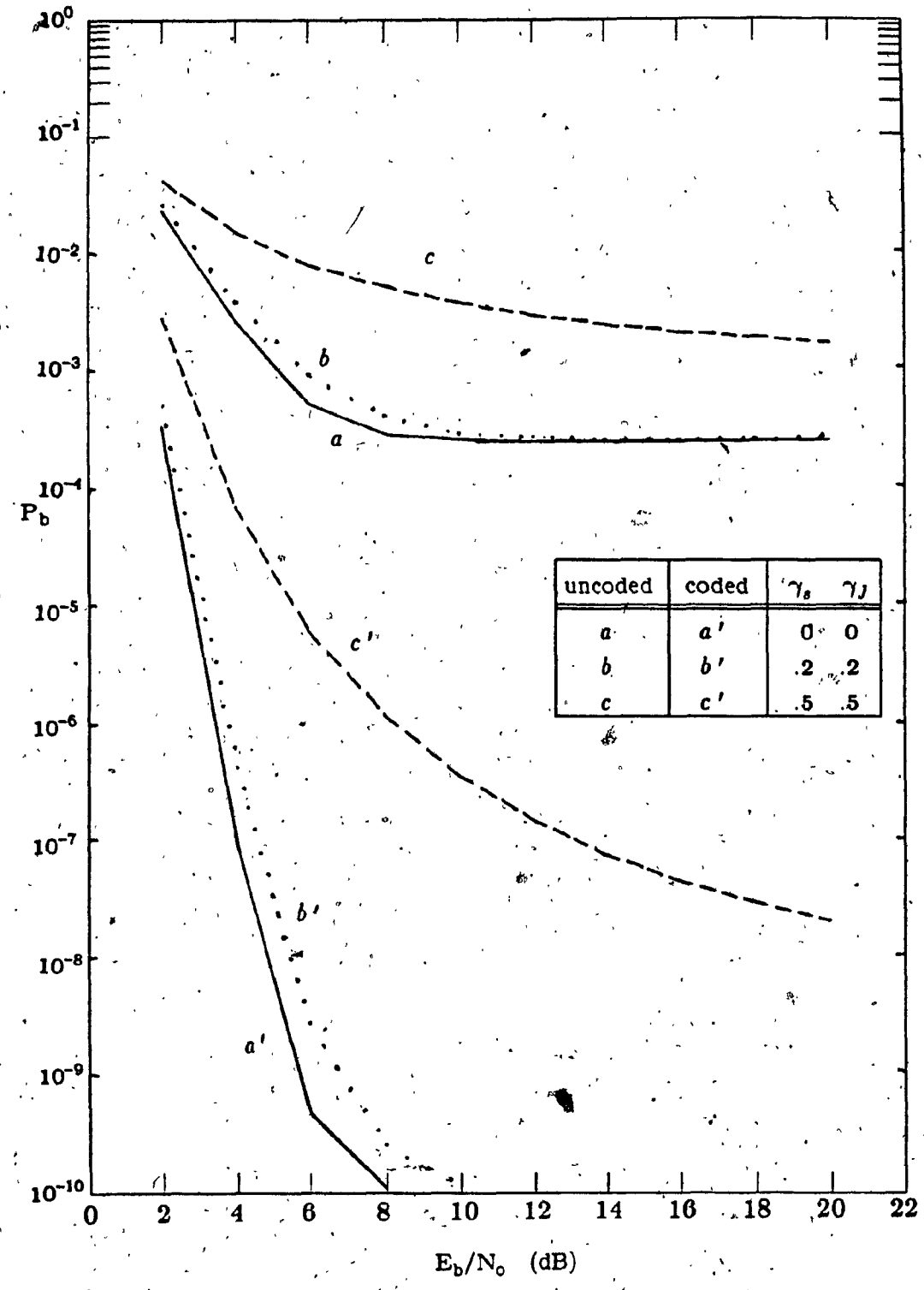

Fig. 8.3-D. P_b versus E_b/N_o for $E_b/N_J = 1$ dB and $M = 1$.

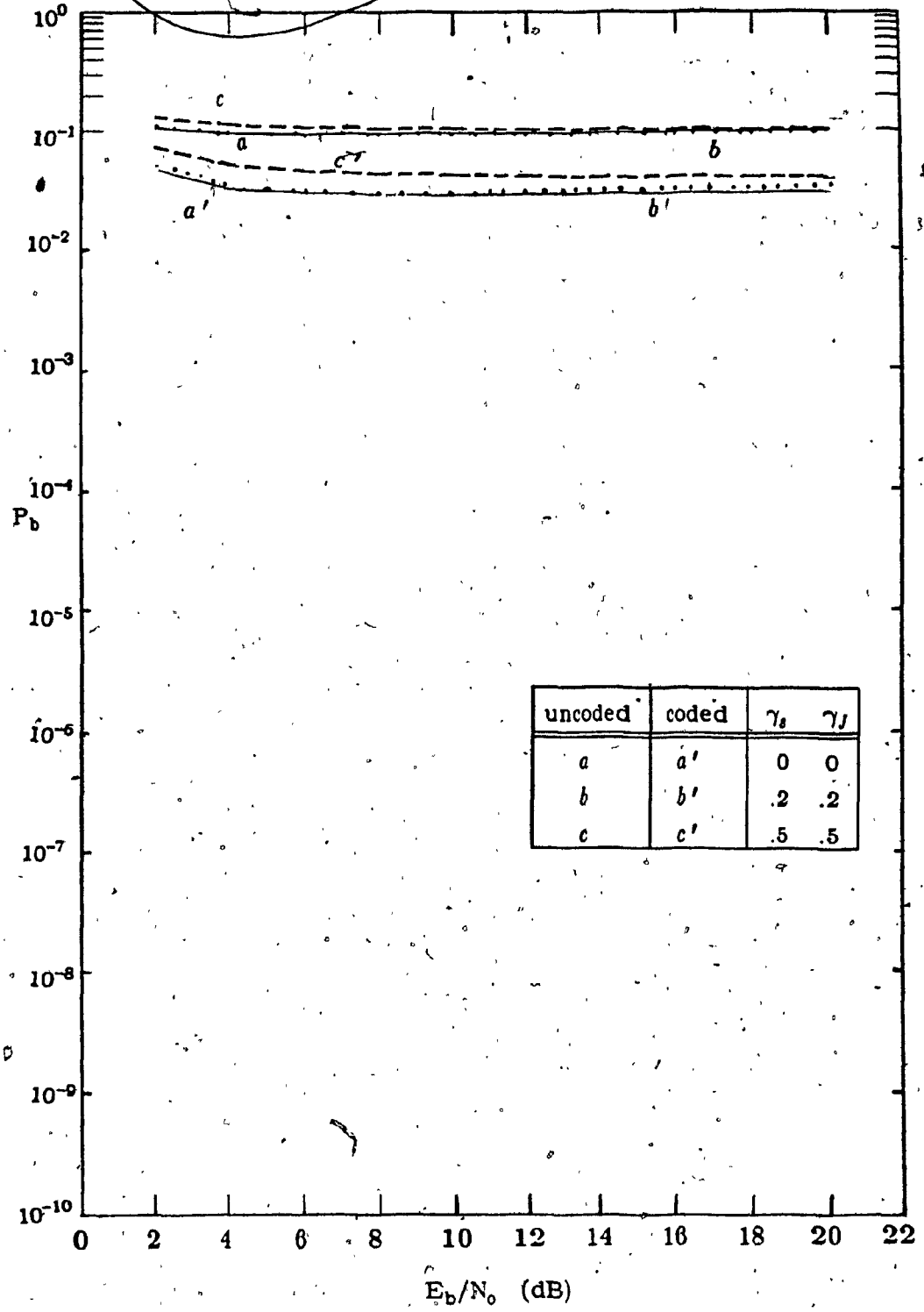

Fig. 3.3-E. P_b versus E_b/N_o for $E_b/N_j = 1$ dB and worst case M.

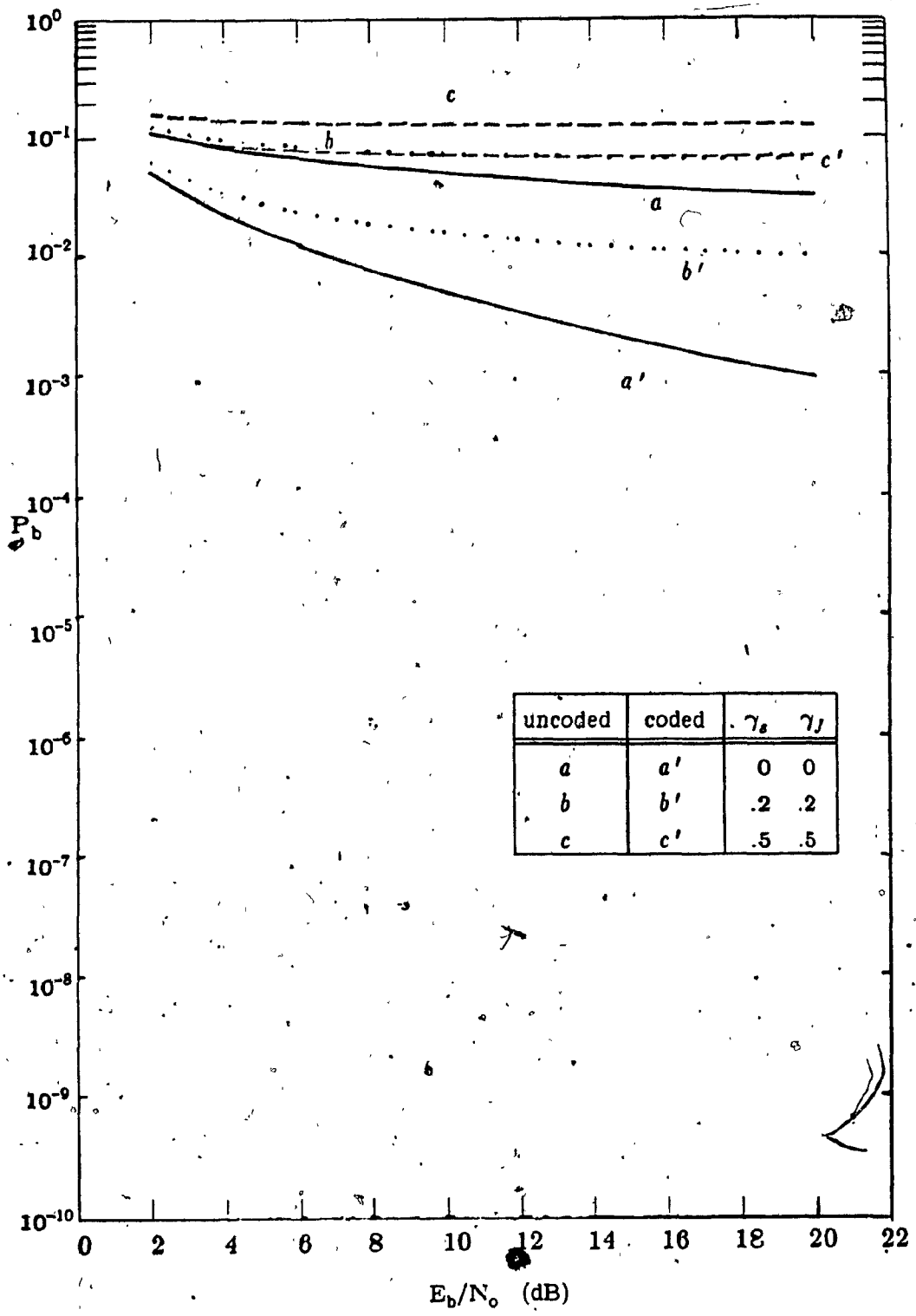

Fig. 3.3-F. P_b versus E_b/N_o for $E_b/N_J = 1$ dB and $M = 1000$ (coded), and $M = 1917$ (uncoded).

CHAPTER FOUR

FH/QPR SYSTEM UNDER FREQUENCY SELECTIVE FADING CHANNEL AND PARTIAL BAND TONE JAMMING

4.1 Introduction:

The performance of frequency-hopping quadrature partial response (FH/QPR) system is presented operating over a frequency-selective channel and partial band tone jamming.

In the analysis of FH/QPR system, conventional type QPR transmitter and receiver structures are employed. QPR is different from the two previous modulation techniques in the sense that this uses controlled intersymbol interference. QPR is essentially a conventional Class I scheme, also referred as a duobinary encoded QPSK in the literature [10],[15]. Because of coherent demodulation necessary at the receiver, the analysis is based on the assumption that a coherent frequency dehopper at the receiver is available. The channel model which assumes wide-sense-stationary-uncorrelated-scattering (WSSUS) described in the introduction is used in the analysis.

In section three, the numerical results are presented by evaluating the expressions for the probability of bit error derived in the analysis.

4.2 Analysis:

The system to be analyzed is shown in fig. 4.1. The modulator and demodulator are the same as those presented in [8]. However, with a frequency selective

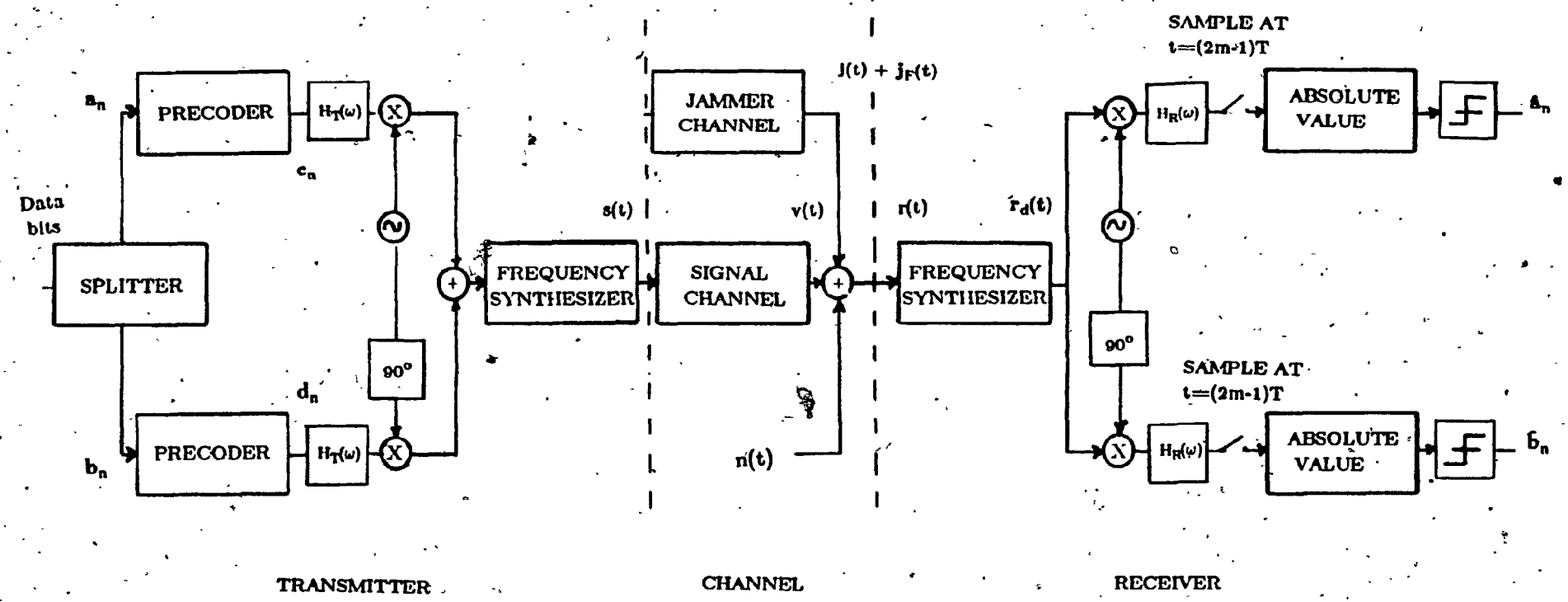

Figure 4.1. Block diagram of FH/QPR system.

fading and the narrowband tone jamming channel far from being an ideal channel we choose for analysis's convenience to concentrate the QPR pulse shaping filter at the transmitter. The transmitter and receiver filters are defined in the frequency domain as

$$H_T(\omega) = \begin{cases} 4T\cos\omega T & |\omega| < \pi/2T \\ 0 & otherwise \end{cases} \tag{4.1}$$

$$H_R(\omega) = \begin{cases} 1 & |\omega| < \pi/2T \\ 0 & otherwise \end{cases} \tag{4.2}$$

and in time domain as

$$h_T(t) = \frac{4}{\pi}\left[\frac{\cos(\pi t/2T)}{1 - t^2/T^2}\right] \tag{4.3}$$

$$h_R(t) = \frac{\sin(\pi t/2T)}{\pi t} \tag{4.4}$$

Here the receiver filter $H_R(\omega)$ merely bandlimits the noise.

The transmitted signal can be expressed as

$$s(t) = \sqrt{2}\,A \sum_k \left\{ \sum_{n=-\infty}^{\infty} c_n\, h_T[t-2nT]\cos[(\omega_k+\omega_o)t+\theta_k] + \sum_{n=-\infty}^{\infty} d_n\, h_T[t-2nT]\sin[(\omega_k+\omega_o)t+\theta_k] \right\} P(t-2kT) \tag{4.5}$$

where A is the signal amplitude, c_n, d_n are the precoded bits in quadrature and in phase channels taking on values ± 1, these are obtained by splitting the information bit array into odd and even arrays in a well known manner, $h_T(t)$ is the transmitter filter defined above, ω_o is the oscillator frequency, ω_k is the *kth* hopping frequency, and θ_k is the random phase generated by the frequency synthesizer in the *kth* interval

$$P(t) = \begin{cases} 1 & 0 \le t \le 2T \\ 0 & elsewhere \end{cases} \tag{4.6}$$

It is to be noted that the first summation with index k is one way of representing a FH signal, while the infinite summation represent the generation process of a QPR signal as is well known.

The received signal is given by

$$r(t) = s(t) + s_F(t) + \bar{J}(t) + \bar{J}_F(t) + n(t) \tag{4.7}$$

where

$s(t)$ is the specular component of the intended signal, given by

$$s(t) = \mathrm{Re}\left[\sqrt{2}A \sum_k P(t-2kT)\left\{\sum_{n=-\infty}^{\infty} c_n h_T(t-2nT) - j\sum_{n=-\infty}^{\infty} d_n h_T(t-2nT)\right\} \cdot \exp j\,[(\omega_k+\omega_o)t + \theta_k]\right] \tag{4.8}$$

$s_F(t)$ is the faded part of the intended signal, given by

$$s_F(t) = \gamma_s\ \mathrm{Re}\left[\sqrt{2}\,A \sum_k \int_{-\infty}^{\infty} \beta_s(\tau)\left[P(t-\tau-2kT)\left\{\sum_{n=-\infty}^{\infty} c_n h_T(t-\tau-2nT) - j\sum_{n=-\infty}^{\infty} d_n h_T[t-\tau-2nT]\right\}\right] d\tau \cdot \exp j\,[(\omega_k+\omega_o)t+\theta_k]\right] \tag{4.9}$$

similarly, the specular received component of the jamming signal is given by

$$\bar{J}(t) = \lambda_J\ \mathrm{Re}\left\{\sqrt{2J}\ \exp j\,[(\omega_k+\omega_o)t + \phi_k]\right\} \tag{4.10}$$

and the faded jamming component is given by

$$\bar{J}_F(t) = \lambda_J\ \mathrm{Re}\left\{\gamma_J\sqrt{2J}\int_{-\infty}^{\infty}\beta_J(\tau)\,d\tau \cdot \exp j\,[(\omega_k+\omega_o)t + \phi_k]\right\} \tag{4.11}$$

$n(t)$ is the additive White Gaussian noise of two-sided spectral density $\eta_0/2$. For the partial-band multi-tone jamming policy assumed, we let the total power of the jammer be denoted as J_T and the number of jamming tones by M. With the

total jamming power of J_T equally divided among the M jamming tones then each tone has power of $J = J_T / M$. The variable λ_J takes a a value of 1 or 0, depending on whether the jammer is present or absent respectively.

Assuming that a coherent frequency synthesizer is available at the receiver. That is it is capable of estimating and correcting for the phase errors caused by the transmitter synthesizer, the channel and the receiver synthesizer. The dehopped signal then can be expressed as

$$
\begin{aligned}
r_d(t) = \mathrm{Re}\Big\{ \sqrt{2}A \Big[& \sum_{n=-\infty}^{\infty} c_n \; h_T(t-2nT) - j \sum_{n=-\infty}^{\infty} d_n \; h_T[t-2nT] \\
& + \gamma_s \sum_k \delta\omega_o \, \omega_k \sum_{n=-\infty}^{\infty} c_n \int_{-\infty}^{\infty} \beta_s(\tau) \, P(t-\tau-2kT) \, h_T(t-\tau-2nT) \, d\tau \\
& - j \; \gamma_s \sum_k \delta\omega_o \, \omega_k \sum_{n=-\infty}^{\infty} d_n \int_{-\infty}^{\infty} \beta_s(\tau) \, P(t-\tau-2kT) \, h_T[t-\tau-2nT] \, d\tau \Big] \\
& \cdot \exp j \, \omega_o t \Big\} \\
& + \lambda_J \mathrm{Re}\Big\{ [\sqrt{2J} + \gamma_J \sqrt{2J} \int_{-\infty}^{\infty} \beta_J(\tau) \, d\tau] \sum_k P(t-2kT) \, \delta\omega_o \, \omega_k \\
& \cdot \exp j \, (\omega_o t + \phi_k) \Big\} \qquad (4.12)
\end{aligned}
$$

then filtering by $H_R(\omega)$ to give the following quadrature and inphase signals,

$$
\begin{aligned}
Z_Q(t) &= y(t)(\sqrt{2} \cos \omega_o t) * h_R(t) \\
&= A \sum_{n=-\infty}^{\infty} c_n \; h_T(t-2nT) \\
&+ \gamma_s A \sum_k \delta\omega_o \, \omega_k \sum_{n=-\infty}^{\infty} c_n \int_{-\infty}^{\infty} \beta_s(\tau) P(t-\tau-2kT) h_T[t-\tau-2nT] d\tau * h_R(t) \\
&+ \lambda_J \sqrt{J} \cos \phi \\
&+ \lambda_J \gamma_J \sqrt{J} \cos \phi \sum_k P(t-2kT) \, \delta\omega_o \, \omega_k \int_{-\infty}^{\infty} \beta_J(\tau) \, d\tau * h_R(t)
\end{aligned}
$$

$$+ N_c(t) \tag{4.13}$$

$$\begin{aligned} Z_I(t) &= y(t)(\sqrt{2}\sin\omega_o t) * h_R(t) \\ &= A\sum_{n=-\infty}^{\infty} d_n\, h_T[t-2nT] \\ &+ \gamma_s A\sum_k \delta\omega_o\,\omega_k \sum_{n=-\infty}^{\infty} c_n \int_{-\infty}^{\infty} \beta_s(\tau)\, P(t-\tau-2kT)\, h_T[t-\tau-2nT]d\tau * h_R(t) \\ &+ \lambda_J\sqrt{J}\,\sin\phi \\ &+ \lambda_J\gamma_J\sqrt{J}\,\sin\phi\sum_k P(t-2kT)\,\delta\omega_o\,\omega_k \int_{-\infty}^{\infty}\beta_J(\tau)d\tau * h_R(t) \\ &+ N_s(t) \end{aligned} \tag{4.14}$$

The baseband signals $Z_Q(t)$ and $Z_I(t)$ are then sampled to give

$$\begin{aligned} Z_{Qm} &= Z_Q[(2m-1)T] \\ &= A(c_m + c_{m-1}) + \lambda_J\sqrt{J}\,\cos\phi \\ &+ \gamma_s A\sum_k \delta\omega_o\,\omega_k \sum_{n=-\infty}^{\infty} c_n \int_{-\infty}^{\infty}\beta_s(\tau)P[(2m-1)T-\tau-2kT] \\ &\qquad h_T[(2m-1)T-\tau-2kT]d\tau * h_R[(2m-1)T] \\ &+ \lambda_J\gamma_J\sqrt{J}\,\cos\phi\sum_k P[(2m-1)T-2kT]\,\delta\omega_o\,\omega_k \\ &\int_{-\infty}^{\infty}\beta_J(\tau)d\tau * h_R[(2m-1)T] \\ &+ N_c[(2m-1)T] \end{aligned} \tag{4.15}$$

$$\begin{aligned} Z_{Im} &= Z_I[(2m-1)T] \\ &= A(d_m + d_{m-1}) + \lambda_J\sqrt{J}\sin\phi \end{aligned}$$

$$+ \gamma_s A \sum_k \delta\omega_o \omega_k \sum_{n=-\infty}^{\infty} d_n \int_{-\infty}^{\infty} \beta_s(\tau)\, P[(2m-1)T-\tau-2kT]$$

$$\cdot h_T[(2m-1)T-\tau-2kT]d\tau * h_R[(2m-1)T]$$

$$+ \lambda_J \gamma_J \sqrt{J} \sin\phi \sum_k P[(2m-1)T-2kT]\, \delta\omega_o \omega_k$$

$$\cdot \int_{-\infty}^{\infty} \beta_J(\tau)d\tau * h_R[(2m-1)T]$$

$$+ N_s[(2m-1)T] \qquad (4.16)$$

To evaluate the probability of bit error, one needs to find the mean and variances of various terms of Z_{Qm} and Z_{Im}. However because of the many parameters involved we choose to fix them first then remove the conditioning later. Before performing this step though we will assume that inter-symbol interference exists only between neighboring adjacent bits and so consider only the quantities c_{-2}, c_{-1}, c_0, c_1, c_2 in equations (15), (16). With this assumption and assuming given values c_{-2}, c_{-1}, c_0, c_1, c_2, d_{-2}, d_{-1}, d_0, d_1, d_2 and inserting the known $h_R(t)$, $P(t)$ in (15), (16) we see that the 3rd term becomes a deterministic term. Also the first term of (15), (16) is deterministic once the data bits c_m, c_{m-1}, d_m, d_{m-1} are assumed. For the computation of probability of bit error we compute the probability of bit error in the I and the Q banks of the receiver. To this objective a normal density is assigned to the decision variables Z_{Qm}, Z_{Im} and the needed variances of faded signal, faded jammer and the noise are presented in the Appendix C. The transmitted data sequences a_l and b_l are then recovered by the well known detection criteria for QPR signals (Table 1).

$$a_l = \begin{cases} +1 & \text{if } |Z_{sl}| > A \\ -1 & \text{if } |Z_{sl}| < A \end{cases} \qquad b_l = \begin{cases} +1 & \text{if } |Z_{cl}| > A \\ -1 & \text{if } |Z_{cl}| < A \end{cases} \qquad (4.17)$$

Table 1.

Transmitted Symbol b_l	Received Symbols c_l	c_{l-1}	Duobinary Value $c_l + c_{l-1}$
-1	+1	-1	0
-1	-1	+1	0
+1	+1	+1	+2
+1	-1	-1	-2

Based on all the above assumptions, conditioning and the results of the Appendix C we get the following for the conditional probability of bit errors in the Q and I channels respectively.

$$P_Q(e \mid \phi, \lambda_J, c_{-2}, c_{-1}, c_0, c_1, c_2, \omega_{-1}, \omega_1)$$
$$= \frac{3}{4}[Q(arg\ 1) + Q(arg\ 2)] - \frac{1}{4}[Q(arg\ 3) + Q(arg\ 4)] \quad (4.18)$$

where

$$Q(x) = \int_x^\infty \frac{1}{\sqrt{2\pi}} e^{\frac{-z^2}{2}} dz \quad (4.19)$$

$$arg\ 1 = \frac{A + \lambda_J \sqrt{J}\ \cos\phi}{\sigma_T} \quad (4.20)$$

$$arg\ 2 = \frac{A - \lambda_J \sqrt{J}\ \cos\phi}{\sigma_T} \quad (4.21)$$

$$arg\ 3 = \frac{3A + \lambda_J \sqrt{J}\ \cos\phi}{\sigma_T} \quad (4.22)$$

$$arg\ 4 = \frac{3A - \lambda_J \sqrt{J}\ \cos\phi}{\sigma_T} \quad (4.23)$$

$$\sigma_T = \left[\frac{N_o}{4T} + \frac{\gamma_s^2 A^2 16 T^3}{\pi^4} I_{s_1} + \frac{\lambda_J \gamma_J J}{\pi^2} I_{J_1}\right]^{1/2} \quad (4.24)$$

Following the same procedure,

$$P_J(e \mid \phi,\lambda_J,c_{-2},c_{-1},c_0,c_1,c_2,\omega_{-1},\omega_1) = \frac{3}{4}[Q(arg\,1)+Q(arg\,2)] - \frac{1}{4}[Q(arg\,3)+Q(arg\,4)] \quad (4.25)$$

the arguments in this case are the same as defined above but with $\cos\phi$ replaced by $\sin\phi$. Defining $\rho = M/N$ as a fraction of the total slots jammed, $N_J = J_T/W$ as the effective jammer power spectral density in the total frequency hopping band W. Using the following relation $S = 4A^2$ (average transmitted power) from the Appendix C, and $J = J_T/M$ as defined above then defining $E_b = ST_b$ as bit energy. Based on these definitions, we may rewrite the arguments in terms of bit energy yielding

$$arg\,1 = \frac{1 + \frac{\sqrt{2}\lambda_J}{\sqrt{\rho E_b/N_J}}\cos\phi}{\left[\frac{N_o}{E_b} + \frac{\gamma_s^2 16T^3}{2\pi^4}I_{s_1} + \frac{2\lambda_J\gamma_J^2}{\pi^2\rho E_b/N_J}I_{J_1}\right]^{1/2}} \quad (4.26)$$

$$arg\,2 = \frac{1 - \frac{\sqrt{2}\lambda_J}{\sqrt{\rho E_b/N_J}}\cos\phi}{\left[\frac{N_o}{E_b} + \frac{\gamma_s^2 16T^3}{2\pi^4}I_{s_1} + \frac{2\lambda_J\gamma_J^2}{\pi^2\rho E_b/N_J}I_{J_1}\right]^{1/2}} \quad (4.27)$$

$$arg\,3 = \frac{3 + \frac{\sqrt{2}\lambda_J}{\sqrt{\rho E_b/N_J}}\cos\phi}{\left[\frac{N_o}{E_b} + \frac{\gamma_s^2 16T^3}{2\pi^4}I_{s_1} + \frac{2\lambda_J\gamma_J^2}{\pi^2\rho E_b/N_J}I_{J_1}\right]^{1/2}} \quad (4.28)$$

$$arg\,4 = \frac{3 - \frac{\sqrt{2}\lambda_J}{\sqrt{\rho E_b/N_J}}\cos\phi}{\left[\frac{N_o}{E_b} + \frac{\gamma_s^2 16T^3}{2\pi^4 I_{s_1}} + \frac{2\lambda_J\gamma_J^2}{\pi^2\rho E_b/N_J}I_{J_1}\right]^{1/2}} \quad (4.29)$$

Averaging over all possible combinations of data bits

$$P_b(e \mid \phi,\lambda_J,\omega_{-1},\omega_1) = \frac{1}{32}\sum_{i=1}^{32} P_b(e \mid \phi,\lambda_J,c_{-2},c_{-1},c_0,c_1,c_2,\omega_{-1},\omega_1) \quad (4.30)$$

where the values of c_{-2}, c_{-1}, c_0, c_1, c_2 take all possible 32 combinations i.e. (1,1,1,1,1), (1,1,1,1,-1), (1,1,1,-1,1)

$$P_b(e \mid \omega_{-1},\omega_1) = \frac{M}{N}\frac{1}{2\pi}\int_0^{2\pi} P(e \mid \lambda_J=1,\phi,\omega_{-1},\omega_1)\, d\phi + \left(1-\frac{M}{N}\right)P(e \mid \lambda_J=0,\omega_{-1},\omega_1) \quad (4.31)$$

Finally, for the four possible cases of intersymbol interference $\delta\omega_0\,\omega_k$ assumed (i.e. conditions of ω_{-1}, ω_1 compared to ω_0).

$$P_b = \frac{1}{N^2}P(e \mid \omega_{-1}=\omega_0,\omega_1=\omega_0) + \frac{N-1}{N^2}P(e \mid \omega_{-1}=\omega_0,\omega_1\neq\omega_0) + \frac{N-1}{N^2}P(e \mid \omega_{-1}\neq\omega_0,\omega_1=\omega_0) + \left(\frac{N-1}{N}\right)^2 P(e \mid \omega_{-1}\neq\omega_0,\omega_1\neq\omega_0) \quad (4.32)$$

In order to improve the performance of the FH/QPR system in the presence of a jammer, it useful to employ error-correction coding. The information rate and spread bandwidth is kept constant, therefore making the number of slots available for hopping decrease by the information rate of the code [9]. For example, if the uncoded FH/QPR system uses N slots, the (23,12) Golay encoded system will then have $\frac{12}{23}N$ slots to hop with. The probability of bit error in the decoded sequence can be shown to be given approximately by [9],

$$P \approx \frac{1}{n}\sum_{i=e+1}^{n} i\binom{n}{i} P_b^{\,i}(1-P_b)^{n-i} \quad (4.33)$$

where P_b is given by (4.32) except that E_b/N_0 is decreased by the rate of the

code. That is the energy-per-symbol of the coded system is 12/23 of the energy-per-symbol of the uncoded system.

4.3 Numerical Results:

Starting with certain values for M and N, the signal to jamming ratio (E_b/N_J) and the signal to noise ratio (E_b/N_o) we were able to compute $\rho = M/N$ and the conditional variances I_{s_i} and I_{J_i} from the Appendix C. The probability of bit error is evaluated for the uncoded and coded system.

Figures 4.2-A to 4.2-C show the effect of varying M, the number of jammed slots on the probability of bit error for the uncoded $(N=1917)$ and coded $(N=1000)$ systems. We consider first the case of no fading $(\gamma_s = 0,\ \gamma_J = 0)$ and compare the curves of figures 4.2-A to 4.2-C for $E_b/N_J = 30,\ 15,\ 1\ dB$, respectively (keeping $E_b/N_o = 20\ dB$ fixed). One observes that for E_b/N_J equal to 15 dB and 30 dB there exists a value of M equal to 80 and 40 for the uncoded and coded systems, respectively, which maximizes the probability of bit error. However, for E_b/N_J equal to 1 dB (fig. 4.2-C) it is seen that P_b increases with an increasing M for both the coded and uncoded systems. Secondly in the case of fading, for the values $\gamma_s = \gamma_J = .2,\ .5$ the performance is seen to be more sensitive for $E_b/N_J = 15,\ 30\ dB$ (figures 4.2-A and 4.2-B) compared to the case of $E_b/N_J = 1\ dB$ (fig. 4.2-C). Although the performance of the coded system is superior to the uncoded system, the coded system is more sensitive to the increase in power of the scatter component than the uncoded system. Also, note the curves are flat under fading for both the uncoded and coded system, only in this situation, and irrespective of the number of jammed slots the performance is the same for that particular γ_s and γ_J.

In figures 4.3-A to 4.3-F, we show the effect of varying E_b/N_o on the performance of P_b. For the set of figures 4.3-A to 4.3-C and 4.3-D to 4.3-F the value of

E_b/N_J is fixed at 15 dB and 1 dB, respectively. Figures 4.3-A and 4.3-C show the performance for suboptimal values of $M = 1$, $M = 1000$ (coded) and $M = 1917$ (uncoded) (from the viewpoint of the jammer). It is observed that P_b decreases with increasing E_b/N_o flatting out at large values of E_b/N_o, whereas in fig. 4.3-B (for worst case M=80), the performance is worst. Worth noting too is the performance sensitivity to values of γ_s and γ_J for both cases of suboptimal and worst case M. It is seen that performance is less sensitive to γ_s, γ_J for worst case M than in the case of suboptimal values of $M = 1$, 1000 (coded), 1917 (uncoded). Similar conclusions are drawn from figures 4.3-D to 4.3-F, the worst case M being 1000 jamming tones for the coded system and 1100 tones for the uncoded system.

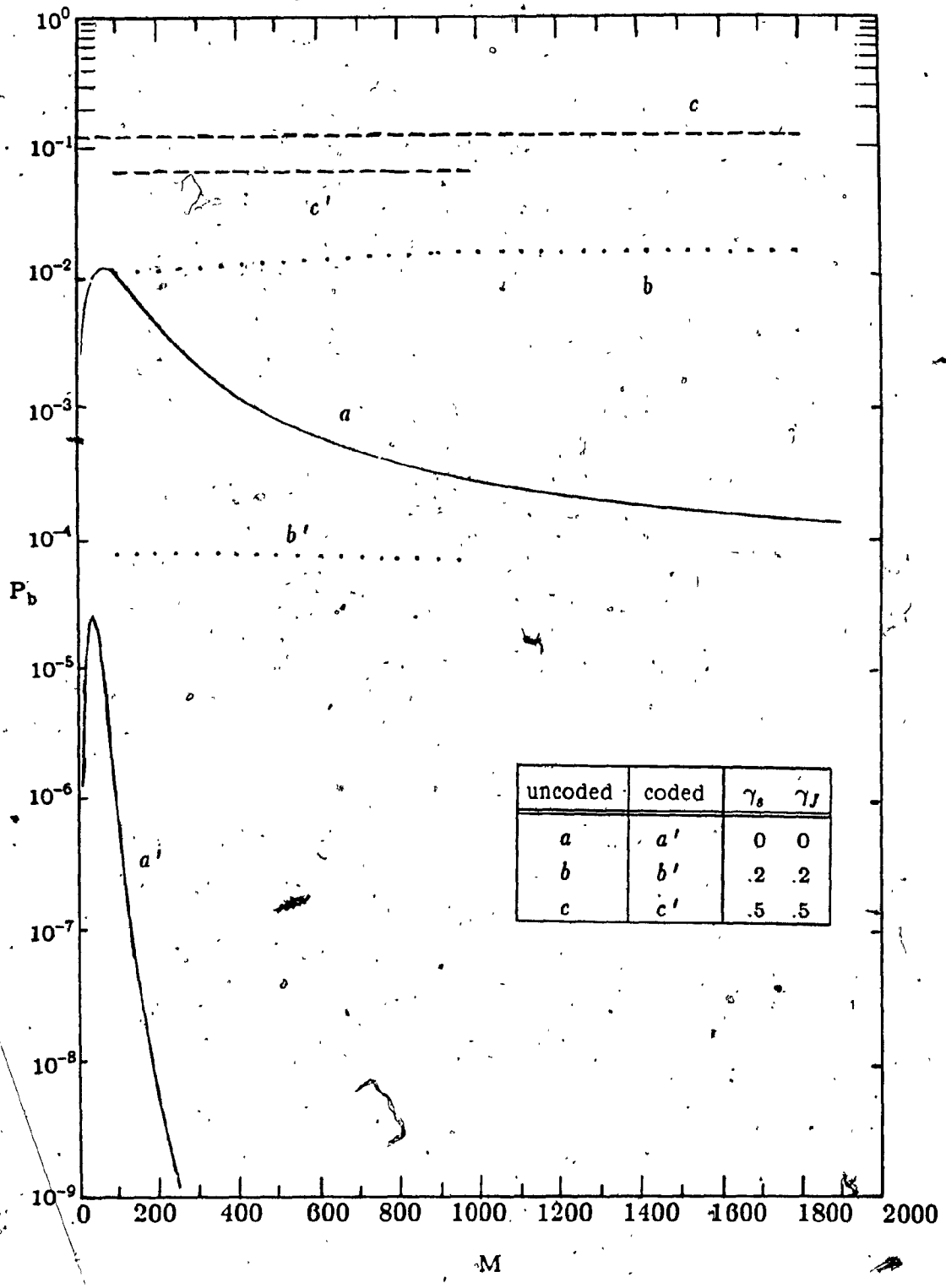

Fig. 4.2-A. P_b versus M for $E_b/N_o = 20$ dB and $E_b/N_J = 30$ dB.

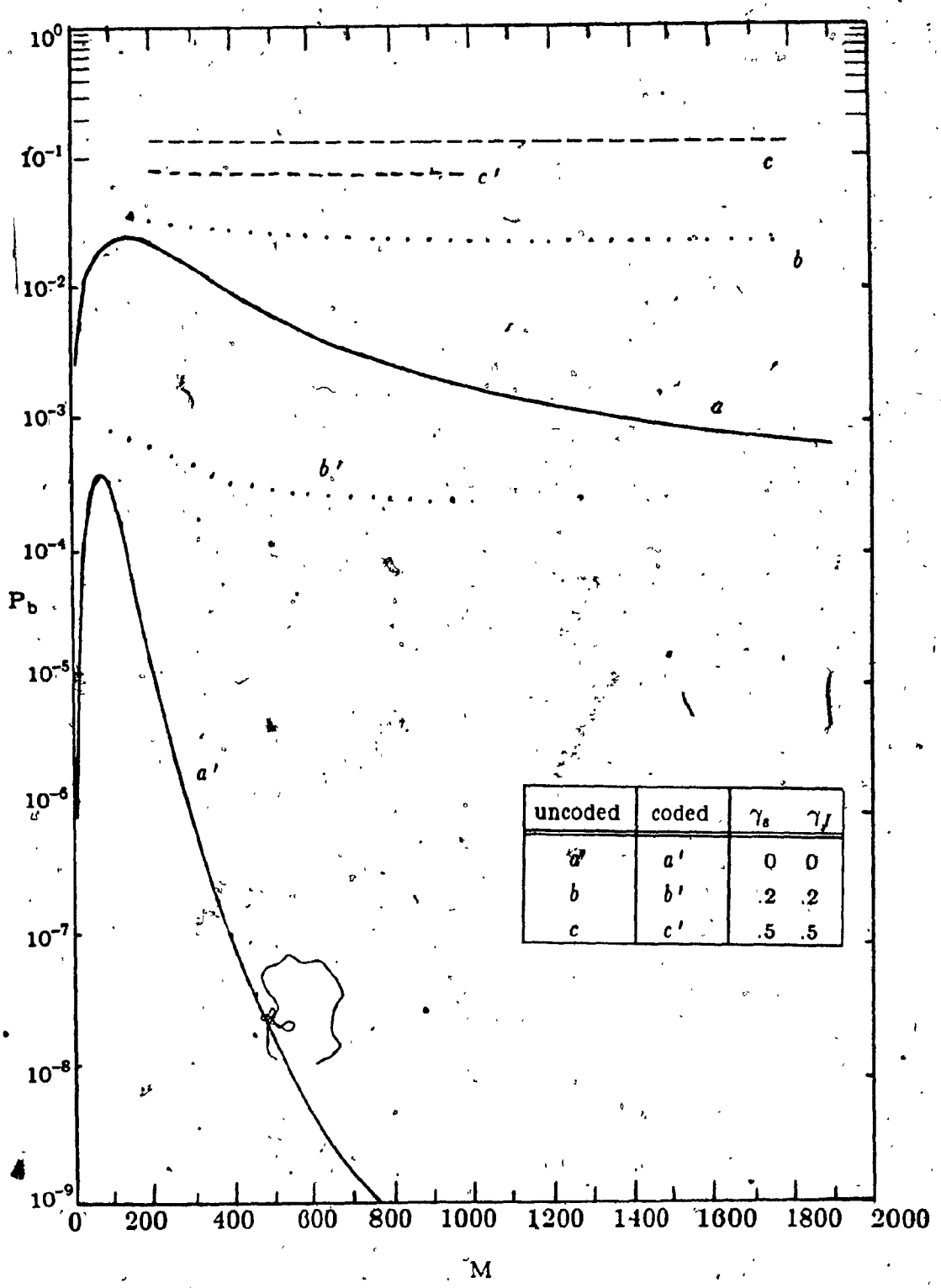

Fig. 4.2-B. P_b versus M for $E_b/N_o = 20$ dB and $E_b/N_j = 15$ dB.

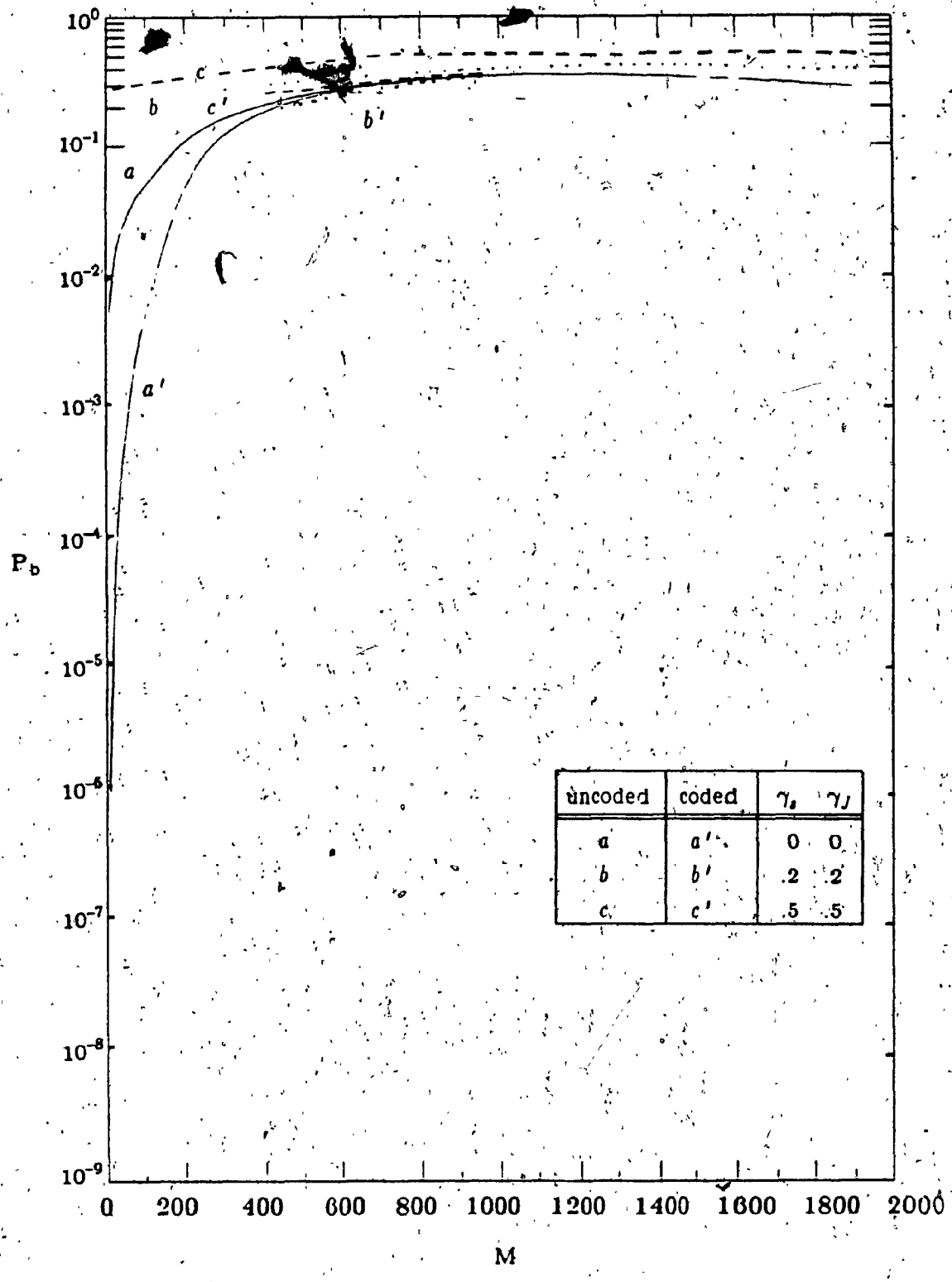

Fig. 4.2-C. P_b versus M for $E_b/N_o = 20$ dB and $E_b/N_J = 1$ dB.

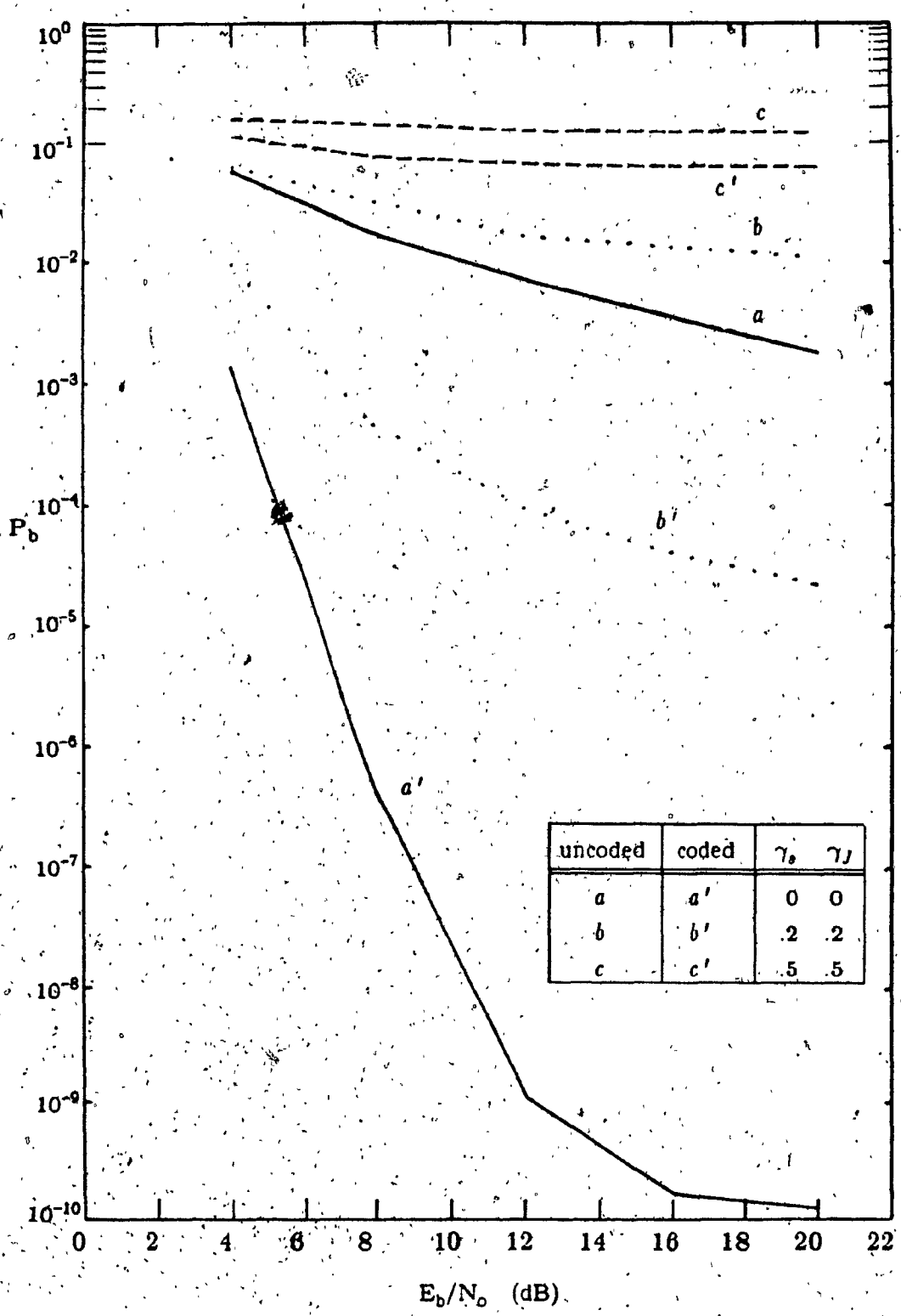

Fig. 4.3-A. P_b versus E_b/N_o for $E_b/N_J = 15$ dB and $M = 1$.

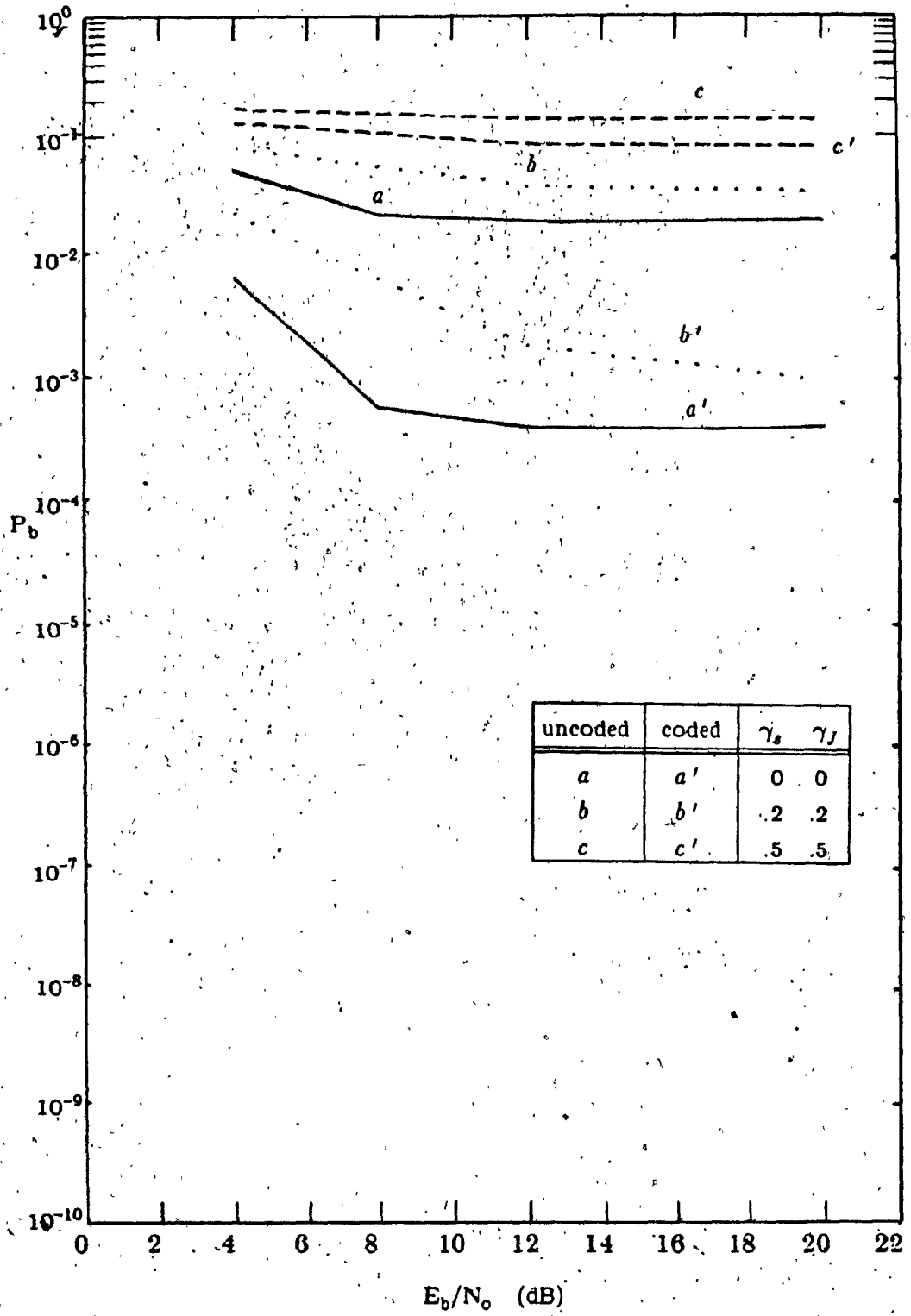

Fig. 4.3-B. P_b versus E_b/N_o for $E_b/N_J = 15$ dB and worst case M.

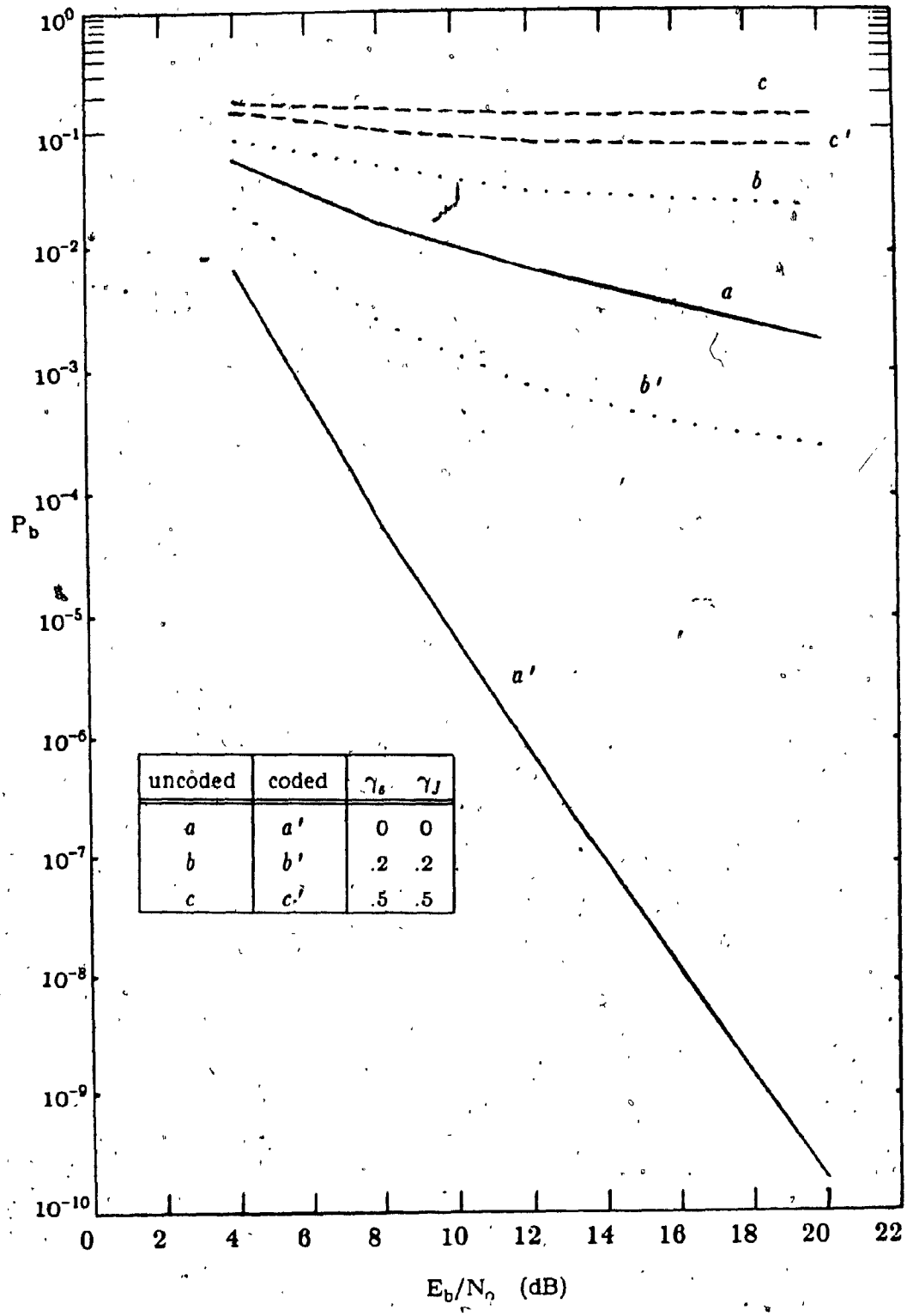

Fig. 4.3-C. P_b versus E_b/N_o for $E_b/N_J = 15$ dB and M = 1000 (coded), M = 1917 (uncoded).

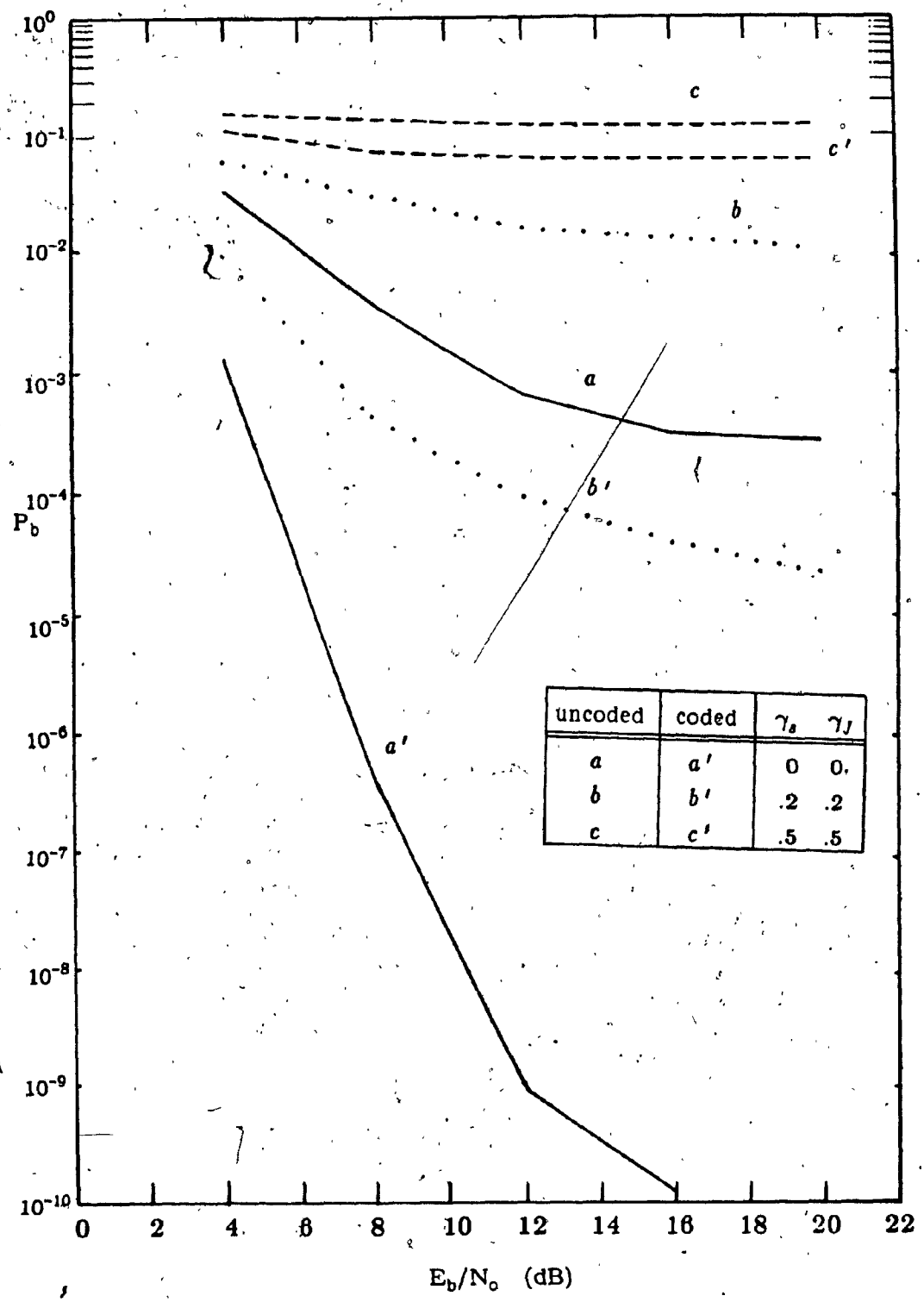

Fig. 4.3-D. P_b versus E_b/N_o for $E_b/N_J = 1$ dB and $M = 1$.

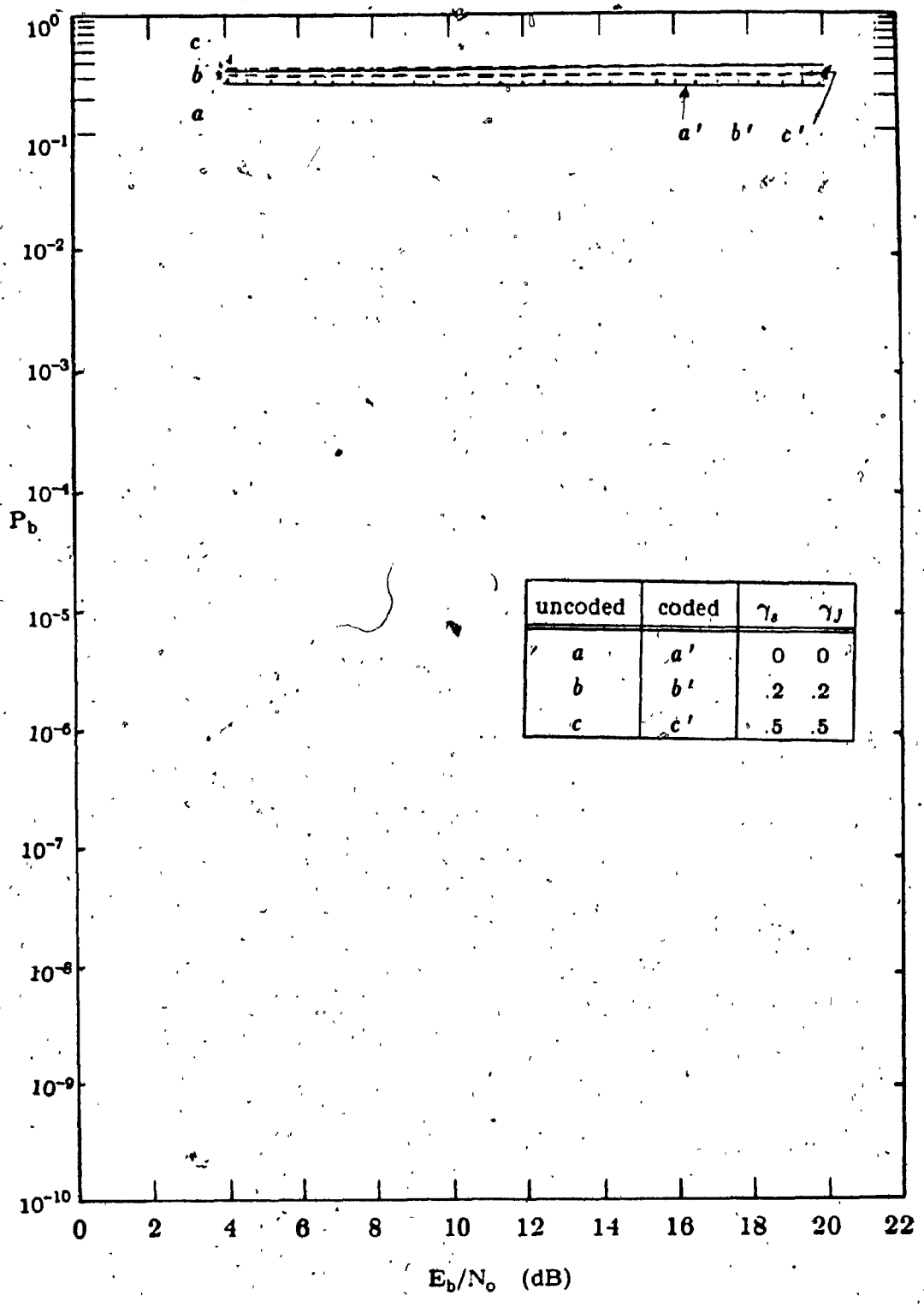

Fig. 4.3-E. P_b versus E_b/N_o for $E_b/N_J = 1$ dB and worst case M.

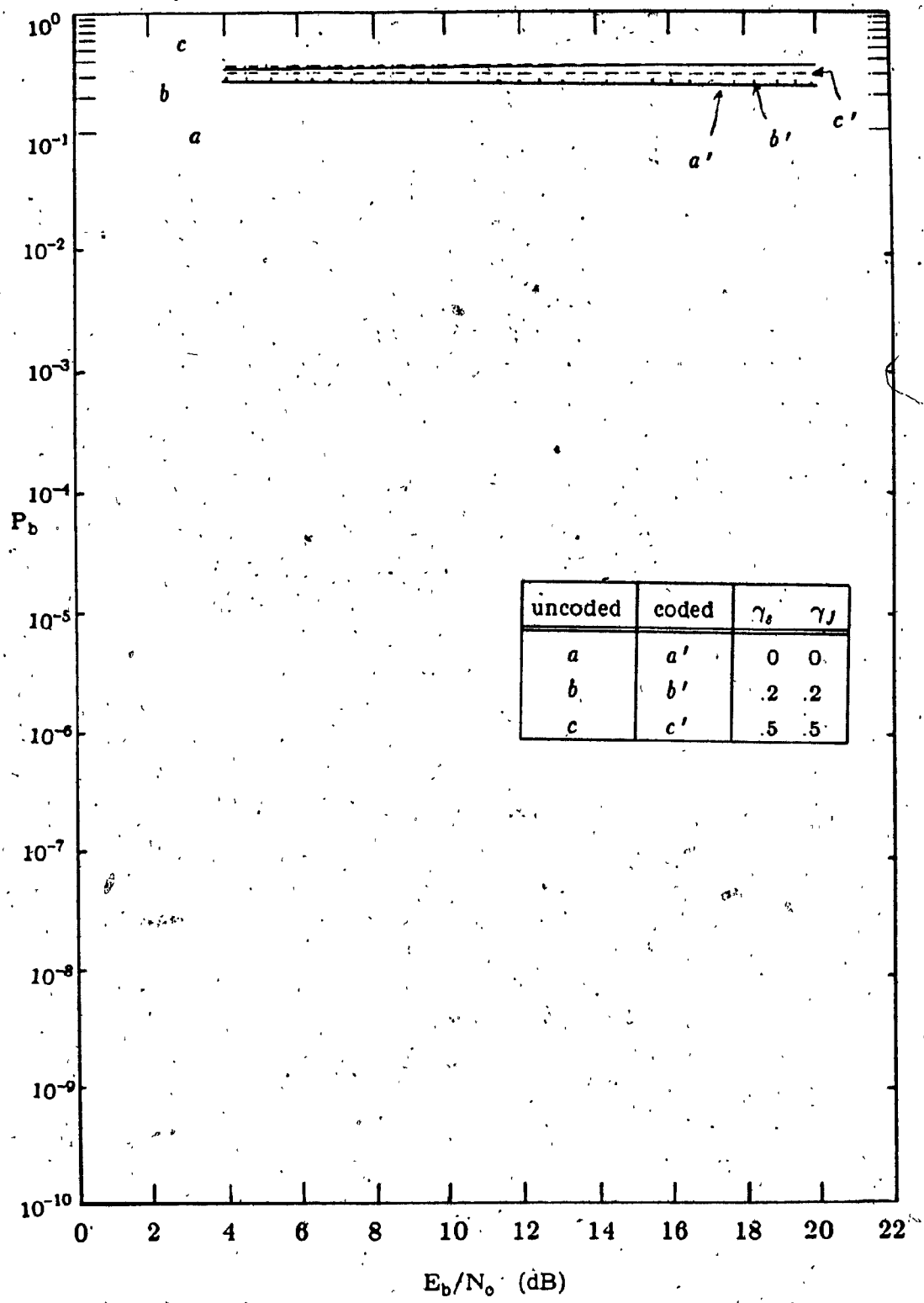

Fig. 4.3-F. P_b versus E_b/N_o for $E_b/N_J = 1$ dB and M = 1000 (coded), M = 1917 (uncoded).

CHAPTER FIVE

COMPARISON OF FH/QPSK, FH/MSK, AND FH/QPR

In this chapter, comparison of FH/QPSK, FH/MSK, FH/QPR is presented. The figures and tables summarize the performance of the modulation techniques for worst case M and suboptimal values of M, keeping $E_b/N_o = 20\ dB$ and for $\gamma_s = \gamma_J = 0, .2, .5$.

In tables 5.1 to 5.3 the results are tabulated for worst case M, $E_b/N_o = 20\ dB$ and $\gamma_s = \gamma_J = 0$ (no fading) and $\gamma_s = \gamma_J = .2, .5$. It is seen from the figures and the tables FH/MSK performs better than FH/QPSK and FH/QPR. For example, from table 5.1 when $E_b/N_J = 30\ dB$ then $M = 30$ and $P_b = 3.27 \times 10^{-3}$ for MSK and $M = 40$ and $P_b = 4.14 \times 10^{-3}$ for QPSK and $M = 80$ and $P_b = 1.20 \times 10^{-2}$ for QPR. Similar conclusion can be drawn for $E_b/N_J = 15$ and $1\ dB$. Also note for large values of E_b/N_J (i.e. 30 dB) the number of jammed channels needed to give maximum probability of error are afewer, than when E_b/N_J is small (i.e. 1 dB).

In tables 5.4 to 5.6 the results are tabulated for $M = 1$, $E_b/N_o = 20\ dB$ and $\gamma_s = \gamma_J = 0, .2, .5$ and in tables 5.7 to 5.9 the results are tabulated for $M = 1000$ (coded) and $M = 1917$ (uncoded). Again it is seen FH/MSK performs best, then FH/QPSK and last FH/QPR.

Looking at figures 5.1-A to 5.1-C we observe FH/QPSK and FH/QPR are more sensitive to fading compared to FH/MSK. For example, comparing the curves of FH/MSK, FH/QPSK, and FH/QPR for $\gamma_s = \gamma_J = .5$, we see

FH/QPSK and FH/QPR result in a higher probability of error and the curves are flatter than for FH/MSK. From figures 5.2-A to 5.2-C we see the following similarity between each other, that is the performance at worst case M (fig. 5.2-B) is less sensitive to fading than at suboptimal values of M (figs. 5.2-A 5.2-C).

Table 5.1

Comparison of FH/QPSK, FH/MSK, FH/QPR for worst case M, $\gamma_s = \gamma_J = 0$ and $E_b/N_o = 20\ dB$.

E_b/N_J dB	FH/QPSK			
	uncoded		coded	
	M	P_b	M	P_b
30	40	4.14×10^{-3}	20	4.37×10^{-7}
15	70	8.32×10^{-3}	40	6.59×10^{-6}
1	1110	1.25×10^{-1}	580	6.66×10^{-2}
E_b/N_J^* dB	FH/MSK			
	uncoded		coded	
	M	P_b	M	P_b
30	30	3.27×10^{-3}	20	1.06×10^{-7}
15	60	6.54×10^{-3}	30	2.59×10^{-6}
1	870	9.81×10^{-2}	460	3.51×10^{-2}
E_b/N_J dB	FH/QPR			
	uncoded		coded	
	M	P_b	M	P_b
30	80	1.20×10^{-2}	40	2.80×10^{-5}
15	140	2.43×10^{-2}	80	3.76×10^{-4}
1	1100	3.64×10^{-1}	1000	3.57×10^{-1}

Table 5.2

Comparison of FH/QPSK, FH/MSK, FH/QPR for worst case M, $\gamma_s = \gamma_J = 0.2$ and $E_b/N_o = 20\ dB$.

E_b/N_J dB	FH/QPSK			
	uncoded		coded	
	M	P_b	M	P_b
30	40	5.01×10^{-3}	20	8.90×10^{-7}
15	70	8.81×10^{-3}	40	8.72×10^{-6}
1	1110	1.27×10^{-1}	580	6.66×10^{-2}
E_b/N_J dB	FH/MSK			
	uncoded		coded	
	M	P_b	M	P_b
30	30	3.11×10^{-3}	20	1.25×10^{-7}
15	60	6.22×10^{-3}	30	2.08×10^{-6}
1	870	9.10×10^{-2}	460	3.07×10^{-2}
E_b/N_J dB	FH/QPR			
	uncoded		coded	
	M	P_b	M	P_b
30	80	2.23×10^{-2}	40	2.75×10^{-4}
15	140	3.50×10^{-2}	80	9.03×10^{-4}
1	1100	3.82×10^{-1}	1000	2.22×10^{-1}

Table 5.3

Comparison of FH/QPSK, FH/MSK, FH/QPR for worst case M, $\gamma_s = \gamma_J = 0.5$ and $E_b/N_o = 20\ dB$.

E_b/N_J dB	FH/QPSK			
	uncoded		coded	
	M	P_b	M	P_b
30	40	8.70×10^{-2}	20	2.60×10^{-2}
15	70	8.98×10^{-2}	40	2.87×10^{-2}
1	1110	1.75×10^{-1}	580	1.35×10^{-1}
E_b/N_J dB	FH/MSK			
	uncoded		coded	
	M	P_b	M	P_b
30	30	4.83×10^{-3}	20	1.03×10^{-6}
15	60	8.22×10^{-3}	30	5.95×10^{-6}
1	870	1.01×10^{-1}	460	4.43×10^{-2}
E_b/N_J dB	FH/QPR			
	uncoded		coded	
	M	P_b	M	P_b
30	80	1.29×10^{-1}	40	7.13×10^{-2}
15	140	1.35×10^{-1}	80	8.04×10^{-2}
1	1100	3.87×10^{-1}	1000	3.10×10^{-1}

Table 5.4

Comparison of FH/QPSK, FH/MSK, FH/QPR for $M = 1$, $\gamma_s = \gamma_J = 0$ and $E_b/N_o = 20$ dB.

E_b/N_J	FH/QPSK P_b		FH/MSK P_b		FH/QPR P_b	
dB	uncoded	coded	uncoded	coded	uncoded	coded
15	2.50×10^{-4}	6.26×10^{-11}	2.42×10^{-4}	6.08×10^{-11}	1.72×10^{-3}	1.22×10^{-10}
1	2.57×10^{-4}	8.85×10^{-11}	2.55×10^{-4}	8.85×10^{-11}	2.57×10^{-4}	8.59×10^{-11}

Table 5.5

Comparison of FH/QPSK, FH/MSK, FH/QPR for $M = 1$, $\gamma_s = \gamma_J = 0.2$ and $E_b/N_o = 20$ dB.

E_b/N_J	FH/QPSK P_b		FH/MSK P_b		FH/QPR P_b	
dB	uncoded	coded	uncoded	coded	uncoded	coded
15	1.43×10^{-3}	1.41×10^{-8}	2.44×10^{-4}	6.56×10^{-11}	1.09×10^{-2}	2.05×10^{-5}
1	1.51×10^{-3}	2.13×10^{-8}	2.57×10^{-4}	8.92×10^{-11}	1.09×10^{-2}	2.03×10^{-5}

Table 5.6

Comparison of FH/QPSK, FH/MSK, FH/QPR for $M = 1$, $\gamma_s = \gamma_J = 0.5$ and $E_b/N_o = 20$ dB.

E_b/N_J	FH/QPSK P_b		FH/MSK P_b		FH/QPR P_b	
dB	uncoded	coded	uncoded	coded	uncoded	coded
15	8.42×10^{-2}	2.40×10^{-2}	1.67×10^{-3}	1.95×10^{-8}	1.21×10^{-1}	6.14×10^{-2}
1	8.43×10^{-2}	2.41×10^{-2}	1.69×10^{-3}	2.11×10^{-8}	1.21×10^{-1}	6.15×10^{-2}

Table 5.7

Comparison of FH/QPSK, FH/MSK, FH/QPR for $M = 1000$ (coded), $M = 1917$ (uncoded), $\gamma_s = \gamma_J = 0$ and $E_b/N_o = 20\ dB$.

E_b/N_J	FH/QPSK P_b		FH/MSK P_b		FH/QPR P_b	
dB	uncoded	coded	uncoded	coded	uncoded	coded
15	1.92×10^{-7}	2.08×10^{-24}	7.94×10^{-8}	6.13×10^{-26}	1.72×10^{-3}	1.90×10^{-10}
1	7.45×10^{-2}	1.67×10^{-2}	3.15×10^{-2}	9.73×10^{-4}	2.43×10^{-2}	2.33×10^{-3}

Table 5.8

Comparison of FH/QPSK, FH/MSK, FH/QPR for $M = 1000$ (coded), $M = 1917$ (uncoded), $\gamma_s = \gamma_J = 0.2$ and $E_b/N_o = 20\ dB$.

E_b/N_J	FH/QPSK P_b		FH/MSK P_b		FH/QPR P_b	
dB	uncoded	coded	uncoded	coded	uncoded	coded
15	3.41×10^{-3}	2.00×10^{-7}	1.36×10^{-5}	5.61×10^{-17}	2.22×10^{-2}	2.26×10^{-4}
1	1.19×10^{-1}	5.85×10^{-2}	6.29×10^{-2}	9.91×10^{-3}	2.75×10^{-1}	3.48×10^{-1}

Table 5.9

Comparison of FH/QPSK, FH/MSK, FH/QPR for $M = 1000$ (coded), $M = 1917$ (uncoded), $\gamma_s = \gamma_J = 0.5$ and $E_b/N_o = 20\ dB$.

E_b/N_J	FH/QPSK P_b		FH/MSK P_b		FH/QPR P_b	
dB	uncoded	coded	uncoded	coded	uncoded	coded
15	9.37×10^{-2}	3.19×10^{-2}	4.85×10^{-3}	8.11×10^{-7}	1.30×10^{-1}	7.10×10^{-2}
1	1.95×10^{-1}	1.62×10^{-1}	1.25×10^{-1}	6.68×10^{-2}	3.13×10^{-1}	3.62×10^{-1}

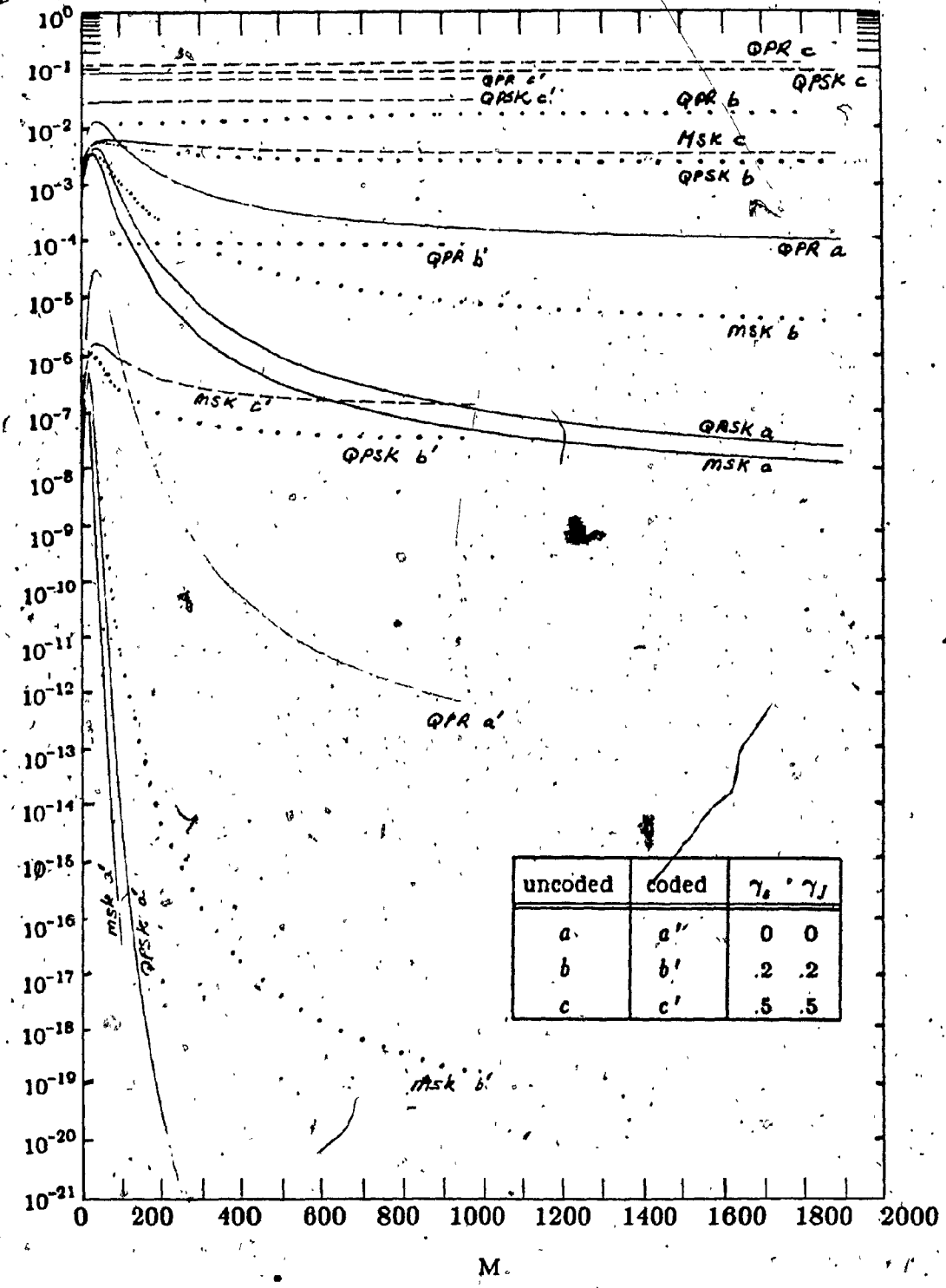

Fig. 5.1-A. P_b versus M for $E_b/N_o = 20$ dB and $E_b/N_J = 30$ dB

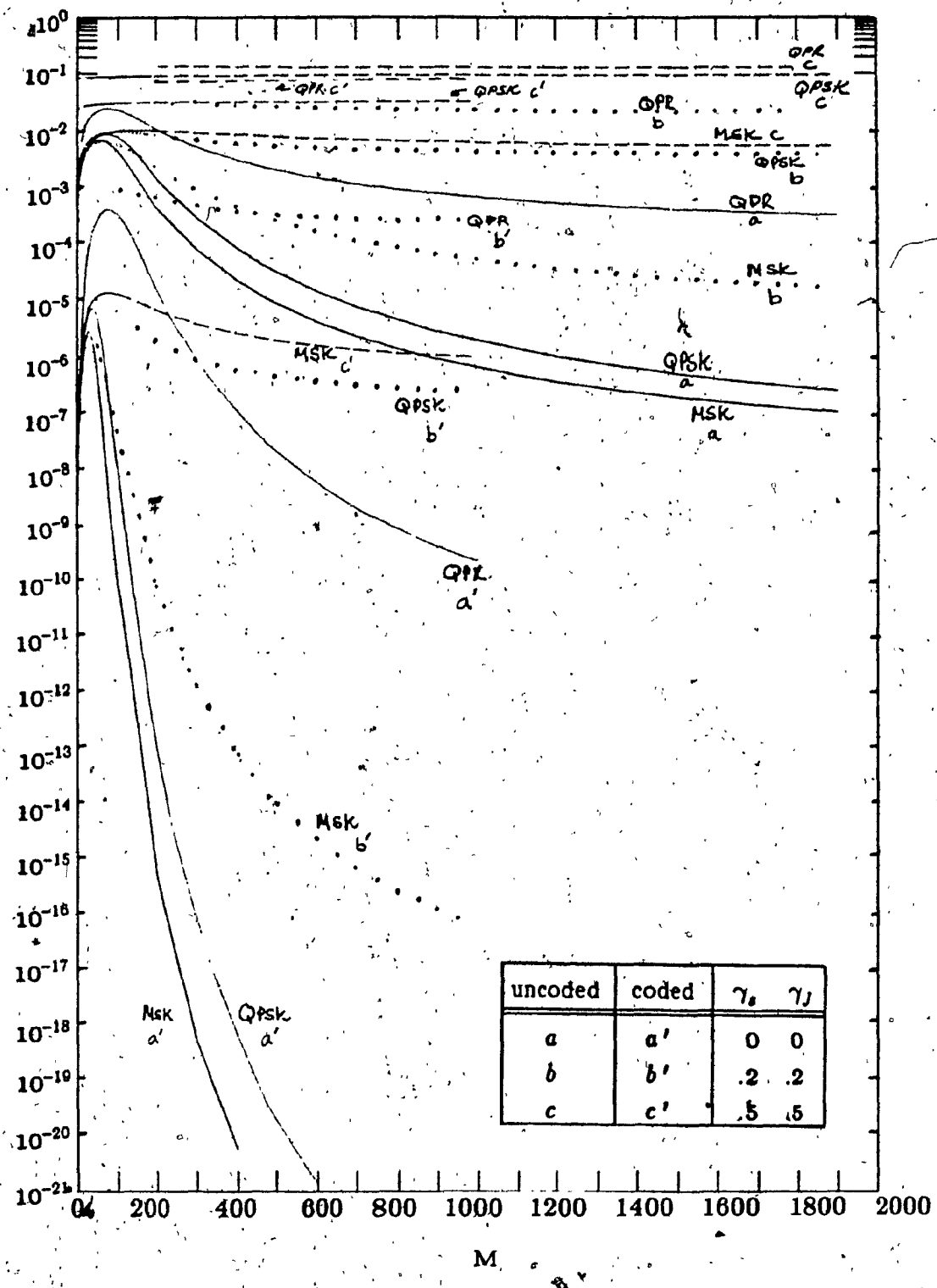

Fig. 5.1-B. P_b versus M for $E_b/N_o = 20$ dB and $E_b/N_J = 15$ dB.

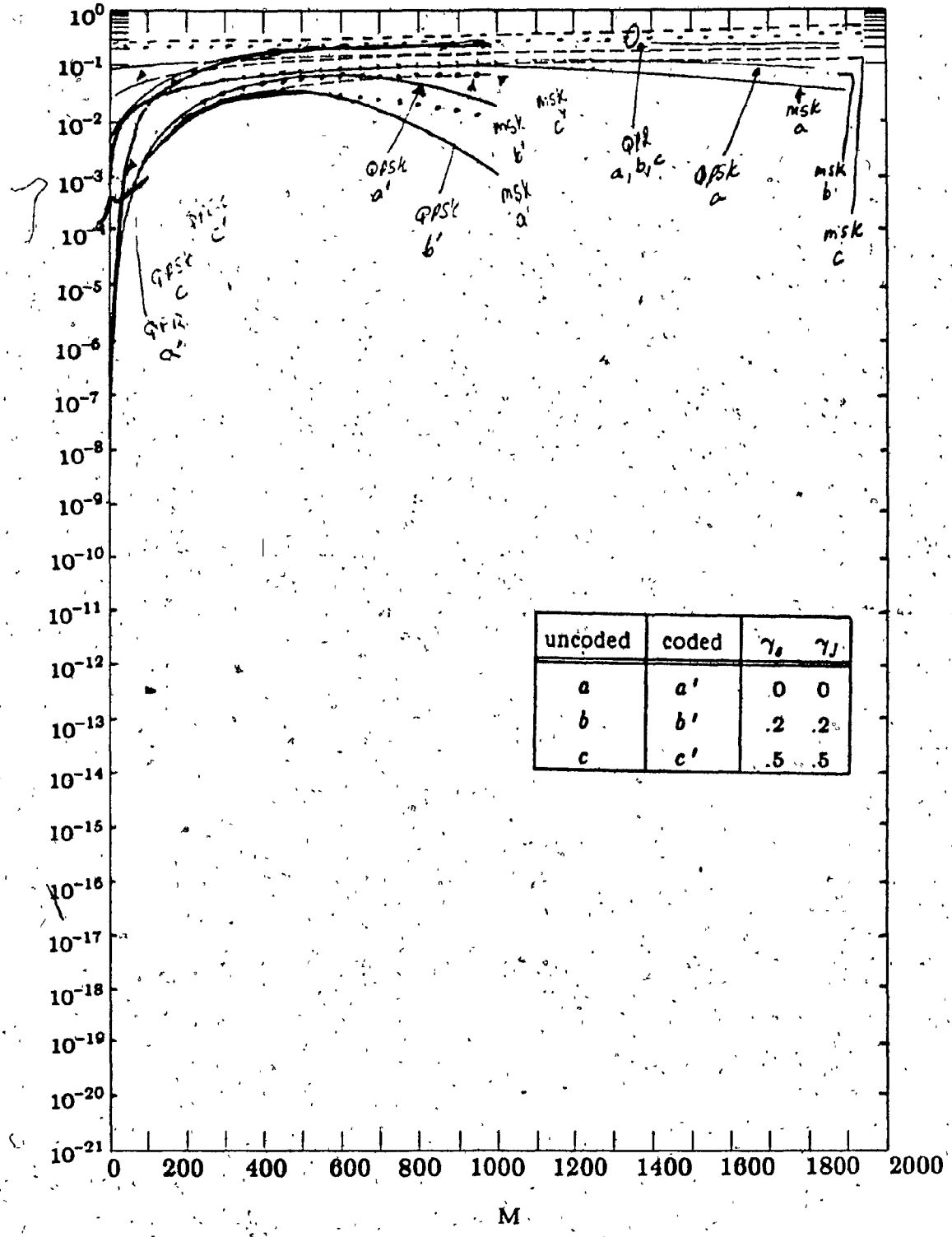

Fig. 5.1-C. P_b versus M for $E_b/N_o = 20$ dB and $E_b/N_J = 1$ dB.

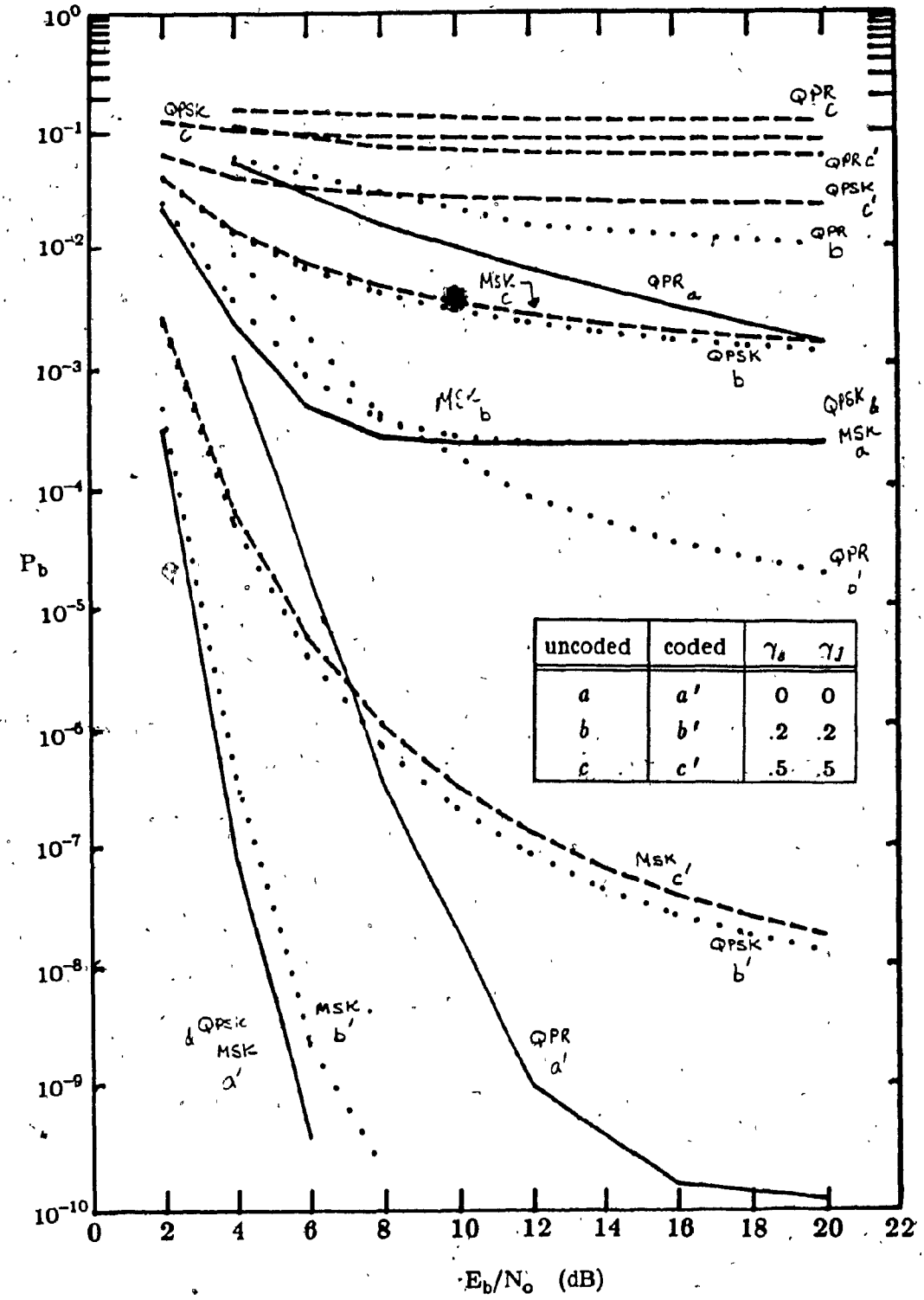

Fig. 5.2-A. P_b versus E_b/N_o for $E_b/N_J = 15$ dB and $M = 1$.

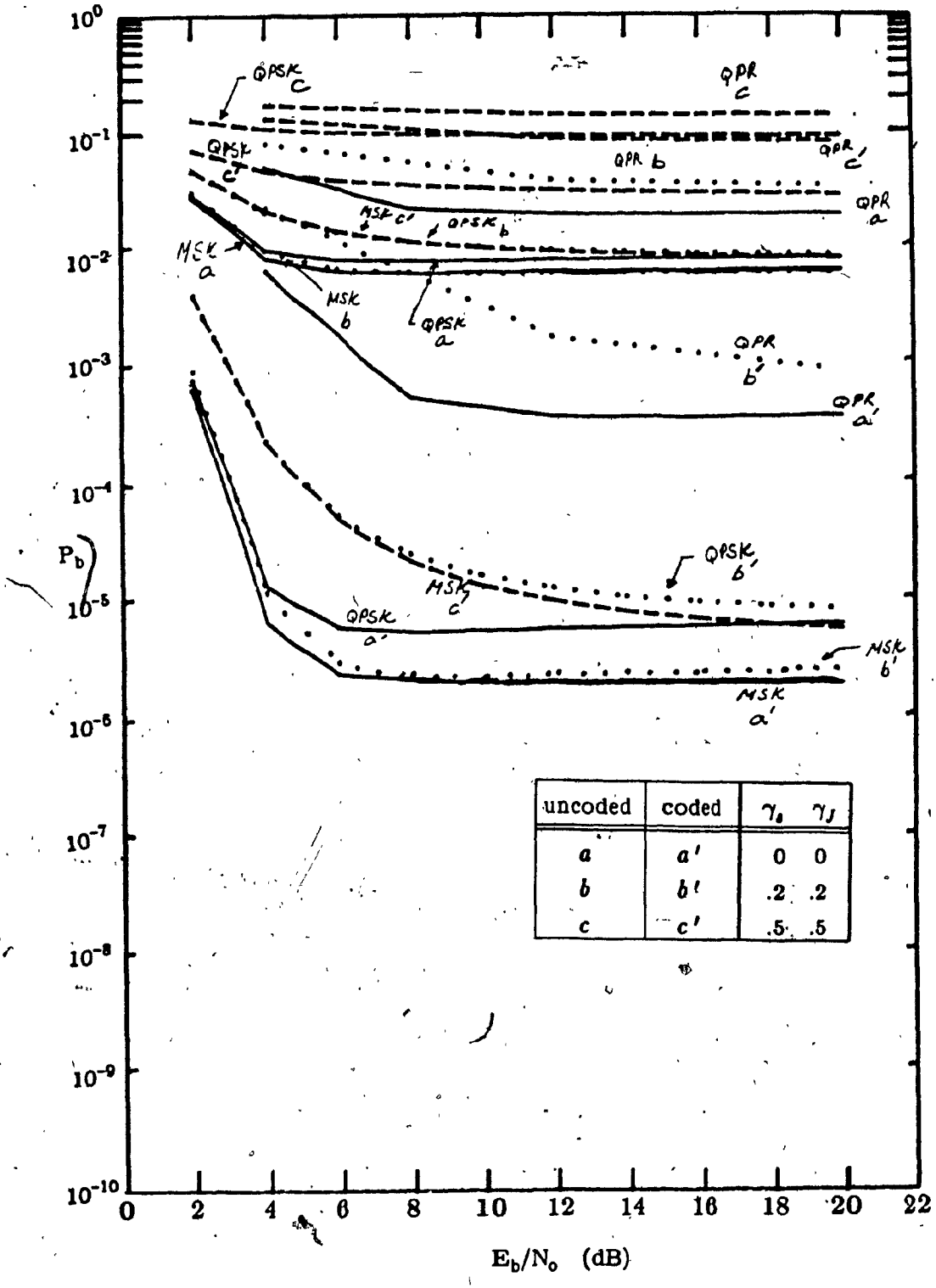

uncoded	coded	γ_s	γ_J
a	*a'*	0	0
b	*b'*	.2	.2
c	*c'*	.5	.5

Fig. 5.2-B. P_b versus E_b/N_o for $E_b/N_J = 15$ dB and worst case M.

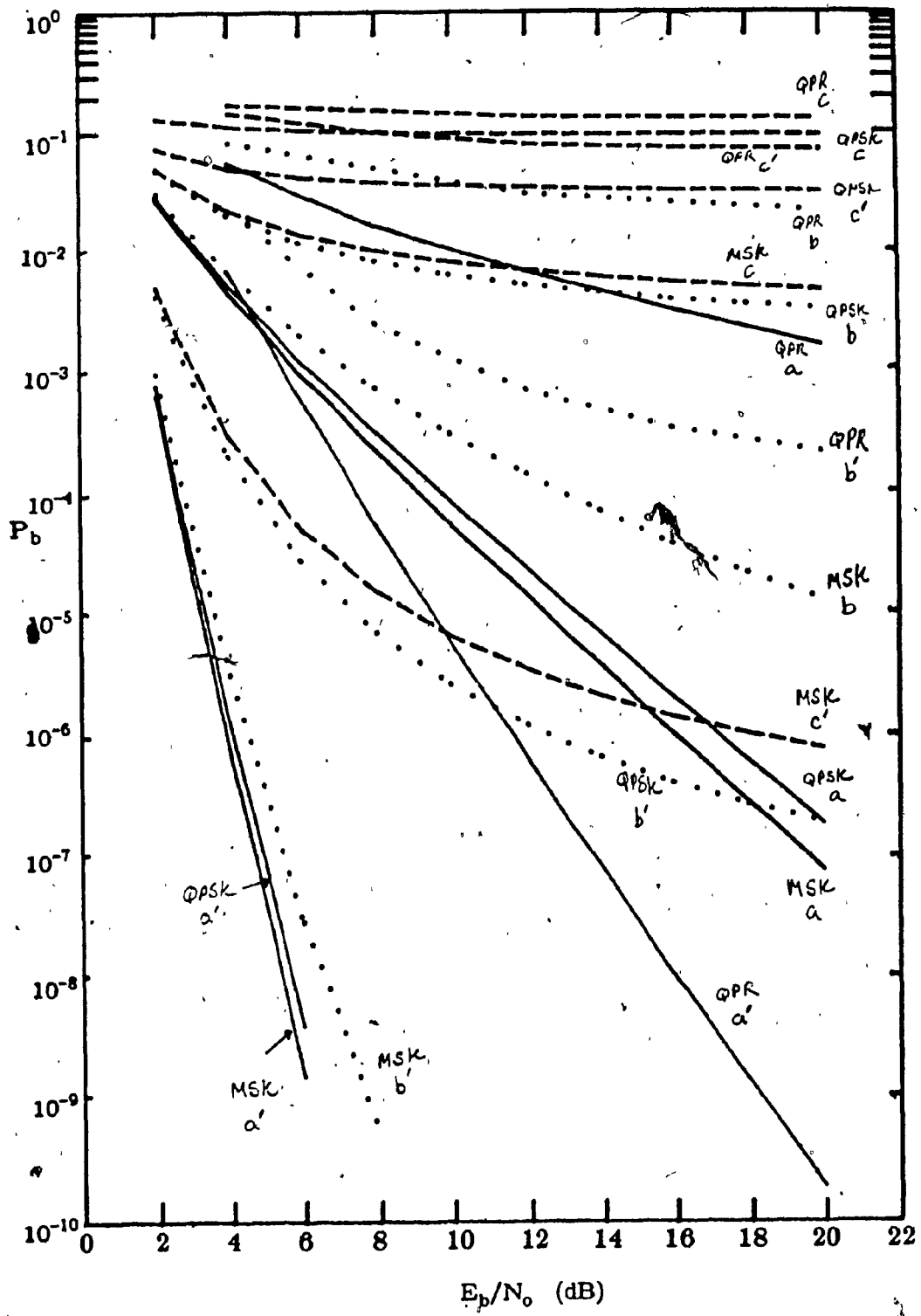

Fig. 5.2-C. P_b versus E_b/N_o for $E_b/N_J = 15$ dB and M = 1000 (coded), and M = 1917 (uncoded).

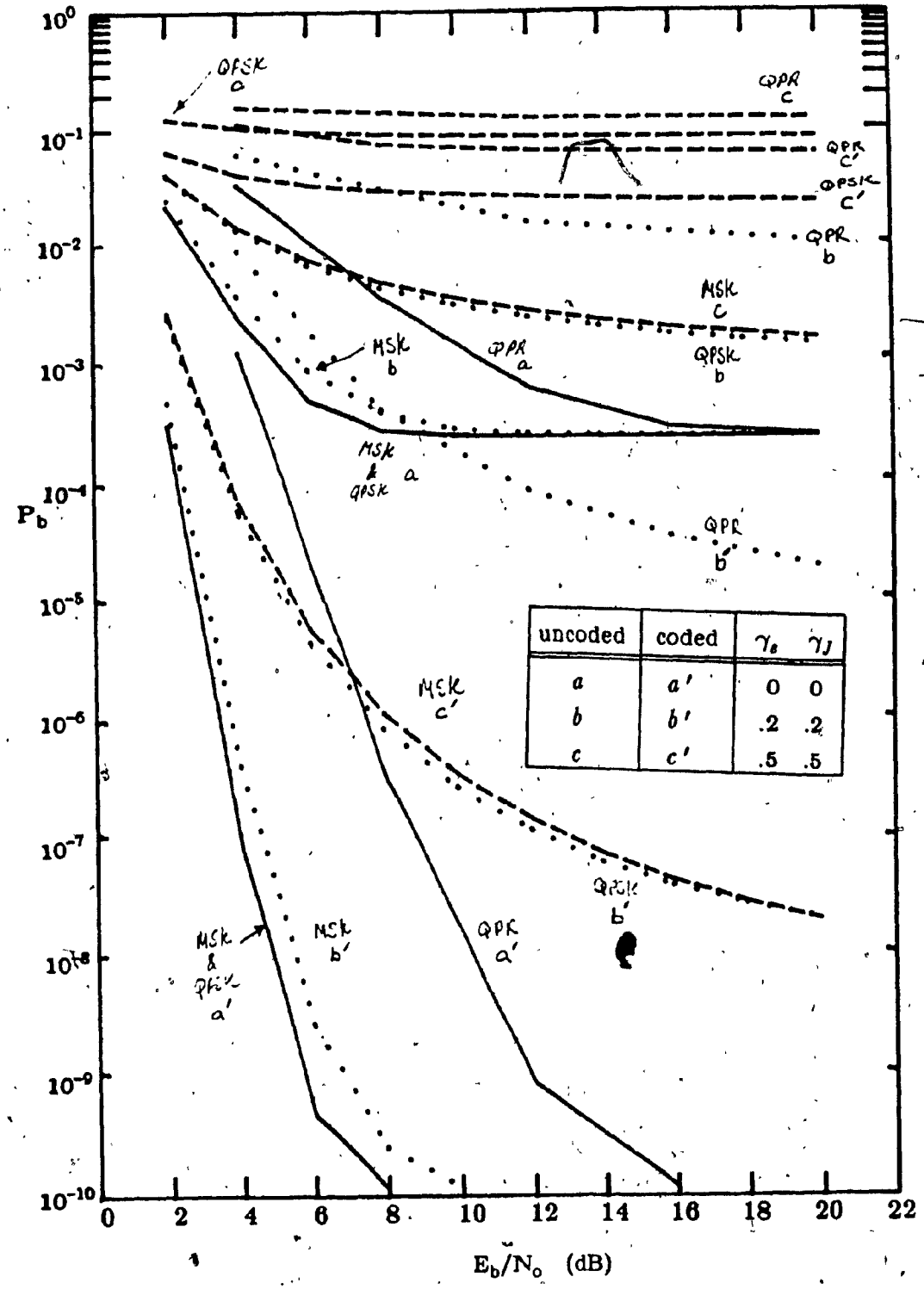

Fig. 5.2-D. P_b versus E_b/N_o for $E_b/N_J = 1$ dB and $M = 1$.

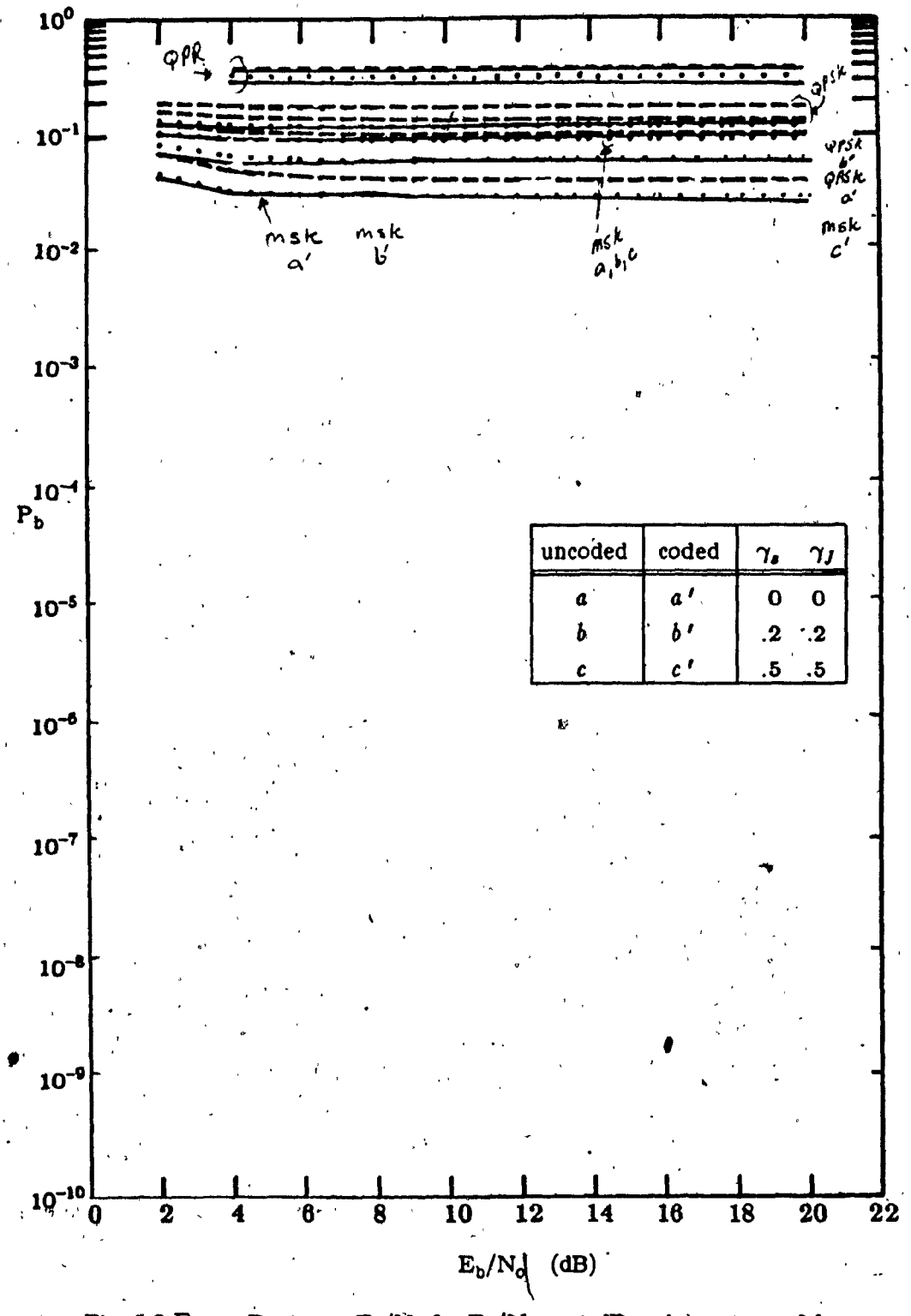

Fig. 5.2-E. P_b versus E_b/N_o for $E_b/N_J = 1$ dB and worst case M.

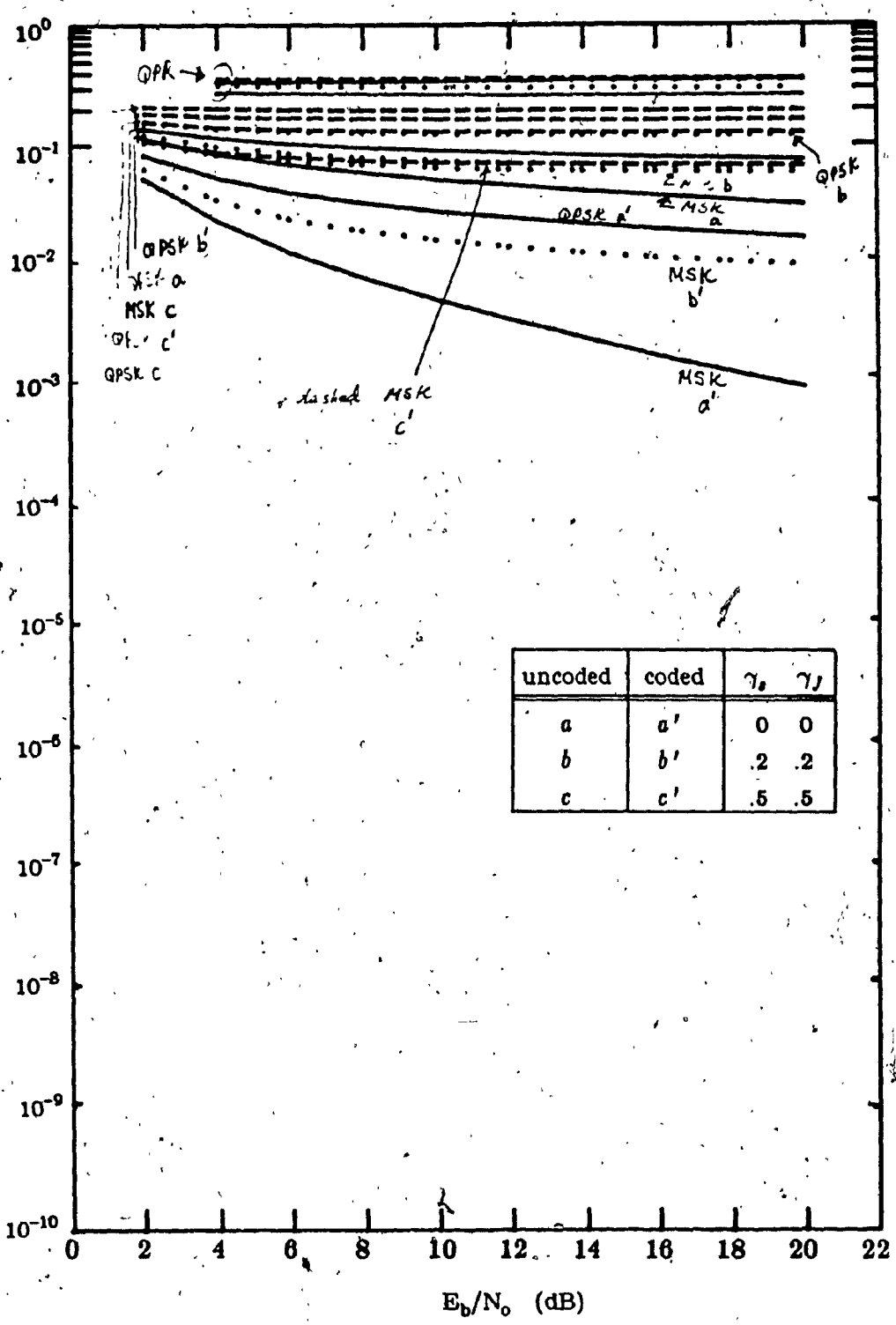

uncoded	coded	γ_s	γ_J
a	a'	0	0
b	b'	.2	.2
c	c'	.5	.5

Fig. 5.2-F. P_b versus E_b/N_o for $E_b/N_J = 1$ dB and $M = 1000$ (coded), and $M = 1917$ (uncoded).

CHAPTER SIX

CONCLUSION

We have presented the performance of the following coherent modulation techniques, quadriphase-shift-keying (QPSK), minimum-shift-keying (MSK), and quadrature-partial-response (QPR), each employing frequency-hopping (FH). The systems were assumed to be operating in the presence of partial band tone jammer. The channel over which the signals were transmitted was modeled as frequency-selective Rician fading known as wide-sense-stationary- uncorrelated-scattering (WSSUS). The probability of bit error for each system was derived both with and without the use of error-correction coding and a comparison for the two cases was made on the basis of equal information rates and equal spread bandwidths.

The probability of bit error derived in the analysis was evaluated numerically and the results plotted for both the uncoded system and coded system employing Golay (23,12) code. It was seen from the figures that under no fading there existed a value of M, the number of jammed tones, for which maximum P_b error occurs, but as γ_s, γ_J increased the performance of the system degraded rapidly. Also we showed the effect of varying E_b/N_o on the performance of P_b for worst case M and suboptimal values of M. It was seen (under fading) the performance of the system is much more sensitive for suboptimal values of M compared to worst case M. In other words, the performance of the system is not sensitive to the presence of the scatter component for worst case M as compared to the cases of suboptimal values of M. It was seen the use of error correction Golay coding improved the performance of the system significantly, but again the

performance is sensitive to γ_s, γ_J, that is as the power in the scatter component increases. It is be emphasized the fact the jammer tries to distribute his tones to match signal power in the uncoded and coded systems such that jammer tone power = signal power which gives worst performance.

Finally, comparison of the three modulation formats was presented. It was seen that FH/MSK scheme resulted in a lower probability of error than FH/QPSK and FH/QPR.

REFERENCES

[1] F.W. Ellersick and D.L. Schilling, *IEEE Journal on Selected Areas in Communications*, Vol. SAC-3, No. 5, September 1985.

[2] S. A. Gronemeyer and A. L. McBRIDE, "MSK and Offset QPSK Modulation", *IEEE Trans. Commun.*, COM-24, No. 8, pp. 809-819, August 1976.

[3] S. Pasupathy, "Correlative Coding: A Bandwidth-Efficient Signaling Scheme", *IEEE Communications Society Magazine*, Vol. 15, No.4, pp.4-11,July 1977.

[4] R.M. Gagliardi, "Frequency Synthesizer Effects in FSK-FH Communications", *IEEE Military Communications Conference*, Vol 3., Session 31, pp. 433-535, October 1984.

[5] M. K. Simon, J. K. Omura, R. A. Scholtz and B. K. Levitt, *Spread Spectrum Communications*, Vol.II, Computer Science Press, Inc., 1985.

[6] O. Yue, "Frequency-Hopping, Multiple-Access, Phase-Shift-Keying System Performance in a Rayleigh Fading Environment", *Bell Syst. Tech. J.*, Vol. 59 pp. 861-878, July 1980.

[7] D. Behraman and W.C. Fifer, "A Low-Cost Spread-Spectrum Packet Radio", *IEEE Military Communications Conference*, Vol. 3, Session 18, pp. 2-10, 1982.

[8] M.K. Simon, "Coherent Detection of Frequency-Hopped Quadrature Modulations in the Presence of Jamming; Part II: QPR Class 1 Modulation", *IEEE Trans. Commun.*, COM-29, No. 11, pp. 1660-1668, November 1981.

[9] L. B. Milstein and D. L. Schilling, "The Effect of Frequency Selective Fading on a Non-Coherent FH-FSK System Operating with Partial Band Tone Interference", *IEEE Trans. Commun.*, vol. COM-30, pp. 904-912, May 1982.

[10] D.P. Taylor and D. Cheung, "The Effect of Carrier Phase Error on the Performance of a Duobinary Shaped QPSK Signal", *IEEE Trans, Commun.*, COM-25, pp. 738-744, July 1977.

[11] D. E. Borth and M. B. Pursley, "Analysis of Direct-Sequence Spread Spectrum Multiple-Access Communication over Rician Fading Channels", *IEEE Trans. Commun.*, COM-28, No 7, 1062-1079, July 1980.

[12] L. B. Milstein, R. L. Pickholtz, and D. L. Schilling, "Optimization of the Processing Gain of an FSK-FH System", *IEEE Trans. Commun.*, COM-28, No. 7, 1062-1079, July 1980.

[13] L. B. Milstein and D. L. Schilling, "Performance of a Spread Spectrum Communication System Operating Over a Frequency-Selective Fading Channel in the Presence of Tone Interference", *IEEE Trans. Commun.*, COM-30, No. 1, pp. 240-247, January 1982.

[14] M. Schwartz, W.R. Bennett, and S. Stein, *Communications Systems and Techniques*, New York: McGraw-Hill, 1966, ch. 9.

[15] P. Kabal and S. Pasupathy, "Partial-Response Signaling", *IEEE Trans. Commun.*, COM-23, pp. 921-935. 1975.

[16] P. Monson, "Fading Channel Communications", *IEEE Communications Society Magazine*, vol. 18, No. 1, pp. 27-36, January 1980.

[17] R. W. Nettleton and G. R. Cooper, "Performance of a Frequency Hopped Differentially Modulated Spread-Spectrum Receiver in a Rayleigh Fading Channel", *IEEE Trans. on Vehicular Technology* vol. VT-30, No.1, pp. 14-29, February 1981.

[18] L. B. Milstein, S. Davidovici, and D. L. Schilling, "The Effect of Multiple-Tone Interfering Signals on a Direct Sequence Spread Spectrum Communication System", *IEEE Trans. Commun.*, COM-30, No. 3, pp. 436-446, March 1982.

[19] H. H. Schreiber, "Self-Noise of Frequency Hopping Signals", *IEEE Trans. Commun. Technology*, vol. Com-17, pp. 588-590, October 1969.

[20] D. H. Morais, A. Sewerinson, and K. Feher, "The Effects of the Amplitude and Delay Slope Components of Frequency Selective Fading on QPSK, Offset QPSK and 8 PSK Systems," *IEEE Trans. Commun.*, COM-27, No. 12, pp. 1849-1853, December 1979.

[21] D. L. Schilling, L. B. Milstein, and R. L. Pickholtz, "Optimization of the Processing Gain of an M-ary Direct Sequence Spread Spectrum Communication System", *IEEE Trans. Commun.*, Com-28, No. 8, pp. 1389-1398, August 1980.

[22] K. Metzger and R. Valentin, "An Analysis of the Sensitivity of Digital Modulation Techniques to Frequency-Selective Fading", *IEEE Trans. Commun.*, vol. Com-33, No. 9, pp. 986-992, September 1985.

APPENDIX A

The dehopped signal (2.7) is multiplied by the reference signal and followed by integrate and dump filtering we get

A.1 Specular signal:

$$\sqrt{S}\int_0^{2T}\left[d_I(t)\cos(\omega_o t)+d_Q(t)\sin(\omega_o t)\right]\cdot\sqrt{2}\cos\omega_o t\ dt$$

$$\approx\sqrt{S}\ \sqrt{2}\frac{1}{2}\int_0^{2T} d_I(t)\ dt$$

$$\approx\sqrt{2S}\ \ T\ d_I, \tag{A.1}$$

A.2 Specular jammer:

$$\int_0^{2T}\sqrt{2J}\ \sum_k P(t-2kT)\,\delta\omega_o\omega_k\cos(\omega_o t+\phi)\cdot\sqrt{2}\cos\omega_o t\ dt$$

$$=\sqrt{2J}\int_0^{2T}\cos(\omega_o t+\phi)\ \sqrt{2}\cos\omega_o t\ dt$$

$$=\sqrt{2J}\ \sqrt{2}\int_0^{2T}\frac{1}{2}\cos\phi\ dt$$

$$=\sqrt{J}\ \ 2T\ \cos\phi \tag{A.2}$$

To evaluate the probability of error (2.15),(2.16) we need the following results results, the conditional variances of the faded signal, faded jammer and of noise. Considering first the variance of the faded jammer.

A.3 Faded Jammer:

$$\sigma_J{}^2=2J\gamma_j^2\,E\left[\int_0^{2T}\mathrm{Re}\left\{\sum_k P(t_1-2kT)\delta\omega_o\omega_k\int_{-\infty}^{\infty}\beta_J(\tau_1)\,d\tau_1\right.\right.$$

$$\cdot \exp\, j\,(\omega_o t_1+\phi)\Big\}\sqrt{2}\cos\omega_o t_1\, dt_1$$

$$\int_0^{2T} \mathrm{Re}\Big\{\sum_{n=-\infty}^{\infty} P(t_2-2nT)\,\delta\omega_o\omega_n \int_{-\infty}^{\infty}\beta_J(\tau_2)\,d\tau_2 \exp\, j\,(\omega_o t_2+\phi)\Big\}$$

$$\sqrt{2}\cos\omega_o t_2\, dt_2\,\Big] \qquad \text{(A.3)}$$

using the relation $Re(a)Re(b) = \frac{1}{2}Re(ab^*) + \frac{1}{2}Re(ab)$ and equations (1.4),(1.5) the above becomes

$$= 2J\gamma_J^2 \int_0^{2T}\int_0^{2T}\int_{-\infty}^{\infty}\int_{-\infty}^{\infty} \rho(\tau_1)\,\delta(\tau_1-\tau_2)\sum_k P(t_1-2kT)\,\delta\omega_o\omega_k$$

$$\cdot \sum_{n=-\infty}^{\infty} P(t_2-2nT)\,\delta\omega_o\omega_n \cos[\omega_o(t_1-t_2)]$$

$$\cdot 2\cos\omega_o t_1 \cos\omega_o t_2 d\tau_1\, d\tau_2\, dt_1\, dt_2 \qquad \text{(A.4)}$$

$$= 2J\gamma_J^2 \frac{2}{4}\int_0^{2T}\rho(\tau)\,d\tau\Big[\sum_k \delta\omega_o\omega_k \int_0^{2T} P(t-2kT)\,dt\Big]^2 \qquad \text{(A.5)}$$

substituting eq. (1.6) the multipath delay spread of the channel which limits the intersymbol interference to just adjacent symbols. Then we get the following four cases

$$\sigma_J^2 = I_{J_i}\,; \qquad i = 1,2,3,4. \qquad \text{(A.6)}$$

case (i) $\omega_{-1} = \omega_o\,,\ \omega_1 = \omega_o$

$$I_{J_1} = \Big[\int_0^{2T} P(t+2T)\,dt + \int_0^{2T} P(t)\,dt + \int_0^{2T} P(t-2T)\,dt,\Big]^2 = 4T^2 \qquad \text{(A.7)}$$

case (ii) $\omega_{-1} \neq \omega_o$, $\omega_1 \neq \omega_o$

$$I_{J_2} = 4T^2 \tag{A.8}$$

case (iii) $\omega_{-1} = \omega_o$, $\omega_1 = \omega_o$

$$I_{J_3} = 4T^2 \tag{A.9}$$

case (iv) $\omega_{-1} = \omega_o$, $\omega_1 \neq \omega_o$

$$I_{J_4} = 4T^2 \tag{A.10}$$

A.4 Faded signal:

Similarly for the faded signal case it can be shown that

$$\sigma_S{}^2 = S\gamma_s^2 E\Big[\int_0^{2T} \mathrm{Re}\Big\{\sum_k \int_{-\infty}^{\infty} \beta_s(\tau_1)\Big[d_I(t_1-\tau_1) + jd_Q(t_1-\tau_1)\Big]$$

$$\cdot P(t_1-2kT-\tau_1)\,\delta\omega_o\omega_k\; d\tau_1 \exp j\,\omega_o t_1\Big\}\sqrt{2}\cos\omega_o t_1\; dt_1$$

$$\int_0^{2T} \mathrm{Re}\Big\{\sum \int_{-\infty}^{\infty} \beta_s(\tau_2)\Big[d_I(t_2-\tau_2) + jd_Q(t_2-\tau_2)\Big]$$

$$\cdot P(t_2-2nT-\tau_2)\,\delta\omega_o\omega_n\; d\tau_2 \exp j\,\omega_o t_2\Big\}\sqrt{2}\cos\omega_o t_2\; dt_2\Big] \tag{A.11}$$

$$\sigma_S^2 = I_{s_i}\,; \qquad i = 1,2,3,4. \tag{A.12}$$

case (i) $\omega_{-1} = \omega_o$, $\omega_1 = \omega_o$

$$I_{s_1} = S\gamma_s^2 \int_{-2T}^{2T} \rho(\tau)\Big\{\Big[\sum_k \delta\omega_o\omega_k \int_0^{2T} d_I(t-\tau)\,P(t-2kT-\tau)\,dt\Big]^2$$

$$+ \Big[\sum_k \delta\omega_o\omega_k \int_0^{2T} d_I(t-\tau)\,P(t-2kT-\tau)\,dt\Big]^2\Big\}\,d\tau \tag{A.13}$$

$$I_{s_1} = S\gamma_s^2 \int_{-2T}^{2T} \rho(\tau) \left\{ \left[\int_{-\tau}^{2T-\tau} d_I(t)\, dt \right]^2 + \left[\int_{-\tau}^{2T-\tau} d_Q(t)\, dt \right]^2 \right\} d\tau \qquad \text{(A.14)}$$

$$I_{s_1} = S\gamma_s^2 T^2 \frac{1}{3} [\, 3\, d_{I_0}^2 + 2\, d_{I_0} d_{I_1} + 4\, d_{I_1}^2 + d_{I_{-1}}^2 + 2\, d_{I_{-1}} d_{I_1} + 3\, d_{Q_0}^2 + 2\, d_{Q_0} d_{Q_1} + 4\, d_{Q_1}^2 + d_{Q_{-1}}^2 + 2\, d_{Q_{-1}} d_{Q_1} \,] \qquad \text{(A.15)}$$

case (ii) $\omega_{-1} \neq \omega_o$, $\omega_1 \neq \omega_o$

$$I_{s_2} = S\gamma_s^2 \int_{-2T}^{0} \rho(\tau) \left\{ \left[\int_{-\tau}^{2T-\tau} d_I(t)\, dt - \int_{2T}^{2T-\tau} d_I(t)\, dt \right]^2 + \left[\int_{-\tau}^{2T-\tau} d_Q(t)\, dt - \int_{2T}^{2T-\tau} d_Q(t)\, dt \right]^2 \right\} d\tau + S\gamma_s^2 \int_{0}^{2T} \rho(\tau) \left\{ \left[\int_{0}^{2T-\tau} d_I(t) dt \right]^2 + \left[\int_{0}^{2T-\tau} d_Q(t) dt \right]^2 \right\} d\tau \qquad \text{(A.16)}$$

$$I_{s_2} = S\gamma_s^2 T^2 [\, 2\, d_{I_0}^2 + 2\, d_{Q_0}^2 \,] \qquad \text{(A.17)}$$

case (iii) $\omega_{-1} \neq \omega_o$, $\omega_1 = \omega_o$

$$I_{s_3} = S\gamma_s^2 \int_{-2T}^{0} \rho(\tau) \left\{ \left[\int_{-\tau}^{2T-\tau} d_I(t) dt \right]^2 + \left[\int_{-\tau}^{2T-\tau} d_Q(t) dt \right]^2 \right\} d\tau + S\gamma_s^2 \int_{0}^{2T} \rho(\tau) \left\{ \left[\int_{0}^{2T-\tau} d_I(t) dt \right]^2 + \left[\int_{0}^{2T-\tau} d_Q(t) dt \right]^2 \right\} d\tau \qquad \text{(A.18)}$$

$$I_{s_3} = S\gamma_s^2 T^2 \left[2\, d_{I_0}^2 + \frac{2}{3}\, d_{I_0} d_{I_1} + \frac{1}{3}\, d_{I_1}^2 + 2\, d_{Q_0}^2 + \frac{2}{3}\, d_{Q_0} d_{Q_1} + \frac{1}{3}\, d_{Q_1}^2 \right] \qquad \text{(A.19)}$$

case (iv) $\omega_{-1} = \omega_o$, $\omega_1 \neq \omega_o$

$$I_{s_4} = S\gamma_s^2 \int_{-2T}^{0} \rho(\tau) \Bigg\{ \left[\int_{-\tau}^{2T-\tau} d_I(t)\, dt - \int_{2T}^{2T-\tau} d_I(t)\, dt \right]^2 + \left[\int_{-\tau}^{2T-\tau} d_Q(t)\, dt - \int_{2T}^{2T-\tau} d_Q(t)\, dt \right]^2 \Bigg\} d\tau + S\gamma_s^2 \int_{0}^{2T} \rho(\tau) \Bigg\{ \left[\int_{-\tau}^{2T-\tau} d_I(t)\, dt \right]^2 + \left[\int_{-\tau}^{2T-\tau} d_Q(t)\, dt \right]^2 \Bigg\} d\tau \tag{A.20}$$

$$I_{s_4} = S\gamma_s^2 T^2 \frac{1}{3} \left[6\, d_{I_0}{}^2 + d_{I_{-1}}{}^2 + 2\, d_{I_{-1}} d_{I_0} + 6\, d_{Q_0}{}^2 + d_{Q_{-1}}{}^2 + 2\, d_{Q_{-1}} d_{Q_0} \right] \tag{A.21}$$

A.5 Probability of bit error:

Assuming $d_{I_0} = 1$ then P_b error is

$$P_b(e \mid \phi, \lambda_J, d_{Q_{-1}}, d_{Q_0}, d_{Q_1}, d_{I_{-1}}, d_{I_1}, \omega_{-1}, \omega_1) = Pr\{Z_i < 0 \mid d_{I_0} = 1\} \tag{A.22}$$

$$P_b = Q\left(\frac{\sqrt{2S} + 2\sqrt{J}T \cos\phi}{\left[N_o T + S\gamma_s^2 T^2 I_{s_4} + J\gamma_J^2 T^2 I_{J_4} \right]^{1/2}} \right) \tag{A.23}$$

Since $E_b = ST$ and

$$\frac{2J}{S} = \frac{2J_T}{\rho NS} \tag{A.24}$$

Also since the hop frequency slots are $1/2T$ wide and total hop frequency band W_{ss} the number of hop slots N is

$$N = 2W_{ss}\, T \tag{A.25}$$

Therefore substituting (A.25) into (A.24) gives

$$\frac{2J}{S} = \frac{J_T / W_{ss}}{\rho ST} = \frac{J_T / W_{ss}}{\rho E_b} = \frac{N_J}{\rho E_b} \tag{A.26}$$

where N_J represents the effective jammer power spectral density in the hop

band. Thus using the above results P_b may be written as,

$$P_b = Q\left(\frac{1+\sqrt{N_{ij}/\rho E_b}\cos\phi}{\left[\frac{N_o}{2E_b}+\frac{\gamma_s^2}{2}I_{s_i}+\frac{\gamma_J^2}{4}\frac{N_J}{\rho E_b}I_{J_i}\right]^{1/2}}\right) \qquad \text{(A.27)}$$

APPENDIX B

B.1 Specular signal:

$$\int_{-T}^{T} r_d(t)I(t)dt = \sqrt{2}A\int_{-T}^{T}\Big[d_I(t)\cos\frac{\pi t}{2T}\cos\omega_o t + I(t)P(t)d_Q(t)\sin\frac{\pi t}{2T}\sin\omega_o t\Big] \cdot \sqrt{2}\cos\frac{\pi t}{2T}\cos\omega_o t \; dt = ATd_{I_0} \tag{B.1}$$

B.2 Specular jammer:

$$\lambda_J\sqrt{J}\;2\int_{-T}^{T}\sum_j P(t-jT)\,\delta\omega_o\omega_j\cos(\omega_o t+\phi)\cos\omega_o t\cos\frac{\pi t}{2T}\,dt = \frac{248\lambda_J\sqrt{J}\,T}{63\pi}\cos\phi \tag{B.2}$$

B.3 Faded signal:

We need the following results to evaluate the probability of error the conditional variances of the faded signal, faded jammer and of noise.

$$\sigma_\delta^2 = 2^2A^2\gamma_s^2\,E\Big[\int_{-T}^{T}\mathrm{Re}\Big\{\sum_j\int_{-\infty}^{\infty}\beta_s(\tau_1)\Big[d_I(t_1-\tau_1)I_j(t_1-\tau_1)\cos\frac{\pi}{2T}(t_1-\tau_1) - j\;d_Q(t_1-\tau_1)P(t_1-2jT-\tau_1)\sin\frac{\pi}{2T}(t_1-\tau_1)\Big]\;\delta\omega_o\omega_j\;d\tau_1\exp j\omega_o t_1\Big\} \cdot \cos\frac{\pi}{2T}t_1\cos\omega_o t_1\;dt_1 \cdot \int_{-T}^{T}\mathrm{Re}\Big\{\sum_k\int_{-\infty}^{\infty}\beta_s(\tau_2)\Big[d_I(t_2-\tau_2)I_j(t_2-\tau_2)\cos\frac{\pi}{2T}(t_2-\tau_2) - j\;d_Q(t_2-\tau_2)P(t_2-2kT-\tau_2)\sin\frac{\pi}{2T}(t_2-\tau_2)\Big]\;\delta\omega_o\omega_k\;d\tau_2\exp j\omega_o t_2\Big\}$$

$$\cdot \cos\frac{\pi}{2T}t_2 \cos\omega_o t_2 \, dt_2 \Big] \qquad \text{(B.3)}$$

Applying the relation $Re(a)Re(b) = \frac{1}{2}Re(ab^*) + \frac{1}{2}Re(ab)$ to the above results in

$$\sigma_s^2 = \frac{4}{2}A^2\gamma_s^2 \int_{-T}^{T}\int_{-T}^{T}\int_{-\infty}^{\infty}\int_{-\infty}^{\infty} E[\beta_s(\tau_1)\beta_s^*(\tau_2)]$$

$$\cdot \sum_j \delta\omega_o \omega_j \Big[d_I(t_1-\tau_1)\, I_j(t_1-\tau_1)\cos\frac{\pi}{2T}(t_1-\tau_1)$$

$$- j\, d_Q(t_1-\tau_1)\, P(t_1-2jT-\tau_1)\sin\frac{\pi}{2T}(t_1-\tau_1)\Big]$$

$$\cdot \sum_k \delta\omega_o \omega_k \Big[d_I(t_2-\tau_2)\, I_k(t_1-\tau_1)\cos\frac{\pi}{2T}(t_2-\tau_2)$$

$$+ j\, d_Q(t_2-\tau_2)\, P(t_2-2kT-\tau_2)\sin\frac{\pi}{2T}(t_2-\tau_2)\Big]$$

$$\cdot \cos\frac{\pi}{2T}t_1 \cos\frac{\pi}{2T}t_2 \, dt_1 dt_2 d\tau_1 d\tau_2 \qquad \text{(B.4)}$$

$$\sigma_s^2 = 4A^2\gamma_s^2 \int_{-2T}^{2T} \rho(\tau)\Big\{ \Big[\sum_j \delta\omega_o \omega_j \int_{-T}^{T} P(t-jT-\tau)\, I_j(t-\tau) d_I(t-\tau)$$

$$\cdot \cos\frac{\pi}{2T}(t-\tau)\cos\frac{\pi t}{2T}dt\Big]^2$$

$$+ \Big[\sum_j \delta\omega_o \omega_j \int_{-T}^{T} P(t-2jT-\tau)\, d_Q(t-\tau)\sin\frac{\pi}{2T}(t-\tau)\cos\frac{\pi t}{2T}dt\Big]^2\Big\} d\tau$$

$$\qquad \text{(B.5)}$$

case (i) $\omega_{-1} = \omega_o$, $\omega_1 = \omega_o$

$$I_{s_1} = 4A^2\gamma_s^2 \int_{-2T}^{T} p(\tau)\Bigg\{ \Bigg[\int_{-T-\tau}^{T-\tau} d_I(t) \cos\frac{\pi}{2T}t \cos\frac{\pi}{2T}(t+\tau)dt \Bigg]^2$$
$$+ \Bigg[\int_{-T-\tau}^{T-\tau} d_Q(t) \sin\frac{\pi}{2T}t \cos\frac{\pi}{2T}(t+\tau)dt$$
$$- \int_{2T}^{T-\tau} d_Q(t) \sin\frac{\pi}{2T}t \cos\frac{\pi}{2T}(t+\tau)dt \Bigg]^2 \Bigg\} d\tau$$
$$+ 4A^2\gamma_s^2 \int_{-T}^{0} \rho(\tau)\Bigg\{ \Bigg[\int_{-T-\tau}^{T-\tau} d_I(t) \cos\frac{\pi}{2T}t \cos\frac{\pi}{2T}(t+\tau)dt \Bigg]^2$$
$$+ \Bigg[\int_{-T-\tau}^{T-\tau} d_Q(t) \sin\frac{\pi}{2T}t \cos\frac{\pi}{2T}(t+\tau)dt \Bigg)^2 \Bigg\} d\tau$$
$$+ 4A^2\gamma_s^2 \int_{0}^{T} \rho(\tau)\Bigg\{ \Bigg[\int_{-T-\tau}^{T-\tau} d_I(t) \cos\frac{\pi}{2T}t \cos\frac{\pi}{2T}(t+\tau)dt \Bigg]^2$$
$$+ \Bigg[\int_{-T-\tau}^{T-\tau} d_Q(t) \sin\frac{\pi}{2T}t \cos\frac{\pi}{2T}(t+\tau)dt \Bigg]^2 \Bigg\} d\tau$$
$$+ 4A^2\gamma_s^2 \int_{T}^{2T} \rho(\tau)\Bigg\{ \Bigg[\int_{-T-\tau}^{T-\tau} d_I(t) \cos\frac{\pi}{2T}t \cos\frac{\pi}{2T}(t+\tau)dt \Bigg]^2$$
$$+ \Bigg[\int_{-2T}^{T-\tau} d_Q(t) \sin\frac{\pi}{2T}t \cos\frac{\pi}{2T}(t+\tau)dt \Bigg]^2 \Bigg\} d\tau \qquad \text{(B.6)}$$

$$I_{s_1} = 4A^2T^2\gamma_s^2 \Bigg\{ d_{I_0}{}^2 \Big[\frac{4}{\pi^2}+\frac{1}{3}\Big] + d_{I_0}d_{I_1}\Big[\frac{-2}{\pi^2}-\frac{1}{6}\Big]$$
$$+ d_{I_1}{}^2\Big[\frac{1}{\pi^2}+\frac{1}{12}\Big] + d_{Q_0}{}^2\Big[\frac{7}{4\pi^2}+\frac{21}{64}+\frac{3}{2\pi^4}\Big]$$
$$+ d_{Q_{-1}}{}^2\Big[\frac{7}{4\pi^2}+\frac{21}{64}+\frac{1}{2\pi^4}\Big] + d_{Q_{-1}}d_{Q_0}\Big[\frac{-4}{\pi^2}-\frac{6}{\pi^4}+\frac{13}{48}\Big]$$
$$+ d_{I_{-1}}{}^2\Big[\frac{1}{\pi^2}+\frac{1}{12}\Big] + d_{I_{-1}}d_{I_0}\Big[\frac{-4}{\pi^2}+\frac{1}{6}\Big] \Bigg\} \qquad \text{(B.7)}$$

case (ii) $\omega_{-1} \neq \omega_0$, $\omega_1 \neq \omega_0$

$$I_{s_2} = 4A^2\gamma_s^2 \int_{-2T}^{-T} \rho(\tau)\Bigg\{ \Bigg[\int_{-T-\tau}^{T-\tau} d_I(t) \cos\frac{\pi}{2T}t \cos\frac{\pi}{2T}(t+\tau)dt$$

$$- \int_{T}^{T-\tau} d_I(t) \cos\frac{\pi}{2T}t \cos\frac{\pi}{2T}(t+\tau)dt \Big]^2$$

$$+ \Big[\int_{-T-\tau}^{T-\tau} d_Q(t) \sin\frac{\pi}{2T}t \cos\frac{\pi}{2T}(t+\tau)dt$$

$$- \int_{2T}^{T-\tau} d_Q(t) \sin\frac{\pi}{2T}t \cos\frac{\pi}{2T}(t+\tau)dt \Big]^2 \Big\} d\tau$$

$$+ 4A^2\gamma_s^2 \int_{-T}^{0} \rho(\tau) \Big\{ \Big[\int_{-T-\tau}^{T-\tau} d_I(t) \cos\frac{\pi}{2T}t \cos\frac{\pi}{2T}(t+\tau)dt$$

$$- \int_{I}^{T-\tau} d_I(t) \cos\frac{\pi}{2T}t \cos\frac{\pi}{2T}(t+\tau)dt \Big]^2$$

$$+ \Big[\int_{0}^{T-\tau} d_Q(t) \sin\frac{\pi}{2T}t \cos\frac{\pi}{2T}(t+\tau)dt \Big]^2 \Big\} d\tau$$

$$+ 4A^2\gamma_s^2 \int_{0}^{T} \rho(\tau) \Big\{ \Big[\int_{0}^{2T-\tau} d_I(t) \cos\frac{\pi}{2T}t \cos\frac{\pi}{2T}(t+\tau)dt \Big]^2$$

$$+ \Big[\int_{0}^{T-\tau} d_Q(t) \sin\frac{\pi}{2T}t \cos\frac{\pi}{2T}(t+\tau)dt \Big]^2 \Big\} d\tau$$

$$+ 4A^2\gamma_s^2 \int_{T}^{2T} \rho(\tau) \Big\{ \Big[\int_{0}^{2T-\tau} d_I(t) \cos\frac{\pi}{2T}t \cos\frac{\pi}{2T}(t+\tau)dt \Big]^2 \Big\} d\tau \qquad \text{(B.8)}$$

$$I_{s_2} = 2A^2\gamma_s^2 T^2 \Big\{ d_{I_0}^2 \Big[\frac{15}{8\pi^2} - \frac{1}{\pi^4} + \frac{37}{192} \Big] + d_{Q_0}^2 \Big[\frac{-3}{2\pi^4} + \frac{21}{64} \Big]$$

$$+ d_{I_0} d_{I_1} \Big[\frac{5}{96} + \frac{1}{2\pi^4} \Big] + d_{I_1}^2 \Big[\frac{1}{8\pi^2} - \frac{1}{192} \Big] \Big\} \qquad \text{(B.9)}$$

case (iii) $\omega_{-1} \neq \omega_0$, $\omega_1 = \omega_0$

$$I_{s_3} = 4A^2\gamma_s^2 \int_{-2T}^{-T} \rho(\tau) \Big\{ \Big[\int_{-T-\tau}^{T-\tau} d_I(t) \cos\frac{\pi}{2T}t \cos\frac{\pi}{2T}(t+\tau)dt \Big]^2$$

$$+ \Big[\int_{-T-\tau}^{T-\tau} d_Q(t) \sin\frac{\pi}{2T}t \cos\frac{\pi}{2T}(t+\tau)dt$$

$$- \int_{2T}^{T-\tau} d_Q(t) \sin \frac{\pi}{2T} t \cos \frac{\pi}{2T}(t+\tau) dt \Big]^2 \Big\} d\tau$$

$$+ 4A^2\gamma_s^2 \int_{-T}^{0} \rho(\tau) \Big\{ \Big[\int_{-T-\tau}^{T-\tau} d_I(t) \cos \frac{\pi}{2T} t \cos \frac{\pi}{2T}(t+\tau) dt \Big]^2$$

$$+ \Big[\int_{0}^{T-\tau} d_Q(t) \sin \frac{\pi}{2T} t \cos \frac{\pi}{2T}(t+\tau) dt \Big]^2 \Big\} d\tau$$

$$+ 4A^2\gamma_s^2 \int_{0}^{T} \rho(\tau) \Big\{ \Big[\int_{-T-\tau}^{T-\tau} d_I(t) \cos \frac{\pi}{2T} t \cos \frac{\pi}{2T}(t+\tau) dt \Big]^2$$

$$+ \Big[\int_{0}^{T-\tau} d_Q(t) \sin \frac{\pi}{2T} t \cos \frac{\pi}{2T}(t+\tau) dt \Big]^2 \Big\} d\tau$$

$$+ 4A^2\gamma_s^2 \int_{T}^{2T} \rho(\tau) \Big\{ \Big[\int_{-T-\tau}^{T-\tau} d_I(t) \cos \frac{\pi}{2T} t \cos \frac{\pi}{2T}(t+\tau) dt \Big]^2 \Big\} d\tau \quad \text{(B.10)}$$

$$I_{s_3} = 4A^2\gamma_s^2 T^2 \Big\{ d_{I_0}{}^2 \Big[\frac{21}{8\pi^2} + \frac{31}{96} + \frac{3}{8\pi^4} \Big] + d_{I_0} d_{I_1} \Big[\frac{-2}{\pi^2} - \frac{1}{6} \Big]$$

$$+ d_{I_1}{}^2 \Big[\frac{1}{\pi^4} + \frac{1}{12} \Big] + d_{Q_0}{}^2 \Big[\frac{5}{4\pi^2} + \frac{21}{64} + \frac{3}{2\pi^4} \Big]$$

$$+ d_{I_{-1}}{}^2 \Big[\frac{1}{\pi^2} + \frac{1}{12} \Big] + d_{I_{-1}} d_{I_0} \Big[\frac{-17}{4\pi^2} + \frac{1}{6} + \frac{1}{\pi^4} \Big] \Big\} \quad \text{(B.11)}$$

case (iv) $\omega_{-1} = \omega_o$, $\omega_1 \neq \omega_o$

$$I_{s_4} = 4A^2\gamma_s^2 \int_{-2T}^{T} \rho(\tau) \Big\{ \Big[\int_{-T-\tau}^{T-\tau} d_I(t) \cos \frac{\pi}{2T} t \cos \frac{\pi}{2T}(t+\tau) dt$$

$$- \int_{T}^{T-\tau} d_I(t) \cos \frac{\pi}{2T} t \cos \frac{\pi}{2T}(t+\tau) dt \Big]^2$$

$$+ \Big[\int_{-T-\tau}^{T-\tau} d_Q(t) \sin \frac{\pi}{2T} t \cos \frac{\pi}{2T}(t+\tau) dt$$

$$- \int_{2T}^{T-\tau} d_Q(t) \sin \frac{\pi}{2T} t \cos \frac{\pi}{2T}(t+\tau) dt \Big]^2 \Big\} d\tau$$

$$+ 4A^2\gamma_s^2 \int_{-T}^{0} \rho(\tau) \Big\{ \Big[\int_{-T-\tau}^{T-\tau} d_I(t) \cos \frac{\pi}{2T} t \cos \frac{\pi}{2T}(t+\tau) dt$$

$$- \int_{T}^{T-\tau} d_I(t) \cos\frac{\pi}{2T}t \cos\frac{\pi}{2T}(t+\tau)dt \Big]^2$$

$$+ \int_{-T-\tau}^{T-\tau} d_Q(t) \sin\frac{\pi}{2T}t \cos\frac{\pi}{2T}(t+\tau)dt \Big]^2 \Big\} d\tau$$

$$+ 4A^2\gamma_s^2 \int_{0}^{T} \rho(\tau) \Big\{ \Big[\int_{-T-\tau}^{T-\tau} d_I(t) \cos\frac{\pi}{2T}t \cos\frac{\pi}{2T}(t+\tau)dt \Big]^2$$

$$+ \Big[\int_{-T-\tau}^{T-\tau} d_Q(t) \sin\frac{\pi}{2T}t \cos\frac{\pi}{2T}(t+\tau)dt \Big]^2 \Big\} d\tau$$

$$+ 4A^2\gamma_s^2 \int_{T}^{2T} \rho(\tau) \Big\{ \Big[\int_{-T-\tau}^{T-\tau} d_I(t) \cos\frac{\pi}{2T}t \cos\frac{\pi}{2T}(t+\tau)dt \Big]^2$$

$$+ \Big[\int_{-2T}^{T-\tau} d_Q(t) \sin\frac{\pi}{2T}t \cos\frac{\pi}{2T}(t+\tau)dt \Big]^2 \Big\} d\tau \qquad \text{(B.12)}$$

$$I_{s_4} = 4A^2\gamma_s^2 \Big\{ d_{I_0}{}^2 \Big[\frac{4}{\pi^2}+\frac{1}{3}\Big] + d_{Q_0}{}^2 \Big[\frac{7}{4\pi^2}+\frac{3}{2\pi^4}+\frac{1}{8}\Big]$$

$$+ d_{Q_{-1}}{}^2 \Big[\frac{7}{4\pi^2}+\frac{3}{2\pi^4}+\frac{21}{64}\Big] + d_{Q_{-1}}d_{Q_0}\Big[\frac{-4}{\pi^2}-\frac{6}{\pi^4}+\frac{13}{48}\Big]$$

$$+ d_{I_{-1}}{}^2 \Big[\frac{1}{\pi^2}+\frac{1}{12}\Big] + d_{I_{-1}}d_{I_0}\Big[\frac{-4}{\pi^2}\frac{-3}{\pi^4}+\frac{1}{6}\Big] \Big\} \qquad \text{(B.13)}$$

B.4 Faded Jammer:

$$\sigma_j^2 = 4\lambda\gamma_j^2 E\Big[\int_{-T}^{T} \mathrm{Re}\Big\{ \sum_j P(t_1 - 2jT)\, \delta\omega_o\, \omega_j \int_{-\infty}^{\infty} \beta_j(\tau_1) \exp j(\omega_o t_1 + \phi) \Big\}$$

$$\cdot \cos\frac{\pi}{2T}t_1 \cos\omega_o t_1\, dt_1$$

$$\int_{-T}^{T} \mathrm{Re}\Big\{ \sum_k P(t_1 - 2kT)\, \delta\omega_o\, \omega_k \int_{-\infty}^{\infty} \beta_j(\tau_2) \exp j(\omega_o t_2 + \phi) \Big\}$$

$$\cdot \cos\frac{\pi}{2T}t_2 \cos\omega_o t_2\, dt_2 \Big] \qquad \text{(B.14)}$$

Applying the relation $Re(a)Re(b) = \frac{1}{2}Re(ab^*) + \frac{1}{2}Re(ab)$ to the above results in

$$\sigma_j^2 = J\gamma_j^2\lambda \int_{-2T}^{2T} \rho(\tau) \left[\int_{-T}^{T} \cos \frac{\pi}{2T} t \ dt \right]^2 d\tau \tag{B.15}$$

For case of jammer

case (i) $\omega_{-1} = \omega_o$; $\omega_1 = \omega_o$

$$I_{J_1} = \lambda J \gamma_j^2 \left(\frac{4T}{\pi} \right)^2 \tag{B.16}$$

case (ii) $\omega_{-1} \neq \omega_o$, $\omega_1 \neq \omega_o$

$$I_{J_2} = \lambda J \gamma_j^2 \left(\frac{4T}{\pi} \right)^2 \tag{B.17}$$

case (iii) $\omega_{-1} \neq \omega_o$, $\omega_1 = \omega_o$

$$I_{J_3} = \lambda J \gamma_j^2 \left(\frac{4T}{\pi} \right)^2 \tag{B.18}$$

case (iv) $\omega_{-1} = \omega_o$, $\omega_1 \neq \omega_o$

$$I_{J_4} = \lambda J \gamma_j^2 \left(\frac{4T}{\pi} \right)^2 \tag{B.19}$$

B.5 Probability of bit error:

$$P_b(e \mid \phi, \lambda_J, d_{Q_{-1}}, d_{Q_0}, d_{Q_1}, d_{I_{-1}}, d_{I_1}, \omega_{-1}, \omega_1)$$

$$= Q\left(\frac{AT + \frac{248\sqrt{J}}{63\pi} T \cos\phi}{\left[\sigma_N^2 + \sigma_S^2 + \sigma_j^2 \right]^{1/2}} \right)$$

As was done in Appendix A, writing in terms of E_b/N_o and E_b/N_j where $S = A^2$ then we get

$$= Q\left(\frac{1 + \frac{248}{63\pi} \sqrt{N_J/2\rho E_b} \cos\phi}{\left[\frac{N_o}{2E_b} + \frac{\gamma_s^2}{2} I_{s_1} + \frac{8\gamma_j^2}{\pi^2} \frac{N_J}{\rho E_b} I_{J_1} \right]^{1/2}} \right) \tag{B.20}$$

APPENDIX C

C.1 Specular signal:

$$Z_Q(t) = \left[r_d(t)(\sqrt{2}\cos w_o t) \right] * h_R(t)$$
$$= 2A \sum_{n=-\infty}^{\infty} c_n \, h_T(t-2nT)\cos^2 w_o t * h_R(t)$$
$$= A \sum_{n=-\infty}^{\infty} c_n \, h(t-2nT) \qquad \text{(C.1)}$$

C.2 Specular jammer:

$$2\sqrt{J}\cos(w_o t+\phi)\cos w_o t * h_R(t)$$
$$= \sqrt{J}\, H_R(0)\cos\phi \qquad \text{(C.2)}$$

C.3 Faded signal:

To evaluate the probability of error (4.32) we need the following results. The conditional variances of the faded signal, faded jammer and of noise. Considering first the variance of the faded signal

$$\sigma_Q^2 = E\Big\{ \mathrm{Re}\Big[\gamma_s A \sum_k \delta\omega_o \omega_k \sum_{n=-\infty}^{\infty} c_n$$
$$\int_{-\infty}^{\infty} \beta_s(\tau_1) P(t-2kT-\tau_1)\, h_T(t-\tau_1-2nT)\, d\tau_1 * h_R(t) \Big]$$
$$\mathrm{Re}\Big[\gamma_s A \sum_l \delta\omega_o \omega_l \sum_{m=-\infty}^{\infty} c_m$$
$$\int_{-\infty}^{\infty} \beta_s(\tau_2)\, P(t-2lT-\tau_2)\, h_T(t-\tau_2-2mT)\, d\tau_2 * h_R(t) \Big] \Big\} \qquad \text{(C.3)}$$

using the relation $Re(a)Re(b) = \frac{1}{2}Re(ab^*) + \frac{1}{2}Re(ab)$ and equations (1.4),(1.5) the above becomes

$$\sigma_Q^2 = \frac{\gamma_s^2 A^2}{2} \int_{-\infty}^{\infty}\int_{-\infty}^{\infty}\int_{-\infty}^{\infty}\int_{-\infty}^{\infty} E\left[\beta_s(\tau_1)\beta_s^*(\tau_2)\right]$$

$$\sum_k \delta\omega_o\,\omega_k \sum_{n=-\infty}^{\infty} c_n\,P(l_1-2kT-\tau_1)\,h_T(l_1-\tau_1-2nT)\,h_R(t-l_1)$$

$$\sum_l \delta\omega_o\,\omega_l \sum_{m=-\infty}^{\infty} c_m\,P(l_2-2lT-\tau)\,h_T(l_2-\tau-2mT)\,h_R(t-l_2)$$

$$d\tau_1 d\tau_2 dl_1 dl_2 \qquad \text{(C.4)}$$

Substituting eq. (1.5) in the above results in

$$\sigma_Q{}^2 = \frac{\gamma_s^2 A^2}{2} \int_{-\infty}^{\infty}\int_{-\infty}^{\infty}\int_{-\infty}^{\infty} \rho(\tau) \sum_k \delta\omega_o\,\omega_k$$

$$\sum_{n=-\infty}^{\infty} c_n\,P(l_1-2kT-\tau)\,h_T(l_1-\tau-2nT)\,h_R(t-l_1)$$

$$\sum_l \delta\omega_o\,\omega_l \sum_{m=-\infty}^{\infty} c_m\,P(l_2-2lT-\tau)\,h_T(l_2-\tau-2mT)\,h_R(t-l_2)\,d\tau\,dl_1\,dl_2$$

(C.5)

$$\sigma_Q{}^2 = \gamma_s^2 A^2 \int_{-2T}^{2T} \rho(\tau) \Big[\sum_k \delta\omega_o\,\omega_k$$

$$\int_{-\infty}^{\infty} \sum_{n=-\infty}^{\infty} c_n\,P(\lambda-2kT-\tau)\,h_T(\lambda-\tau-2nT)\,h_R(t-\lambda)\,d\lambda \Big]^2 d\tau$$

(C.6)

Substituting eq. (1.6) the multipath-delay spread of the channel which limits the intersymbol interference to just adjacent symbols. Then we get the following four cases

$$\sigma_Q{}^2 = \frac{\gamma_s^2 A^2 16 T^3}{2\pi^4} I_{s_i} \; ; \qquad i = 1,2,3,4. \qquad \text{(C.7)}$$

case (i) $\omega_{-1} = \omega_o\,,\ \omega_1 = \omega_o$

$$I_{s_1} = \int_{-2T}^{0} \left(1 + \frac{\tau}{2T}\right) \Big[\sum_{n=-2}^{2} c_n \int_{-2T+\tau}^{4T+\tau} h_T(\lambda-\tau-2nT)\,h_R(t-\lambda)\,d\lambda \Big]^2 d\tau$$

$$+\int_{0}^{2T}\left[1-\frac{\tau}{2T}\right]\left[\sum_{n=-2}^{2}c_n\int_{-2T+\tau}^{4T+\tau}h_T(\lambda-\tau-2nT)h_R(t-\lambda)d\lambda\right]^2 d\tau \quad \text{(C.8)}$$

case (ii) $\omega_{-1}\neq\omega_o$, $\omega_1\neq\omega_o$

$$I_{s_2}=\int_{-2T}^{0}\left[1+\frac{\tau}{2T}\right]\left[\sum_{n=-2}^{2}c_n\int_{\tau}^{2T+\tau}h_T(\lambda-\tau-2nT)h_R(t-\lambda)d\lambda\right]^2 d\tau$$
$$+\int_{0}^{2T}\left[1-\frac{\tau}{2T}\right]\left[\sum_{n=-2}^{2}c_n\int_{\tau}^{2T+\tau}h_T(\lambda-\tau-2nT)h_R(t-\lambda)d\lambda\right]^2 d\tau \quad \text{(C.9)}$$

case (iii) $\omega_{-1}\neq\omega_o$, $\omega_1=\omega_o$

$$I_{s_3}=\int_{-2T}^{0}\left[1+\frac{\tau}{2T}\right]\left[\sum_{n=-2}^{2}c_n\int_{\tau}^{4T+\tau}h_T(\lambda-\tau-2nT)h_R(t-\lambda)d\lambda\right]^2 d\tau$$
$$+\int_{0}^{2T}\left[1-\frac{\tau}{2T}\right]\left[\sum_{n=-2}^{2}c_n\int_{\tau}^{4T+\tau}h_T(\lambda-\tau-2nT)h_R(t-\lambda)d\lambda\right]^2 d\tau \quad \text{(C.10)}$$

case (iv) $\omega_{-1}=\omega_o$, $\omega_1\neq\omega_o$

$$I_{s_4}=\int_{-2T}^{0}\left[1+\frac{\tau}{2T}\right]\left[\sum_{n=-2}^{2}c_n\int_{-2T+\tau}^{2T+\tau}h_T(\lambda-\tau-2nT)h_R(t-\lambda)d\lambda\right]^2 d\tau$$
$$+\int_{0}^{2T}\left[1-\frac{\tau}{2T}\right]\left[\sum_{n=-2}^{2}c_n\int_{-2T+\tau}^{2T+\tau}h_T(\lambda-\tau-2nT)h_R(t-\lambda)d\lambda\right]^2 d\tau \quad \text{(C.11)}$$

where

$$h_T(\lambda-\tau-2nT)\,h_R(t-\lambda)=\frac{\cos\frac{\pi(\lambda-\tau-2nT)}{2T}}{\left[1-\frac{(\lambda-\tau-2nT)^2}{T^2}\right]}\,\frac{\sin\frac{\pi(t-\lambda)}{2T}}{(t-\lambda)} \quad \text{(C.12)}$$

sampled at $t=(2m-1)T$. Using trignometric identities and knowing m takes on integer values (A10) may be written as

$$h_T(\lambda-\tau-2nT)\,h_R(t-\lambda)=\frac{Num}{Denom} \quad \text{(C.13)}$$

where

$$Num = \{(.5 + .5\cos\frac{\lambda\pi}{T})\cos\frac{\pi\tau}{2T} + 2\sin\frac{\pi\lambda}{T}\sin\frac{\pi\tau}{2T}\}$$
$$\cdot \cos n\pi \cos k\pi \qquad (C.14)$$

$$Denom = -\lambda^3 + \lambda^2[(2m-1)T + 2(\tau+2nT)]$$
$$+ \lambda[T^2 - (\tau+2nT)^2 - 2(\tau+2nT)(2m-1)T]$$
$$+ (2m-1)T[(\tau+2nT)^2 - T^2] \qquad (C.15)$$

C.4 Faded jammer:

Similarly for the jammer case it can be shown that

$$\sigma_J^2 = \frac{\gamma_j^2 J}{\pi^2} I_{J_i}\ ; \quad i=1,2,3,4. \qquad (C.16)$$

case (i) $\omega_{-1} = \omega_0\ ,\ \omega_1 = \omega_0$

$$I_{J_1} = Si^2(6\omega T) \qquad (C.17)$$

case (ii) $\omega_{-1} \neq \omega_0\ ,\ \omega_1 \neq \omega_0$

$$I_{J_2} = [Si(4\omega T) - Si(2\omega T)]^2 \qquad (C.18)$$

case (iii) $\omega_{-1} \neq \omega_0\ ,\ \omega_1 = \omega_0$

$$I_{J_3} = [Si(6\omega T) - Si(2\omega T)]^2 \qquad (C.19)$$

case (iv) $\omega_{-1} = \omega_0\ ,\ \omega_1 \neq \omega_0$

$$I_{J_4} = Si^2(4\omega T) \qquad (C.20)$$

where

$$Si(x) = \int_0^x \frac{\sin z}{z}\,dz \qquad (C.21)$$

Next the variance of the noise is

$$\sigma_N^2 = \frac{N_0}{2}\left[\frac{1}{2\pi}\int_{-\pi/2T}^{\pi/2T} |H_R(\omega)|^2 d\omega\right] = \frac{N_0}{4T} \qquad (C.22)$$

In addition to the above results, to characterize the performance of the system by the probability of bit error as a function of bit energy to noise ratio, bit energy to jamming noise ratio we need the following, a relation between signal amplitude A to the average transmitted power S.

$$S = (\sqrt{2}A)^2 \left[\frac{1}{2T}\int_0^{2T} \sum_{n=-\infty}^{\infty} h_T^2(t-2nT)dt\right] = \frac{2A^2}{2T}\left[\frac{1}{2\pi}\int_{-\pi/2T}^{\pi/2T} |H_T(\omega)|^2 d\omega\right]$$

$$= 4A^2 \qquad \text{(C.23)}$$

C.5 Probability of bit error:

From the detection criteria eq. (4.17), the bit error probabilities are for the quadrature and in-phase channel are

$$P_Q(e \mid \phi,\lambda_J,c_{-2},c_{-1},c_0,c_1,c_2,\omega_{-1},\omega_1) = Pr(\hat{a}_l \neq a_l)$$
$$= \frac{1}{2}Pr\{|Z_{Qm}| > A \mid c_l + c_{l-1} = 0\}$$
$$+ \frac{1}{4}Pr\{|Z_{Qm}| < A \mid c_l + c_{l-1} = 2\}$$
$$+ \frac{1}{4}Pr\{|Z_{Qm}| < A \mid c_l + c_{l-1} = -2\} \qquad \text{(C.24)}$$

$$P_I(e \mid \phi,\lambda_J,d_{-2},d_{-1},d_0,d_1,d_2,\omega_{-1},\omega_1) = Pr(\hat{b}_l \neq b_l)$$
$$= \frac{1}{2}Pr\{|Z_{Qm}| > A \mid d_l + d_{l-1} = 0\}$$
$$+ \frac{1}{4}Pr\{|Z_{Qm}| < A \mid d_l + d_{l-1} = 2\}$$
$$+ \frac{1}{4}Pr\{|Z_{Qm}| < A \mid d_l + d_{l-1} = -2\} \qquad \text{(C.25)}$$